Individual roles of *p53* and *NF1* in OPC competition and gliomagenesis

Phillippe P. Gonzalez
Chandler, Arizona

M.S., University of Oregon, 2012
B.S., University of the Incarnate Word, 2007

A Dissertation presented to the Graduate Faculty
of the University of Virginia in Candidacy for the Degree of
Doctor of Philosophy

Department of Microbiology, Immunology and Cancer Biology

University of Virginia
May, 2017

ABSTRACT

Glioblastoma remains one of the most deadly cancers due to their rapid onset and the limited effectiveness of therapies. Here we use a mouse genetic system termed Mosaic Analysis with Double Markers (MADM) to study progression towards malignancy in oligodendrocyte progenitor cells (OPC), the cell of origin of glioma. We use gene deletions to uncover individual roles of two commonly mutated tumor suppressor genes, *p53* and *NF1*. *NF1* acts as a negative regulator of OPC self-renewal and promoter of OPC differentiation, and *p53* increases the permanent arrest of OPC proliferation during times of stress. Subsequent analysis revealed that the downstream *NF1* effector, *mTOR*, is critical for OPC transformation. Furthermore, mutant OPCs expand at the expense of surrounding non-mutant OPCs through a mechanism termed cell competition, to maintain proper density in the brain. This cell competition phenomenon is critical for OPC transformation as the complete inhibition of this property leads to inhibition of gliomagenesis irrespective of *p53* and *NF1* mutations. In summary, our findings reveal distinct roles for *p53* and *NF1* during gliomagenesis and a unique cell-cell interaction during the progression that is critical for malignancy.

ACKNOWLEDGEMENTS

TABLE OF CONTENTS

List of Figures

LIST OF ABBREVIATIONS

4EBP1= eukaryotic translation initiation factor 4E-binding protein 1

AKT= protein kinase B

AML= acute myeloid leukemia

APC/CC1= adenomatous polyposis coli

Bax= bcl-2-like protein 4

BrdU = 5-bromo-2′-deoxyuridine

CD34 = cluster of differentiation 34, Hematopoietic Progenitor Cell Antigen CD34

CD68 = cluster of differentiation 68, macrophage antigen CD68

CD133= prominin-1

CDK4= cyclin-dependent kinase 4

CDKN2A/CDKN2B= cyclin-dependent kinase inhibitor 2A/B

CDKN2C= cyclin-dependent kinase 4 inhibitor C

CKO = conditional knockout

CNS= central nervous system

Cre = cre recombinase

CreER= estrogen receptor-fused cre recombinase

CSC = cancer stem cell

DAPI = 4',6-diamidino-2-phenylindole

DIV = days in vitro

dMyc= *drosophila* myc

DNA = deoxyribonucleic acid

Dox = doxycycline

dpi = days post injection

E# = embryonic day #

EdU = 5-ethynyl-2′-deoxyuridine

EGFR= epidermal growth factor receptor

ERK= extracellular signal-related kinaase

FACS = fluorescence-activated cell sorting

G1/S= G1 to S phase transition

GAP= gtpase activating protein

GBM = glioblastoma

GDP=guanosine diphosphate

GFAP = glial fibrillary acidic protein

GFP = green fluorescent protein

GOI = gene-of-interest

G/R= green to red ratio

GTP= guanosine triphosphate

hGFAP= human glial fibrillary acidic protein

INK4, ARF = cyclin-dependent kinase inhibitor 2A

IR= irradiation

Ki67 = marker of proliferation Ki67

KO= knock-out

KRas= Kirsten rat sarcoma viral oncogene homolog

LGG= low-grade glioma

MADM = Mosaic Analysis with Double Markers

MAPK = mitogen-activated protein kinase

MBP= myelin basic protein

MDM2= mouse double minute 2 homolog

miRNA= micro RNA

MPNST=malignant peripheral nerve sheath tumor

mTOR= mammalian target of rapamycin

NDS = normal donkey serum

NeuN = Neuronal Nuclei

NG2= neuron-glial antigen 2

NF1=neurofibromin 1

NSC = neural stem cell

O1= oligodendrocyte marker 1

O4= oligodendrocyte marker 4

Olig2= oligodendrocyte lineage transcription factor 2

OPC = oligodendrocyte precursor cells

P# = postnatal day #

P21=cyclin-dependent kinase inhibitor 1

PBS = phosphate buffered saline solution

PBT = PBS plus Triton-X 100

PCR = polymerase chain reaction

PDGFRα = platelet-derived growth factor alpha receptor

PFA = paraformaldehyde

PI3K= phosphoinositide 3-kinase

PLP= proteolipid protein

PreT= pre-transforming/ed

PTEN= phosphatase and tensin homolog

PUMA= p53 upregulated modulator of apoptosis

Rb= retinoblastoma protein

RFP = red fluorescent protein

RNA = ribonucleic acid

RT = room temperature

RTK= receptor tyrosine kinase

S6K= ribosomal protein S6 kinase beta-1

SEM = standard error of mean

SPARC= secreted protein acidic and rich in cysteine

Sos= son of sevenless

Sox10= SRY-box 10

tdT= tdTomato reporter protein

TSG= tumor suppressor gene

TP53, p53 = tumor protein 53

TUNEL= terminal deoxynucleotidyl transferase dUTP nick end labeling

Wnt= wingless-related integration site

WT= wild-type

YAP= yes-associated protein

Chapter 1: Introduction

1.1 Clinical aspects of glioblastoma

Gliomas are the most frequent primary malignant brain tumor in adults which arise from glial tissue (Brennan et al., 2009; Chen et al., 2012; Cloughesy et al., 2014; Dunn et al., 2012; Lawrence et al., 2012; Moser, 1988). Gliomas are defined pathologically as tumors that display histological, immunohistochemical, and structural evidence of glial cells. Gliomas are classified by their line of differentiation and graded on a scale of I to IV according to malignancy (Lassman et al., 2005; Maher et al., 2001; Ostrom et al., 2014; Schwartzbaum et al., 2006). Grades I and II tend to be less malignant and the overall survival time post diagnosis is high (3-20yrs) (Maher et al., 2001). Grade III and IV gliomas make up a majority of new glioma cases annually in adults. Grade IV glioma, also referred to as glioblastoma (GBM), is the most common glioma grade, constituting over 70% of all glioma cases. With 10,000 new cases per year in the U.S. GBM is the most deadly glioma, with an average survival time post diagnosis of 14.6 months, even with therapy (Ostrom et al., 2014; Seymour et al., 2015).

Glioblastoma incidence increases with age with a peak between 75-84 years of age (Sturm et al., 2014). GBM are classified by the manner in which the tumor develops in the brain. Primary GBM originate *de novo* and account for a majority, 95%, of annual GBM cases (Lote et al., 1997; Sanai et al., 2011). Secondary GBM make up roughly 5% of total annual GBM cases and develop from lower grade gliomas, Grade I/II. While secondary GBM typically progress over many years, primary GBM is characterized by quick onset of symptoms with no recognizable symptoms beforehand.

Current therapeutic strategies involve surgical resection followed by chemotherapy and localized radiotherapy (Agnihotri et al., 2013; Ali and Trafalis, 2015; Huse and Holland, 2010; Stupp et al., 2005). Complete resection of the tumor is impossible due to the infiltrative nature of the tumor cells. However, even with this aggressive treatment program, over 80% of patients inevitably relapse within 9 months following treatment (De Bonis et al., 2013).

This lethality is due in part to the location of the tumor which decreases the accessibility of drug delivery in addition to the aggressiveness of residual tumor cells following resection, resulting in inevitable relapse (Chipuk, 2015; Sherriff et al., 2013; Wen and Kesari, 2008). The majority of relapsed gliomas are resistant to secondary treatments, making relapse a fatal outcome for glioma patients (Ramirez et al., 2013; Weller et al., 2012). Additionally, while low-grade gliomas (LGG) rarely have noticeable symptoms in patients, these tumors invariably progress to malignant high-grade gliomas, a process which current therapies have yet to effectively stop (Kleihues and Ohgaki, 1999; Ohgaki and Kleihues, 2013; Pouratian and Schiff, 2010; Schomas et al., 2009). Thus, more research is needed to understand the progression from LGG to GBM and also to understand the basic biological mechanism affected during GBM malignancy.

1.2 Core pathway mutations in Glioblastoma

To gain a better understanding of the fundamental molecular pathways involved in GBM, The Cancer Genome Atlas analyzed hundreds of human glioma samples at the genomic level to identify commonly perturbed pathways (Brennan et al., 2013; McLendon et al., 2008). From these studies 3 "core" pathways were identified, including the *Ras/*RTK, *p53*, and *Rb* signaling pathways (Figure 1.1). The majority of GBMs have

alterations in all three signaling pathways, which allows tumor cells to proliferate, invade, and survive, while also allowing these cells to escape cell-cycle arrest, senescence, and apoptosis. These studies highlight the importance of these signaling pathways in GBM. Treating patients would benefit from better understanding the roles these signaling pathways play during malignant progression.

1.2.1 RTK/Ras signaling

The RAS/RTK signaling pathway plays an important role in normal development and is one of the most frequently mutated pathways in human cancers. Receptor tyrosine kinases (RTKs) are a family of cell surface proteins which act as receptors for growth factors, cytokines, and other extracellular signaling molecules (Lemmon and Schlessinger, 2010; Schlessinger, 2000). Once activated, RTKs signaling results in recruitment of *Sos*, a RAS guanine exchange factor, which results in nucleotide exchange from GDP to GTP, resulting in activation of the Ras protein (Karnoub and Weinberg, 2008; McClatchey, 2007; Scheffzek et al., 1998; Wiesmuller and Wittinghofer, 1992; Zhu et al., 2001). Activated Ras is regulated by another family of proteins, GTPase Activate Proteins (GAPs), which stimulate the GTPase activity of Ras, resulting in hydrolysis of GTP to GDP and inactivation of Ras (Tarik 2009). In tumor cells, aberrant RAS signaling leads to uncontrolled proliferation. The importance of RAS signaling to GBM became apparent when initial reports of the frequency of mutations, which led to improper activation, were first reported. It has been found that in 90% of human patient biopsies harbor mutations within the canonical RAS/RTK (Brennan et al., 2013; McLendon et al., 2008). The most frequently mutated components of this signaling pathway include *EGFR* (57%), *PTEN* (41%), *PI3K* (25%), *PDGFR*α (10%), and *NF1* (10%). *NF1* is a large cytoplasmic protein that has been studied extensively as a RAS-

GAP, but little else is known about functions outside its GAP activity (Corral et al., 2003; Dasgupta and Gutmann, 2003; Gutmann et al., 2012; Klose et al., 1998; Morcos et al., 1996; Park et al., 1998; Shin et al., 2012).

1.2.2 The p53 pathway

The *p53* pathway is known to regulate numerous different tumor suppressive processes, including cell-cycle arrest, apoptosis, and senescence. Normally *p53* is regulated tightly by *MDM2*, which has been shown to lead to both p53 degradation and inhibition of *p53* transcriptional activity, both of which lead to low levels of p53 protein (Kruse and Gu, 2009; Prives and Hall, 1999; Vousden and Lu, 2002). However, upon cellular stresses, *p53* becomes activated through the dissociation of the p53-MDM2 complex and an overall increase in p53 levels (Freed-pastor and Prives, 2012; Harajly et al., 2016; Khoo et al., 2014; Kruse and Gu, 2009; Lambert et al., 2009; Levine and Oren, 2009). Since p53 is a transcription factor, p53's activation causes transcriptional activation of various genes depending on the stress including p21, which leads to cell-cycle arrest, and Bax and PUMA, which leads to apoptosis. However, recent work has identified numerous different functions of *p53* outside the canonical cell-cycle arrest, apoptosis, and senescence, including metabolic adaptation and suppression of stem cell properties (Hong et al., 2009; Lujambio et al., 2013; Menendez et al., 2009; Montero et al., 2013). Additionally, some studies have shown p53-mediated apoptosis, cell-cycle arrest, and senescence are dispensable for *p53* mediated tumor suppression. These studies showed that when mutations within *p53* that lead to *p53*'s inability to induce apoptosis, cell-cycle arrest, and senescence activities, tumor suppression was still achieved in a *p53*-dependent manner. These studies highlighted the lack of complete

understanding of *p53* functions (Li et al., 2012; Valente et al., 2013a). It has been found that, while *p53* is attenuated in over 50% of all human cancers, a large number of the remaining cancers harbor *p53* mutations. These mutations within *p53* normally lead to dominant negative isoforms of the p53 protein (Wang and Sun, 2010; Young et al., 2011; Yu et al., 2012). In the TCGA study of GBM patient samples, the frequency of mutations within the *p53* signaling pathway includes *CDKN2A* (57.8%), *p53* (28%), and *MDM2* (7.6%) (Brennan et al., 2013; McLendon et al., 2008). Among p53 mutations, 8.1% is loss and 19.9% is point mutations.

1.2.3 The RB pathway

The RB pathway is a key check point for cell cycle progression in most mammalian cells (Bremner et al., 2004; Giacinti and Giordano, 2006; Sherr and Mccormick, 2002). The ability of a cell to proliferate is determined by extracellular signals that cue downstream transcriptional and protein level changes. During cell division there is up-regulation of D-type cyclins and cyclin kinases, which phosphorylate and negatively regulate *RB* (Khleif et al., 1996; Lim and Kaldis, 2013; Ren and Rollins, 2004; Sherr and Roberts, 1999). *RB* is known to inhibit the progression from G1 to S during the cell cycle by sequestering the transcription factors of the E2F family and phosphorylation of Rb causes release of E2F and leads to a loss of *RB* dependent cell cycle arrest. It should come as no surprise that RB pathway mutations are found in nearly 4/5 (79%) of all GBM samples, including CDKN2A/CDKN2B (61%), CDK4 (14%), RB1 (7.6%), and CDKN2C (5.6%), thereby highlighting *RB*'s critical role in GBM malignancy.

Figure 1.1 Core signaling pathways frequently mutated in Glioblastoma Multiforme according to TCGA
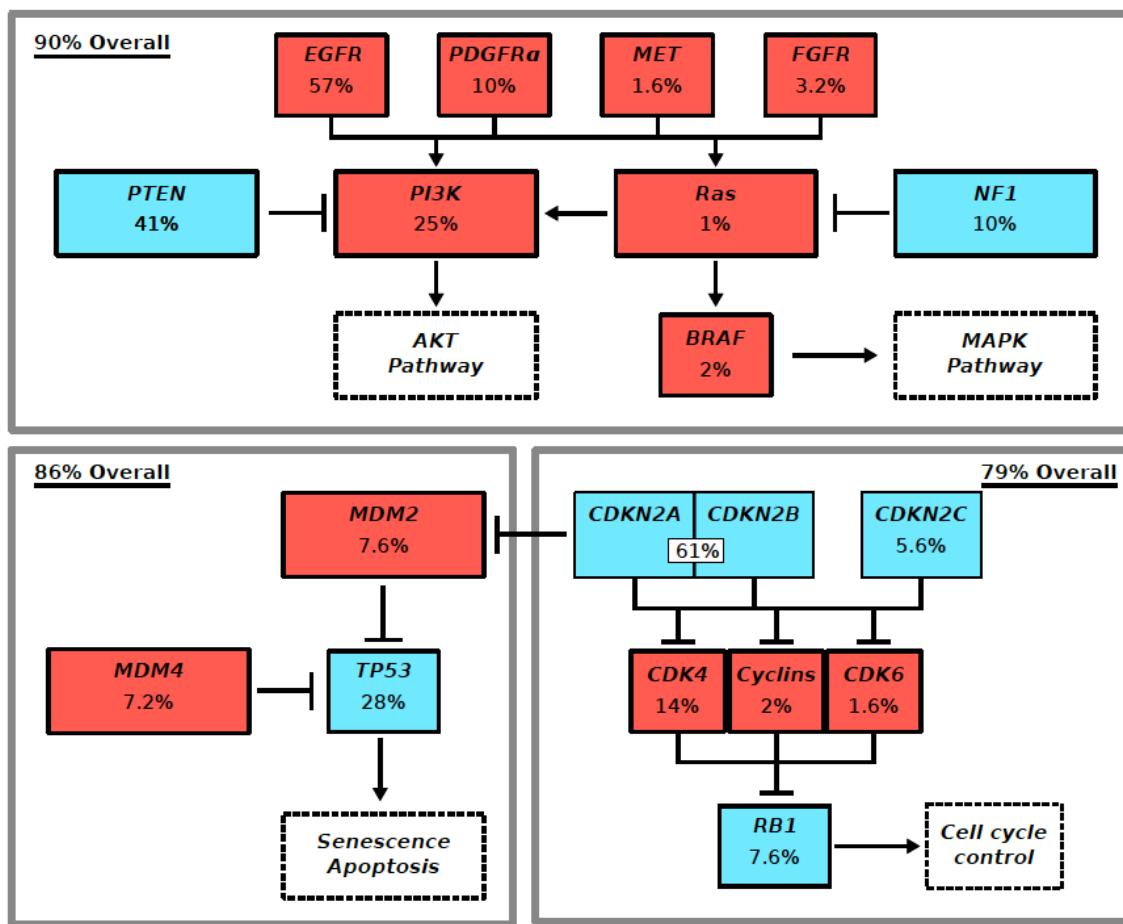
Figure 1.1 Pathway mutations in Glioblastoma Multiforme

Following analysis of over 500 human glioma samples, 3 "core" pathways were identified that were commonly mutated in most tumors. The *Ras/RTK* pathway was mutated in 90% of all patients, the *p53* pathway was mutated in 86% of all patients, and the *Rb* pathway was mutated in 79% of all patients. Over 70% of all samples contained mutations in all 3 pathways highlighting the importance of all three pathways in gliomagenesis. Red indicates activating mutations while blue indicates inactivating mutations.

1.3 Pre-Transforming stage studies reveal distinct molecular and cellular aberrations

Due to the onset of glioma at later ages in life, it is important to understand the entire process of gliomagenesis. By studying both pre-transforming and malignant states, one can gain a more in depth understanding of the gliomagenic process. Analysis of pre-transforming stages could help one find the alterations that are necessary for transformation rather then 'passenger' mutations, which are less critical. Finding these key alterations could provide critical insights for designing novel therapies that target these critical pathways. Since these changes occur only in at the malignant stages, they may be more important and better targets for tumor cells since their change only occurs at the switch to malignancy. Additionally, identification of the changes between pre-malignant and malignant stages could provide new treatment options for halting low-grade glioma to high-grade glioma progression by using therapies designed to maintain pathway integrity to block the malignant switch.

However, one limitation with current glioma studies is the inability to analyze precancerous lesions before malignancy occurs. These studies use end-point analyses and by doing so are limited to addressing how tumor cells behave after transformation but fail to address how Pre-Transforming cells ultimately achieves malignancy. The progression from an initial precancerous lesion to the manifestation of symptoms involves an accumulation of alterations, some of which are necessary for transformation. These alterations could involve critical changes at the DNA, RNA, protein, or cellular levels. However, by only studying the tumor stage, we limit our ability to see differences in any of these levels. Therefore, studying cells at both the Pre-Transforming stage and the tumor stage can give us unique perspectives on the changes at the genomic,

transcriptomic, proteomic, and cellular activities level, either preceding or following transformation.

Previous work in human colon, skin, and lung cancers studies has helped identify unique genetic and signaling differences between Pre-Transforming cells and tumor cells. Hyperplasias found in both the skin and lung showed increased levels of DNA damage, which resulted in accumulation of *p53* (Gorgoulis et al., 2005). However, following transformation, *p53* was altered at the genomic level resulting in no activation of *p53* in response to DNA damage, and as a consequence, they found decreased apoptosis and decreased DNA damage response, suggesting that *p53* inactivation was the critical step needed for transformation. Thus, by studying pre-malignant stages of these tumors, this group found that the tumor suppressor genes (TSG) *p53* can be highly active in benign lesions, yet is completely absent from tumors. If they had in fact only studied the end-stage they might assume that *p53* inactivation was an early step needed for the hyperplasias to accumulate.

A separate study analyzed precancerous and malignant colon lesions to identify how transcriptional activation was changed between the two stages of tumorigenesis. In pre-invasive lesions, cell-cycle arrest pathways were up regulated while in late pre-invasive lesions, there was down regulation of differentiation pathways (Maglietta et al., 2012). Following transformation, tumor cells had altered the expression of cell-cycle pathways such that the *G1>S* transition was hyper-activated. Additionally, patients with neurofibroma, a benign tumor found in patients with familial *NF1* mutations, sometimes acquire malignant peripheral nerve sheath tumors (MPNSTs). These malignant tumors are the result of neurofibromas becoming deadly and thus serve as a perfect system for comparing changes between benign and malignant states. In these patients, they found

that the *Wnt* pathway was gradually up regulated as malignancy increased (Watson et al., 2013).

Together these studies emphasize that unique pathways are differentially regulated at both the Pre-Transforming stage and the tumor stage. By only analyzing tumor cells, none of the above studies would have noted that particular pathways, such as the *Wnt* pathway, would have close to normal activity levels in Pre-Transforming cells yet somehow becomes hyperactive in malignant cells. If analyzed at just an end-point, these groups might have concluded that *Wnt* was activated initially and was therefore not unique to tumor cells. Yet by looking at both stages these groups were able to determine which changes were unique to tumor cells and which changes were necessary to Pre-Transforming cells.

1.4 Glioma cell of origin studies

One of the biggest challenges to these types of studies in mouse glioma models is being able to identify Pre-Transforming cells accurately and precisely to characterize only a pure population of the Pre-Transforming cells without contamination from other cell types. Therefore, in order to accurately make these comparisons, identification of the cell of origin in glioma is vital so that the characterization can be done properly.

The identification of the cell responsible any given cancer also carries with it the possibility of uncovering specific details that could help tailor therapies to more effectively treat these cancers. The problem with identification is that most tumors are composed of a heterogeneous population of cells and also that the multiplicity of mutations may have also altered cellular properties enough which could lead to a

misidentification. Despite these issues, different theories have been postulated in an attempt to identify the cell of origin in cancer.

1.4.1 Cancer Stem Cell theory

The Cancer Stem Cell (CSC) theory was first experimentally backed up in 1997 in a study looking at acute myeloid leukemia (AML) (Bonnet and Dick, 1997). The theory posits that tumor heterogeneity is not a consequence of random mutations but rather results from a hierarchy of cells with CSCs at the top (Fabian et al., 2013). A key feature of the CSC theory is that despite the large number of cells found within the tumor, CSCs only make up less than 1% of the total population and are the only population capable of generating a tumor. These small populations of CSCs have several characteristics reminiscent of normal stem cells in that they can differentiate into multiple lineages, indefinitely self-renew, and are less susceptible to genotoxic stress. These combined characteristics make treating tumors difficult. Furthermore, CSCs are thought to be resistant to standard therapies due in part to their ability to remain quiescent (Chipuk, 2015).

One of the main issues in early studies that tried to identify CSCs in AML was that many studies did not provide direct evidence that this unique population could generate tumors of their own. However by 1997 it was shown that by injecting $CD34^{+}CD38^{-}$ cells, or AML CSCs, into immune-compromised mice, tumors were generated consistently and morphologically similar to the parental tumor (Bonnet and Dick, 1997). Additionally, they showed that despite the original heterogeneity of these CSCs from different patients, all the tumors that formed were similar and that they all displayed the same capacity to differentiate and self-renew as normal stem cells. They

concluded that AML contains CSCs, which are derived from normal SCs, and this small pool of cells can continually generate tumors.

CSCs were then identified in other types of other cancers including brain tumors shortly thereafter. Human tumors originating in the brain contained a small population of cells that were $CD133^+$, whereas a majority of the tumor cells were $CD133^-$. By grafting as little as 100 of these $CD133^-$, tumors were generated that mimicked the original tumor type, while grafting $CD133^-$ cells generated no such tumors (Singh et al., 2004a, 2004b). Additionally these cells behaved similarly to normal neural stem cells in that they generated multiple lineages, self-renewed, and actively proliferated. Additional reports found CSCs in various central nervous system tumors including medulloblastoma, pilocytic astrocytomas, and ependymomas, giving more evidence that CSCs may serve as the cell of origin in all brain tumors including gliomas (Singh et al., 2003). Since these glioma CSCs behaved similarly to neural stem cells (NSCs), they concluded that these CSCs must have originated from NSCs.

However, one of the main caveats with this theory, as it relates to brain tumors, is its assumption that tumor cells function the same as the cell of origin. Because tumors gain large numbers of mutations during tumorigenesis, the biological consequences of all these mutations are unknown. In addition, while NSCs may be one of the reservoirs of proliferating cells in the brain, they are by no means the only cell population capable of this as previous reports have shown astrocytes and glial progenitors also proliferate well into adulthood (Sadgrove et al., 2003; Yong et al., 1991). Thus, the CSC theory has obvious caveats with regards to gliomagenesis since several different cell types potentially share the characteristics needed for tumor formation.

1.4.2 Neurons and Astrocytes as the possible glioma cell of origin.

Because the brain is composed of several specific cells, it has been proposed that most of the neural lineage cells can give rise to glioma. Mutations in the *p53*, *RB*, and *PTEN* pathways have been shown to transform both astrocytes and glial progenitors (Chow et al., 2011; Uhrbom et al., 2004). A separate study showed that concurrent loss of *Ink4a-Arf* along with *KRas* activation leads to GBM formation from both astrocytes and neural progenitors (Uhrbom et al., 2002). Additional studies showed that not only could astrocytes successfully transform but with the right mutations neurons could also form gliomas through a process of dedifferentiation (Friedmann-Morvinski et al., 2012). However, one caveat of these studies is that they analyzed tumors at the end stage, when tumor cells have acquired multiple changes which could result in their altered expression patterns and trans differentiation which has been previously reported (Scully et al., 2012; Soda et al., 2011).

OPCs as the glioma the glioma cell of origin

The last potential source put forth for the glioma cell of origin is the oligodendrocyte progenitor cells (OPCs). One of the reasons people thought that OPCs could serve as the cell of origin was because of their unique ability to continually proliferate and self-renew throughout adulthood, similar to NSCs. Several studies have shown that mutations commonly found in human patients can drive OPCs to transform and develop high-grade GBM (Assanah et al., 2006; Lindberg et al., 2009, 2014; Llaguno et al., 2015).

While these studies elegantly showed the OPCs could indeed generate GBM, there was still debate whether these cells were truly OPCs. The reason for this debate stemmed from the notion that following all of these mutations; NSCs could simply have altered expression patterns or could have undergone some differentiation during this process. If this were true then the idea that OPCs were the cell of origin did not hold true since NSCs truly were the cell responsible for the tumor. To address this our lab established a genetic mosaic tool that allows for permanent labeling of both WT and mutant cells at the same type at an infrequent rate, which mimics the sporadic and clonal nature of cancer.

1.4.4 *Mosaic Analysis with Double Markers*

Conventional knockout models generate a whole population of cells that are genetically altered in the same way. However, early reports by Peter Nowell and more recent papers have shown that cancers are clonal by nature and thus, to study them precisely, one must use a model which recapitulates the disease state as closely as possible (Greaves and Maley, 2012; Nowell, 1976). To address this issue, our lab has developed a clonal model of glioma with Mosaic Analysis with Double Markers (MADM) in mice (Henner et al., 2013; Zong et al., 2005). MADM tumors progress in a clonal fashion from a small population of mutant cells that are permanently labeled with a fluorescent protein. Similar to the human disease state, these mutant cells are surrounded by non-mutant cells, which more closely mimics how most human cancers are thought to develop.

The MADM system was originally generated to study the clonal nature of both mutant and wildtype cells in the same tissues using permanent fluorescent protein

labeling. MADM enables lineage analysis and the ability to observe different cell behaviors between different cell types (Muzumdar et al., 2007; Zong et al., 2005). This genetic mosaic system is an ideal tool to study the clonal nature of human cancer in mice due to the ability to track sparsely labeled cells in an otherwise unaffected tissue (Liu et al., 2011a). The genetic design of MADM includes two reciprocal chimeric cassettes, whereby the green fluorescent protein (*GFP*) and red fluorescent protein (*RFP*) are interrupted with loxP sites and the N-terminal and C-terminal halves of the genes are separated to generate chimeric alleles in the same chromosome (Figure 1.2). In the presence of a Cre-recombinase, intrachromosomal recombination of the chimeric cassettes can occur at a low frequency when the cell undergoes division and the chromosomes are duplicated during S-phase. If recombination occurs and the recombined chromosomes are segregated in either an X- or Z-pattern into daughter cells, this imparts the two daughter cells with either an intact GFP gene or an intact RFP gene, both GFP and RFP genes, or neither gene. These will generate a green, red, yellow, or colorless cell, respectively. If a mutant allele of a gene-of-interest (GOI) is present telomeric to the cassette, it is linked to the fluorescent gene half of the MADM cassette on the same allelic side. For example, if the mutant allele is linked to the GFP-half, then upon Cre-mediated recombination and X-patterned chromosomal segregation into two daughter cells, one green cell would be homozygous-mutant for the GOI and the red sister cell would be wildtype for the GOI. If instead Z-patterned chromosomal segregation occurred, then one of the daughter cells would be identical to the mother cell (colorless and heterozygous for the GOI), while the other daughter cell would be yellow due to the intact *GFP* and *RFP* genes and also heterozygous for the GOI. The sparse labeling of sibling cells, which are distinguished by fluorescent proteins, provides

a useful tool to observe the progression from initial mutant clones all the way to fully malignant tumors.

Figure 1.2 <u>M</u>osaic <u>A</u>nalysis with <u>D</u>ouble <u>M</u>arkers
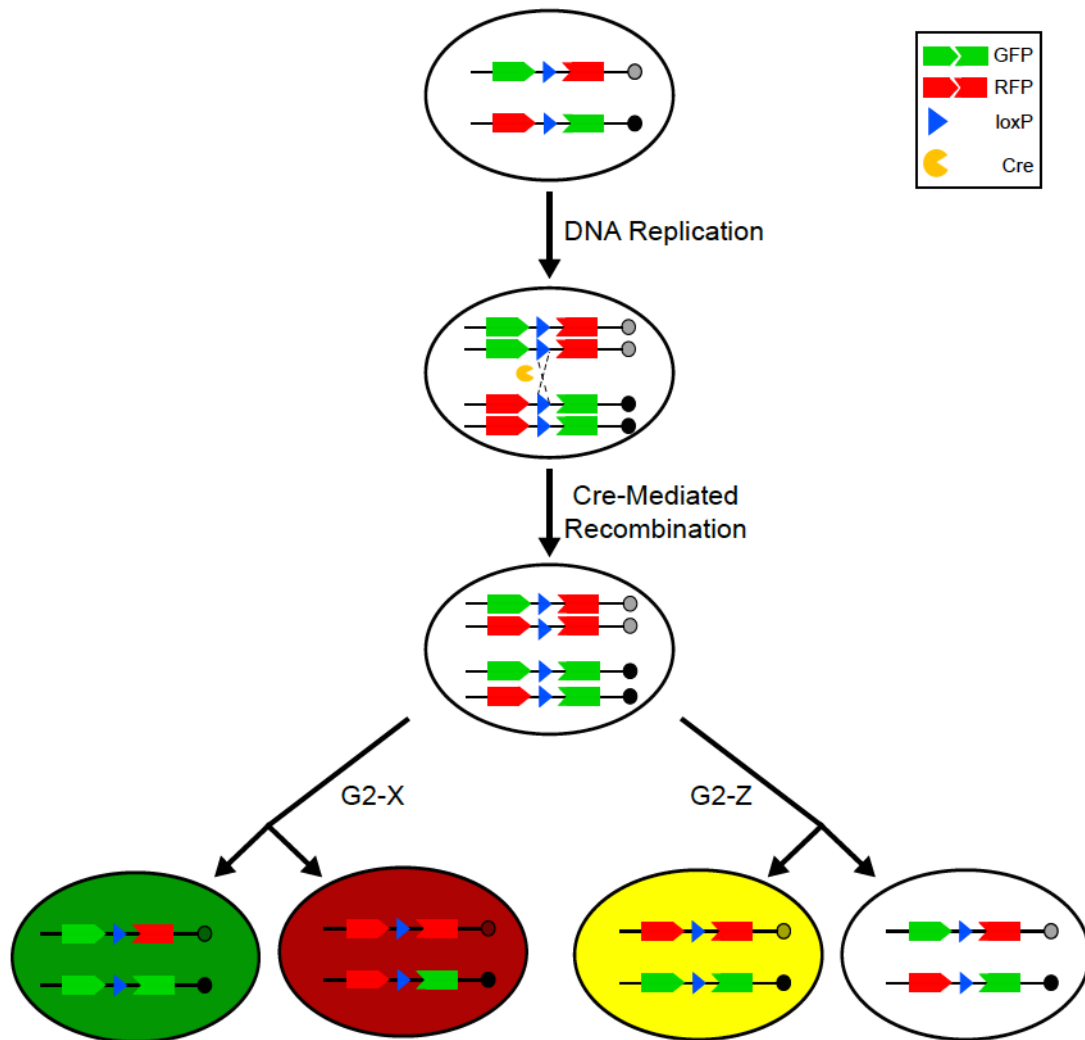
Figure 1.2 <u>M</u>osaic <u>A</u>nalysis with <u>D</u>ouble <u>M</u>arkers

MADM is comprised of two chimeric fluorescent protein cassettes separated by a loxP site on both alleles in a chromosome. When Cre-recombinase is present, it can mediate intrachromosomal recombination between loxP sites of MADM cassettes at a low frequency upon cell division. Duplicated chromosomes, which have undergone recombination, will segregate into two daughters cells following a G2-X or G2-Z pattern. In the G2-X separation pattern, one daughter cell will receive an intact *RFP* allele and the other allele is still chimeric which results in permanent labeling of this cell and all of its lineage with *RFP*. The sister cell will receive an intact *GFP* allele and is permanently labeled with *GFP*. In G2-Z segregation, one daughter cells receives both GFP and RFP alleles, resulting in one cell being permanently labeled as yellow while the sister cell receives both chimeric alleles, like the mother cell, and is colorless. To assess gene function, a GOI is incorporated telomeric to the MADM cassettes. When the GOI is linked with the *GFP* half of the cassette, then following G2-X recombination and segregation, both mutant alleles segregate into a GFP+ cell while the sister RFP+ sister cell serves as a wildtype control.

1.4.5 MADM reveals OPCs as the glioma cell of origin

Using MADM, our lab generated a glioma model by incorporating two commonly mutated TSGs in glioma, *p53* and *NF1*. Because the purpose of our original study was to determine cell serving as the cell of origin for glioma, we chose to use a Cre-recombinase that would label all the cell lineages in the brain. We generated a MADM mouse with *p53* and *NF1* mutant alleles linked to the GFP-half of MADM and used *hGFAP*-Cre to specifically delete both genes in NSCs, thereby allowing for all the neural lineages to have equal opportunity to transform (Zhuo et al., 2001). Following deletion of both TSGs, MADM-Tumor mice (*p53,NF1*-null) and MADM-WT mice were analyzed at different stages of development including Postnatal day 10 (P10), P60, and P150. At P10, MADM-WT and MADM-Tumor mice had no obvious changes in the number of GFP+ mutant cells compared to RFP+ WT cells. However, by P60 there was an obvious increase in the number of GFP+ cells and by P150, mice had formed tumors, which were histo-pathologically identified as glioblastoma (Liu et al., 2011a).

Because P60 mice had obvious increases in mutant cells, an analysis of the cellular identity of the mutant cells in these brains was necessary to identify the cell type that was expanding following *p53* and *NF1* deletion. Due to the nature of MADM labeling, a simple quantification of the number of GFP+ cells compared to RFP+ cells (G/R ratio) allows for a quick analysis of the effect on cell numbers in respect to the genetic alterations. While neurons, astrocytes, and oligodendrocytes all showed minimal if any increases in G/R ratio, OPCs showed a substantial 150-fold increase in G/R ratio. Further analysis of the tumors revealed that not only did the tumor cells share OPC specific expression patterns histologically, but they also had similar transcriptome

profiles to OPCs, suggesting that these tumors did indeed form from OPCs and not NSCs, neurons, astrocytes, or oligodendrocytes.

Following this, however, there remained important unanswered questions. The first question was whether OPCs could directly transform to form GBM. To address this, our lab then used the MADM system to generate MADM mice using an OPC specific Cre (NG2-Cre) and analyzed whether these mice formed similar tumors to the previous mice (Zhu et al., 2007). Not surprisingly, these mice formed tumors that resembled the original tumors albeit at a later latency but with the same penetrance. Thus, OPCs can indeed directly transform and form GBM.

However, an even more important question remained regarding the applicability of this system to the human disease. GBM is generally an adult-onset tumor type, which manifests itself later in life, while the MADM system generates mutant cells embryonically using the Cre lines. Thus, whether or not this system recapitulated the human disease was left unanswered. To resolve this issue, our lab then made use of a traditional condition knockout system (CKO) that allowed for *p53* and *NF1* deletion in OPCs using an NG2-CreER that is inducible upon tamoxifen administration(Galvao et al., 2014). Starting at either P45 of P180, mice were treated with tamoxifen and the effects of *p53* and *NF1* deletion were analyzed. Following the initial deletion, PreT-OPCs increased their proliferation and their cell numbers during a reactivation phase. Following the reactivation stage, these cells then underwent a quiescent period where proliferation rates were normalized before undergoing further, currently unknown, changes that resulted in transformation. These tumors resembled OPCs in their transcriptomic profile but also the original MADM tumors generated previously. This demonstrated that not only can OPCs directly transform into GBM but also that adult OPCs can generate GBMs that are similar to the MADM tumors generated.

Consequently, while others have shown other cells capable of forming tumors following genetic deletions, our group showed that given the same genetic lesions and chance to become malignant, only OPCs expand and eventually transform into tumor cells (Chow et al., 2011; Friedmann-Morvinski et al., 2012; Uhrbom et al., 2002). While our findings were not the first to put forth the idea that OPCs are the cell of origin, our unique ability to label all neural cells and track the effects on all the cells gave us an unprecedented ability to analyze pre-malignant stages in addition to malignant stages. Moreover, while most glioma models use a Cre-loxP system, our system generates mutant cells at such a low frequency that is mimics the clonal nature of cancer. Additionally, now that we have identified OPCs as the cell of origin, targeting these cells can now be made a priority since previous therapeutics have used end stage cells as their basis for therapeutic intervention. Given that OPCs have distinct biological properties compared to all other cells, designing novel treatments tailored for OPC biology can perhaps increase the efficacy of said treatments.

1.5 OPC Biology

1.5.1 OPC Development

Oligodendrocyte progenitor cells constitute around 5% of all cells in the adult brain and generate oligodendrocytes throughout life (Billon et al., 2002; De Castro and Bribián, 2005; Dawson, 2003; Dimou et al., 2008; Nishiyama et al., 2009; Richardson et al., 2006; Rowitch and Kriegstein, 2010). OPCs were first identified in the rat optic nerve and later in the adult mammalian central nervous system (CNS) (Engel and Wolswijk, 1996; Ffrench-Constant and Raff, 1986; Raff et al., 1983; Wolswijk and Noble, 1989).

OPCs are first detected late during brain development and originate from the neuroepithelial progenitor cells of the ventricular zone (Richardson et al., 2006). During this time, generally around embryonic day 12.5 (E12.5), OPCs are characterized by their high proliferation rate and high migratory activity throughout the parenchyma. From this ventral area of origin, these OPCs are able to efficiently populate most of the CNS before a second wave of OPCs, around E15.5 (Kessaris et al., 2006). Around birth, a third wave of OPCs thought to be of cortical origin replaces the original OPC population. During this process the cortex is expanding some 20-fold in size and it is thought that part of the reason for the replacement of the first wave of OPCs is through the dilution of these cells among the entire OPC population. By P20, most OPCs in the brain have slowed their division rate and enter into a quiescent state that they remain in throughout adulthood.

1.5.2 Developmental and adult OPC characteristics

OPCs develop embryonically and are considered a developmental cell type until P20. During development these cells express various genes including *Oligodendrocyte Transcription Factor 2* (*OLIG2*), which is present in all cells of the oligo-lineage. As these cells leave the ventricular zone, both *platelet-derived growth factor receptor alpha* (*PDGFRa*) and the transcription factor *SRY-Box 10* (*Sox10*) are up regulated while *neural/glial antigen 2* (*NG2*) expression starts slightly later (Cavaliere et al., 2012; Crawford et al., 2014; Dimou and Wegner, 2015; Hill et al., 2013; Young et al., 2013). In particular, PDGFRa is the major growth factor receptor in OPCs and as such has been studied extensively in OPCs. Previous studies have shown that KO of PDGFRa results in low numbers of OPCs initially that eventually recovers to near WT levels (Fruttiger et

al., 1999). Because these cells have to migrate and expand in number quickly, the expression profile of embryonic and perinatal OPCs resembles most highly proliferative cells with high expression of cell-cycle related genes which allows them to divide once every 4 days (Psachoulia et al., 2009; Young et al., 2013).

Normally, perinatal OPCs are responsible for migrating throughout the parenchyma and differentiating into myelin-forming oligodendrocytes, which wrap the axons of neurons (Canoll and Goldman, 2008). This process involves up regulation of different genes including *oligodendrocyte marker 4* (*O4*), and *oligodendrocyte marker 1* (*O1*) and differentiation into a pre-myelinating oligodendrocyte. Following this, these cells then differentiate further into mature myelinating oligodendrocytes which are characterized by their expression of myelin related genes including *myelin basic protein* (*MBP*), *proteolipid protein* (*PLP*), and *adenomatous polyposis coli* (*APC/CC1*)

In contrast to perinatal OPCs, adult OPCs are relatively quiescent (Engel and Wolswijk, 1996; Shi et al., 1998; Wolswijk and Noble, 1989; Young et al., 2013). While adult OPCs maintain the ability to proliferate, they do so at a much slower rate then perinatal OPCs, about once every 36 days. In line with decreased proliferation, adult OPCs adopt an mRNA expression profile with relatively low levels of cell cycle related genes (Belachew et al., 2002; Lin et al., 2009). However, the main function of adult OPCs is to become reactivated in response to either injury or neuronal activity. This reactivation causes an increase in proliferation, which results in the intended de-differentiation of fully differentiated myelinating oligodendrocytes (Franklin and Ffrench-Constant, 2008; Gibson et al., 2014; McTigue and Tripathi, 2008). Thus, while perinatal OPCs are highly proliferative and differentiate into myelinating oligodendrocytes, adult OPCs act as responders to signals within the brain, ready to be called upon to form more oligodendrocytes.

1.5.3 OPC Homeostasis

Because OPCs have to respond to signals that arise from injury and neuronal activity, their patterning in the brain must be tightly regulated to ensure that proper density is maintained at all times. This is even more critical in the CNS since there is a finite amount of space for cells to occupy. While it is known that many glial cells self-renew in response to loss after injury, the mechanisms in place for this response was not known (Ajami et al., 2007; Franklin and Barnett, 1997). It has been shown that OPCs in the adult brain form a grid-like or tiled pattern within the brain and continue to generate oligodendrocytes into adulthood (Rivers et al., 2008). However, the dynamics and control of OPC density in the adult CNS had never been properly studied in an intact brain.

In 2013, Hughes et al. examined the dynamics of OPCs by generating a *NG2-mEGFP* transgenic line that labeled all OPCs with a membrane bound GFP protein (Hughes et al., 2013a). Using this system they found that OPCs in the adult are highly dynamic and constantly survey they surroundings by extension and retraction of filopodia. During this sensing, they reorganized their processes continuously and moved through the parenchyma throughout the study. Interestingly, OPCs did not stay in a fixed position within the brain but did maintain their own independent territory through a self-repulsion mechanism. Furthermore, ablation or differentiation of OPCs triggered a swift migration and proliferation of neighboring OPCs to preserve OPC density. Therefore, OPCs balance density through both a self-repulsion and constant surveying mechanism in order to be ready to promptly respond to injury or neuronal induced stimulation.

1.6 Cell Competition

The evolution from single cellular organisms to advanced multicellular organisms with specialized organs to carry out different functions occurred over billions of years. Until Charles Darwin's theory of evolution however, no one understood how such a complex and varied process could result in the multitude of organisms we see today. One of the most spectacular aspects of evolution was the development of specialized cells within organisms that carry out functions that are, many times, unique to only those particular cells. It seems inconceivable that organs such as the brain, who have several types of cell lineages all of which carry out unique and critical functions, do not have a mechanism in place wherein cells are not constantly competing for space and factors that allow for proper brain function. Yet it wasn't until 1881 that Wilhelm Roux proposed the idea of a cellular struggle for survival during development from applying Darwin's theory of evolution to the process of ontogenesis (Roux, W. et al 1881). While unknown to him at the time, his idea would become the cornerstone of a biological process termed cell competition that is critical for not only proper development but also homeostasis during organismal life. Cell competition can be defined as the process by which cells that are normally viable on their own, die in the presence of a more competitive cell.

1.6.1 Cell competition in development

While the concept of competition has been studied in microbiology intensively, biologists studying multicellular organism had never found examples of this until 1975. Morata and Ripoll discovered the phenomenon of cell competition initially in *Drosophila*. By studying the developing wing imaginal disc of *Drosophila*, they were able to first study

the behavior of cells that contained a dominant mutation in a group of genes termed *Minute*. These Minute mutations reduced the proliferation of the mutant cell in a cell-autonomous manner. Not surprisingly, flies heterozygous for *Minute (M/+)*, developed more slowly than WT flies due to a defect in their ribosomal proteins but were still viable and were of normal body size (Morata and Ripoll, 1975). Knowing this, they generated a fly in which only a few cells were WT while the surrounding majority of cells *M/+*. They found that WT clones eventually occupy most areas of the adult wing and concurrently, *M/+* cells were eliminated from the wing. In 1981, in a similar study, *M/+* cells were analyzed by their proximity to WT cells (Simpson and Morata, 1981). It was found that *M/+* cells near WT cells died more frequently while WT cells proliferated at a higher rate when situated adjacently to *M/+* clones. Interestingly, *M/+* cells that were not in contact with WT cells were not eliminated, thus this phenomenon depended on short-range cell-cell interactions in order to occur (Simpson, 1981). Because this phenomenon, which seemed to regulate the balance between proliferation of faster-growing WT cells and the elimination of *M/+* cells depended on cell-cell interactions, they termed the phenomenon "cell competition".

From these foundational studies, the basic rules for cell competition were laid with one of the most fundamental being that competition is dependent on growth rates (Simpson, 1979). Additional evidence for this crucial role of growth rates in competition was shown through the starvation of animals. While normally WT cells would out-compete *M/+* cells, in starvation conditions, this competition was suppressed (Simpson, 1979). An interesting finding in these studies was that once development was finished, competition was abolished, suggesting that this mechanism in the imaginal discs was a developmental mechanism for proper ontogenesis. Another critical component of cell competition is that it does not alter total tissue size, thus cell competition is

phenotypically silent. The only way to observe competition is by analyzing the relative contributions of each cell within a genetically mosaic tissue to observe competition (Amoyel and Bach, 2014).

After the initial findings of the *Minute* mutations, several classes of other genes were found to lead to similar phenotypes. Using a mosaic system in *Drosophila*, Johnston et al. showed that the loss of *dMyc* slows cell growth and reduces cell size (Johnston et al., 1999). However, the overexpression of *dMyc* increases cell proliferation and cell size. When WT cells surround the heterozygous *dMyc* cells, similar to *Minute* mutants, they are readily outcompeted and undergo apoptosis. Interestingly, it was also found that when *dMyc* overexpressing cells are in a field of WT cells, WT cells are now "loser" cells and undergo rapid cell death. These *dMYC* overexpressing cells were termed "super-competitors" since they contained increased levels of *dMYC* which suggested that the relative expression level of *dMyc* determines who is outcompeted (De La Cova et al., 2004; Moreno and Basler, 2004). Other pathways that have been shown to be involved in competition include Ras, Wingless/Wnt, Hippo, and Mahjong, most of which have now been implicated in tumorigenesis (Diaz-Benjumea and Hafen, 1994; Li et al., 2010; Neto-Silva et al., 2010; Pierce et al., 2008; Prober and Edgar, 2000; Tamori and Deng, 2011; Tyler et al., 2007; Vincent et al., 2011; Ziosi et al., 2010).

1.6.2 Cell Competition in cancer

Recent work has suggested that cell competition is highly relevant to the initial stages of tumorigenesis (Baker and Li, 2008; Hogan et al., 2011; Johnston, 2009; Moreno, 2008). During the initial stages of tumorigenesis, mutations can cause aberrant growth or increased survival of mutant cells that need to expand within the tissue.

Nevertheless, most tissues have homeostatic mechanisms in place that allow precise control of cell numbers and tissue size. However, as shown in the previous studies, once a cell acquires particular favorable mutations, it can outcompete surrounding cells, which do not possess these advantageous mutations.

Recent work has shed light on the role of cell competition in both the promotion and suppression of tumorigenesis. Beginning with *dMYC*, several related genes have been shown to be highly relevant to the ability of mutant cells to out compete WT cells and promote tumor formation. Profiling of cells undergoing *Myc* competition revealed that the membrane protein *Flower* and the secreted *SPARC* mediate cell competition (Portela et al., 2010; Rhiner et al., 2010). *Flower* expression is up regulated in some papillomas and *Flower*-null mice have an increased susceptibility to papilloma formation (Petrova et al., 2012). Additionally, *SPARC*'s role in cancer has been known for some time but it seems to be more convoluted since in some cases it promotes cancer while in other cases it suppresses progression (Chlenski and Cohn, 2010; Petrova et al., 2011). Additionally, the recently identified *Hippo-YAP* pathway was discovered to act as a tumor suppressor and regulator of organ size in *Drosophila* over ten years ago (Halder and Johnson, 2011; Pan, 2010; Zhao Li, L., Lei, Q. and Guan, K. L., 2010). In 2007, it was demonstrated that this pathway converges on *Myc* and thus is again related to tumor promoting properties (Neto-Silva et al., 2010; Tyler et al., 2007; Ziosi et al., 2010). Lastly, the *Wnt* pathway has been shown to be involved in carcinomas and colorectal cancers and is known to regulate competition (Torisu et al., 2008; Vincent et al., 2011).

While this data may suggest that it would be difficult to restrain mutant cells during tumorigenesis, there are examples of genes involved in competition that could serve as tumor suppressors in the right context. The most classic example of this is the polarity genes, which included *scribble*, *lethal giant larvae*, *discs large*, and *crumbs*.

Various studies have shown that mutations in these genes allow for over proliferation of cells and tissue structure integrity is lost. However, mosaic animals have shown that when these mutant cells are in a pool of WT cells, they are readily eliminated through apoptosis (Bilder et al., 2000; Brumby and Richardson, 2003; Ellenbroek et al., 2012; Enomoto and Igaki, 2011; Froldi et al., 2010; Igaki et al., 2009; Menéndez et al., 2010; St Johnston and Ahringer, 2010). Surprisingly, while *Ras* has been shown to be a potent oncogene, when surrounded by WT cells, *Ras* mutant cells are extruded from the epithelium through cell death (Hogan et al., 2009; Kajita et al., 2010; Vidal et al., 2006). Lastly, miRNAs secreted from WT prostate cells have been shown to reduce the proliferation rate of prostate cancer cells suggesting that the regulation of cell competition may be mediated through miRNA regulation as well (Chen and Silver, 2012; Kosaka et al., 2012). Thus cell competition, while originally demonstrated in developmental studies of Drosophila, has a more broad applicability to other processes that include tumorigenesis.

1.7 Rationale and Hypothesis

The inability to effectively treat glioma patients creates a need for a better understanding of both the process leading to glioma and also the cellular aspects of tumor cells that are affected following mutations. Our previous data has shown that not only can OPCs serve as the cell origin and also that mutant cells have a limited capacity to differentiate and continually proliferate (Galvao et al., 2014; Liu et al., 2011a). However, how this occurs, when this occurs, and whether targeted therapies against the common pathway mutations in glioma can effectively block OPC transformation remains to be seen. In this thesis project, I sought to understand how *p53* and *NF1* mutations

individually impact PreT-OPC biology, whether these pathways can be targeted for tumor therapy, and what are the downstream effectors of these pathways. In the second part of my thesis project I seek to understand how cell competition plays a role in gliomagenesis and whether this mechanism can be used to design novel anti-tumor therapies.

For the first part of my thesis I hypothesized that *p53* and *NF1* play distinct roles during the progression towards gliomagenesis. Because our previous data that showed that PreT-OPCs have altered self-renewal and differentiation capabilities, I hypothesized that one of these TSGs blocked the self-renewal ability of OPCs and that the other TSG promoted differentiation of OPCs to oligodendrocytes (Figure 1.3). To address this I used a MADM model with either individual *p53* or *NF1* deletion and assayed the changes in cell number, proliferation, and differentiation in addition to the ability of these single mutant OPCs to transform. Secondly, I determined whether the restoration of either TSG could have anti-tumor effects using primary Tumor OPCs (Tu-OPCs) *in vitro*. Third, I analyzed the signaling changes in WT, PreT, and Tu-OPCs downstream of *Ras* to uncover unique signaling activation signatures and finally with these data I determined whether blocking specific pathways could prevent gliomagenesis.

For the second part of my thesis I initially found that while PreT-OPC numbers go dramatically up in number, the overall density of OPCs, regardless of genotype, remain quite steady. From this I hypothesized that during the process of gliomagenesis PreT-OPCs out-compete other OPCs and that this process is necessary for gliomagenesis. To address this I first quantified the relative proportion of WT, heterozygous, and PreT-OPCs in MADM-Tumor mice and compared them to MADM single *p53* KO (MADM-*p53)* and MADM single *NF*1 KO (MADM-*NF1)* mice to determine which gene was responsible for this process. I then generated a new MADM model to try to increase the competitive

fitness of non-GFP+ OPCs. Finally, I show that this cell competition between PreT-OPCs and WT OPCs is vital for OPC transformation.

Figure 1.3 Hypothesis for the role of *p53* and *NF1* during OPC transformation
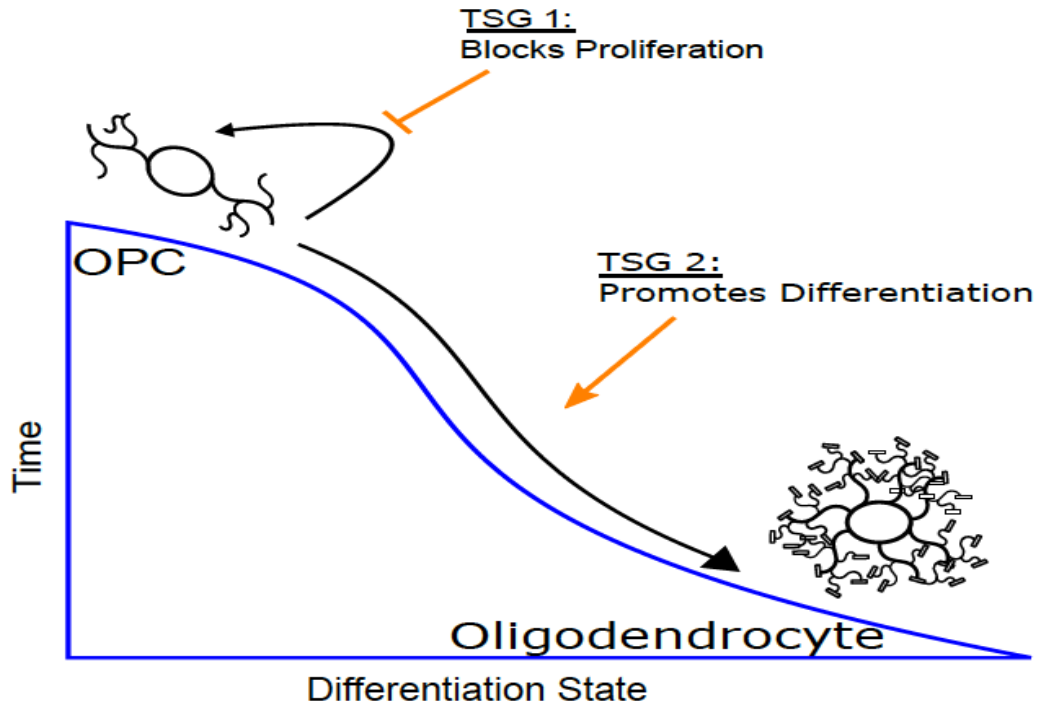
Figure 1.3 Hypothesis for the role of *p53* and *NF1* during OPC transformation

A schematic drawing showing the hypothesis that *p53* and *NF1* play individual roles during OPC transformation. One of the TSGs controls the self-renewal ability of OPCs while the other TSG promotes differentiation. The loss of both TSGs allows PreT-OPCs to continually self-renew while not differentiating into oligodendrocytes.

Chapter 2 Individual roles of p53 and NF1 during the progression towards malignancy in the glioma cell of origin

Introduction

Glioma is the most common primary brain tumor in adults with a high mortality rate due to resistance of glioma cells to traditional therapies and the highly aggressive nature of the tumor cells (Agnihotri et al., 2013; Chen et al., 2012; Chipuk, 2015; Cloughesy et al., 2014; Haar et al., 2012; Lawrence et al., 2012). A majority of glioma patients have only a 15-month median survival time due to the nature of these tumors (Huse and Holland, 2010; Wen and Kesari, 2008). To better understand the molecular mechanisms that lead to gliomagenesis, the Cancer Genome Atlas (TCGA) sequenced a few hundred human GBM samples to find common "core" pathway mutations (Brennan et al., 2013; McLendon et al., 2008). Not surprisingly, they found that the *p53*, *Ras/RTK*, and *RB* pathways are almost always all mutated in patient samples (79%) thereby highlighting the importance of these pathways during gliomagenesis. While other studies have highlighted the roles of these pathways in either tumor suppression or tumor progression, recent work has demonstrated that these pathways are more complex than originally thought in different contexts (Li et al., 2012; Valente et al., 2013b). However, how these pathways drive normal neural cells to malignancy remains unclear with current studies. One potential solution is to identify the cell of origin for glioma, then to study the impact of each mutated pathway on tumor initiation, progression, and transformation.

Unequivocal identification of the cell of origin is generally impossible with patient samples due to significant alterations of cellular morphologies and marker gene

expression in malignant tumor cells and the unavailability of human tissues at pre-transforming stages. Therefore, mouse genetic models have been widely used to pinpoint the glioma cell of origin among all cell types in the brain. While conventional mouse models still cannot reveal pre-malignant mutant cells, our lab uses a mouse genetic system termed MADM (Mosaic Analysis with Double Markers) to circumvent the problem. Through *inter*-chromosomal mitotic recombination, MADM generates mutant (mt) cells labeled with GFP, and its sibling WT cells labeled with RFP (Figure 1.2 in Chapter 1). The sparseness of mutant cells resulted from the low frequency of *inter*-chromosomal recombination not only closely mimics the clonal nature of human cancer, but also allows one to visualize the previously inaccessible tumor initiation and progression stages. Most importantly, the definitive correlation between color and genotype greatly facilitates the revelation of the tumor initiation events based on the increased ratio of green-to-red cell numbers (G/R ratio). In our previous studies, we found that, upon the introduction of *p53*/*NF1* mutations into neural stem cells, cell lineage-specific analysis revealed a dramatic increase of G/R ratio at pre-malignant stage only in oligodendrocyte precursor cells (OPCs) but not in any other brain cell types (Liu et al., 2011b). Along with other evidences, we pinpointed OPC as the cell-of-origin in this model, a finding supported by other studies (Assanah et al., 2006; Galvao et al., 2014; Lindberg et al., 2009, 2014; Persson et al., 2010).

Yet pinpointing the cell of origin still does not address how the deletion of *NF1* and *p53* contribute to OPC malignancy. Therefore, the next important question is how the deletion of *p53* and *NF1* leads to OPC transformation. During normal mouse development, OPCs originate from NSCs embryonically, which continue to proliferate after birth and migrate throughout the brain while differentiating into oligodendrocytes by the weaning age (postnatal day 20, P20). Adult OPCs enter the quiescent stage and

only re-enter cell cycle at a low frequency (Psachoulia et al., 2009; Wolswijk and

Noble, 1989; Young et al., 2013). Based on normal OPC biology, it is conceivable that,

once mutated, either increased proliferation or decreased differentiation of OPCs (or

both) could lead to tumor initiation. Our previous data showed that the concurrent

deletion of *p53* and *NF1* led to both increased proliferation and decreased differentiation

of OPCs, subsequently promoting glioma initiation. However, the individual roles of *p53*

and *NF1* in suppressing gliomagenesis remain unknown. Therefore, in this chapter, we

set out to deconstruct the contribution of individual tumor suppressor gene deletion

during the progression toward gliomagenesis, using the MADM system to delete *p53* or

NF1, respectively. We hypothesized that the loss of p53 and NF1 could play distinct

roles in gliomagenesis. While the loss of one would promote proliferation, the loss of the

other would lead to reduced differentiation, thereby loss of both cooperatively lead to

tumor formation (Figure 1.4 in Chapter 1). In addition to *in vivo* analysis, we also purified

both pre-transforming mutant OPCs (Pre-T OPCs) and malignant tumor cells using the

OPC-specific surface marker PDGFRα, then examined the activities of commonly

studied signaling nodes (Cadinu et al., 2014; Gorgoulis et al., 2005; Maglietta et al.,

2012; Watson et al., 2013). Since NF1 is known as a RasGAP (Klose et al., 1998;

Morcos et al., 1996; Scheffzek et al., 1998; Shin et al., 2012), we focused on analyzing

the downstream effectors of the Ras pathway in this study, specifically on the

progressive activation of these molecules from pre-malignant to malignant stages.

Based on our findings, we hope to develop therapeutic strategies that are tailored to

target malignant tumor cells and pre-transforming mutant cells in a precise fashion to

achieve the best efficacy.

Results

2.1 Establishment of tools and analytical methods for determining individual roles of *p53* and *NF1 in vivo*.

2.1.1 Establishment of MADM models for analyzing the roles of p53 and NF1 in PreT-OPCs.

To investigate the individual roles of *p53* and *NF1* in gliomagenesis, we first needed to establish two MADM models to allow for individual *p53* or *NF1* deletions. By combining the MADM cassettes with either single *NF1* mutant alleles (MADM-*NF1*) or *p53* mutant alleles (MADM-*p53*), we were able to generate mutant GFP+ cells with single *NF1* or *p53* deletions in their respective MADM models and WT RFP+ sibling cells (Figure 2.1). We also analyzed the original MADM tumor model in which GFP+ OPCs are null for both *p53* and *NF1* (MADM-Tumor) and MADM mice with no mutations (MADM-WT) as controls. To delineate the roles of *p53* and *NF1* in OPC transformation we examined four aspects of OPC biology following the deletion of one or both TSGs. First we analyzed how individual TSG deletion affected G/R ratio, which is indicative of mutant cell expansion. We then analyzed whether this effect was due to increases in proliferative rates or the loss of differentiation capability. Lastly, we examined whether single TSG deletion was sufficient for OPC transformation.

2.1.2 Time course analysis and systematic sampling scheme.

Because we have previously shown particular time points are important for the progression of PreT-OPCs in our MADM model, we chose three distinct time points to analyze. We first analyzed postnatal day 10 (P10) when normal OPCs proliferate rapidly during normal development. We then analyzed P60 a time when both WT and PreT-OPCs are mostly quiescent. Lastly we chose P240, since this is when tumors start forming in the MADM-Tumor model as previously shown (Liu et al., 2011b).

To analyze these aspects in a systematic fashion, we sectioned each brain sagitally at 20 μm thickness and performed quantification on 7 sections that are 200 μm apart medialaterally (7 distinct areas per section, Figure 2.2a). To assess the effect of gene deletion on mutant OPC expansion, the total number of GFP+ OPCs were divided by the total number of RFP+ OPCs to give us a G:R ratio (Figure 2.2b). Next, to assess the effect of gene deletion on OPC proliferation, the number of dividing mutant OPCs (BrdU+ GFP+ PDGFRα+) were divided by the total number of mutant OPCs (GFP+ PDGFRα+) (Figure 2.2c). Proliferative rate of WT OPCs was calculated with a similar method by focusing the analysis on RFP+ PDGFRα+ cells (Figure 2.2c). Last, to quantify the effect of gene deletion on the differentiation potential of mutant and WT cells, MADM brains were stained with markers for both OPCs (PDGFRα) and oligodendrocytes (CC1) and the percent of each population within total mutant (GFP+) or WT (RFP+) cells were calculated (Figure 2.2e). The MADM system is unique in that it generates both WT and mt cells at the same time, thus allowing for precise analysis of even subtle changes in mutant cells while having a control within the same animal.

Figure 2.1 Simplified schematic for various MADM models used during this study
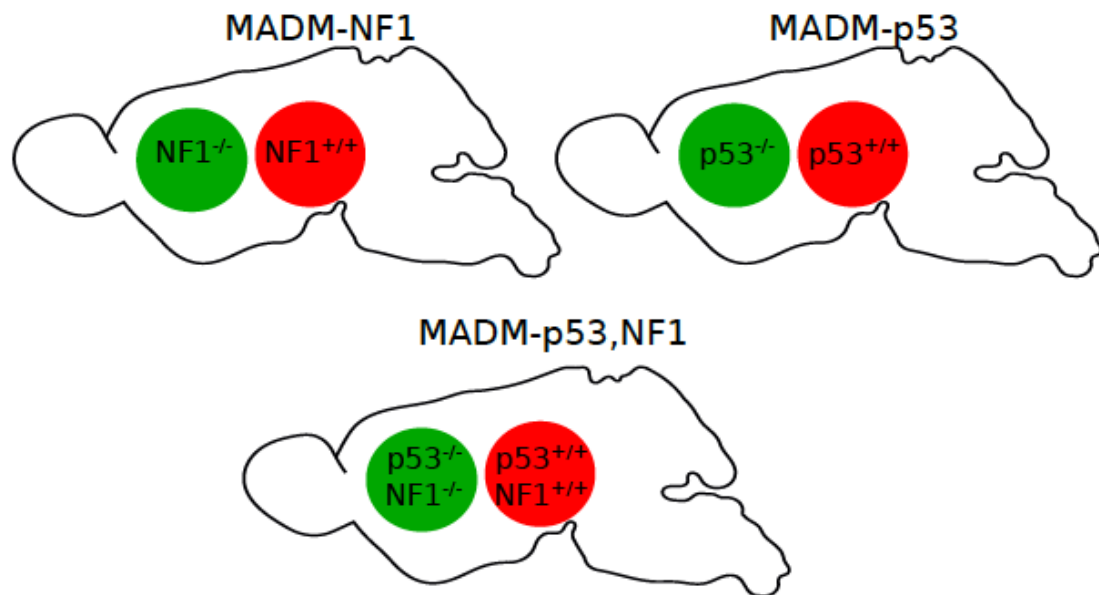
Figure 2.1 Simplified schematic for various MADM models used during this study

Simplified schematics to show the various genotypes of different colored cells within various MADM models. MADM-*NF1* mice have GFP+ *NF1*-null cells and RFP+ WT cells. MADM-*p53* mice have GFP+ *p53*-null cells and RFP+ WT cells. MADM-Tumor mice have GFP+ *p53,NF1*-null cells and RFP+ WT cells. All uncolored OPCs in these systems are heterozygous for the genes that are deleted in GFP+ OPCs.

Figure 2.2 Systematic sampling and quantification examples for determining the role of *p53* and *NF1* during gliomagenesis.
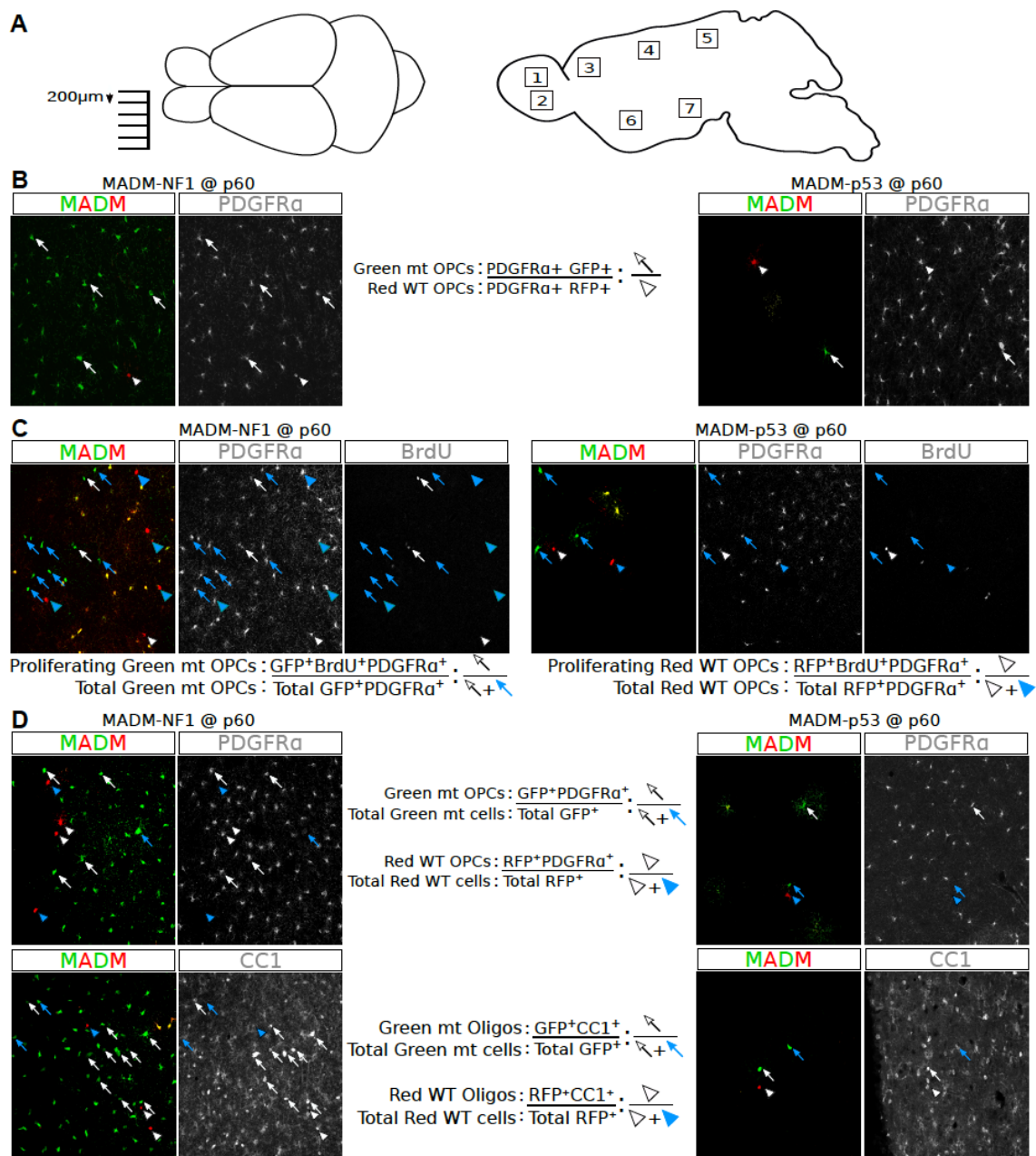
Figure 2.2 Systematic sampling and quantification examples for determining the role of *p53* and *NF1* during gliomagenesis.

(A) Brains were sectioned medialaterally with 200 µm between each slice collected. 6 sections were collected per brain to accurately sample the brain. Within each slice, 7 areas were sampled to ensure thorough sampling of the parenchyma.

(B) To determine the G/R ratio, MADM brains were stained for PDGFRα, GFP, and RFP and the total amount of PDGFRα+, GFP+ OPCs were divided by the total amount of PDGFRα+, RFP+ OPCs.

(C) To calculate the percentage of proliferating OPCs, the total number of GFP+ cells that are BrdU+ and PDGFRα+ are divided by the total number of GFP+ PDGFRα+ cells. The same quantification is done for WT OPCs. The sum of all 42 areas is used to calculate the final percentage of proliferating OPCs in both the WT and mt populations.

(D) To calculate the proportion of OPCs and oligodendrocytes within either the mutant or WT populations, brains are stained for either PDGFRα or CC-1. The total number of GFP+, PDGFRα+ cells is counted and divided by the total GFP+ to determine the relative proportion of OPCs within the mutant population. The sum of all 42 areas is used to calculate the percent of OPCs within the mutant population. The same calculation is done for WT OPCs in addition to using CC1 to determine the proportion of oligodendrocytes within both the WT and mutant populations.

2.2 Deletion of individual TSG led to distinct aberrations of OPCs but did not lead to malignant transformation.

2.2.1 Deletion of NF1 but not p53 is sufficient for an increase in G/R ratio.

First, to assess how each gene mutation contributes to the previously reported pre-malignant expansion of OPCs in the MADM-Tumor model (Liu et al., 2011b), we systematically quantified G/R ratio throughout the brains of MADM-*p53* and MADM-*NF1* models at P10, P60, and P240 (Figure 2.2a). While we expected that deletion of *p53* or *NF1* would each partially contributes to OPC expansion, we were surprised to find that the deletion of *NF1* resulted in a G/R ratio that phenocopied the co-deletion of *p53* and *NF1* at all time points that we examined, while the loss of *p53* had minimal impact (G/R ratio of approximately 1, comparable to MADM-WT mice) (Figure 2.3). This indicates that *NF1* deletion but not *p53* deletion confers mutant OPC growth advantages.

2.2.2 Deletion of NF1 but not p53 is sufficient for an increase in mutant OPC proliferation.

Next we quantitatively measured the proliferative rate of OPCs via BrdU labeling at P10, P60, and P240 (see Materials and Methods for detailed procedures). First, we noticed that the proliferative rate of normal OPCs dramatically decreases after early development, from ~25% in 3 hr time window at P10 to ~0.4% at P60, then to ~0.1% at P240 (Figure 2.4), which matches well with previous independent studies (Stolt et al., 2006; Young et al., 2013). When gliomas form in our model, the proliferative rate returns

to the level of neonatal stage, especially at the tumor edge (Figure 2.4, bottom right).

Furthermore, while *p53*-null OPCs showed no significant difference in proliferative rate

when compared to WT OPCs, *NF1*-null OPCs proliferated at significantly higher rate

than WT counterparts in the MADM-*NF1* model, comparable to *p53,NF1*-null OPCs (Fig.

2.4). Interestingly, in both MADM-*NF1* and MADM-Tumor models, the proliferative rate

of WT cells appeared to be suppressed to a level lower than those in WT or MADM-*p53*

brains, which eventually became undetectable at P240 (Figure 2.4, red asterisk),

suggesting possible non-cell autonomous suppression from *NF1*-null or *p53,NF1*-null

OPCs toward their WT counterparts in the same brain. These findings demonstrated that

the *NF1* deletion but not *p53* deletion led to enhanced proliferation of mutant OPCs.

2.2.3 Deletion of NF1 but not p53 is sufficient for a decrease in OPC differentiation.

To evaluate the differentiating potential of OPCs in each mouse model, we

immunostained brain sections with markers specifically for OPCs (PDGFRα) and

oligodendrocytes (CC1), and quantified the percentage of both cell types within either

the mutant or WT populations (Figure 2.5). While *p53* deletion showed little effect, the

deletion of *NF1* led to a nearly 1.5-fold increase (p<0.001) in OPC composition and a

50% reduction in oligodendrocyte composition (p<0.001) (Fig 2.5), replicating the

observations in the MADM-Tumor model. These data suggest that the loss of *NF1* but

not *p53* lead to a decrease in differentiation potentials of mutant OPCs.

2.2.4 Deletion of NF1 or p53 individually is not sufficient for gliomagenesis.

Our data so far showed that, while the *NF1*-null OPCs recapitulated *p53,NF1*-null OPCs in every aspect including massive cell number expansion, increased proliferation and compromised differentiation, *p53* deletion seemed to lead to no effect whatsoever. Therefore, we dissected mice of all three models at the tumor latency age of the MADM-Tumor model to see if MADM-*NF1* model would generate gliomas as MADM-Tumor model does. While it was expected that we didn't find tumors in the MADM-*p53* model, surprisingly we found no glioma in all 18 MADM-*NF1* mice examined despite massive expansion of mutant OPCs in the entire brain of these mice (Figure 2.6). This finding suggests that the over-expansion of mutant OPCs caused by *NF1* deletion is insufficient for malignant transformation, and that *p53* is a critical gatekeeper to prevent tumor formation.

Figure 2.3 Deletion of *NF1* but not *p53* is sufficient for mutant OPC expansion.
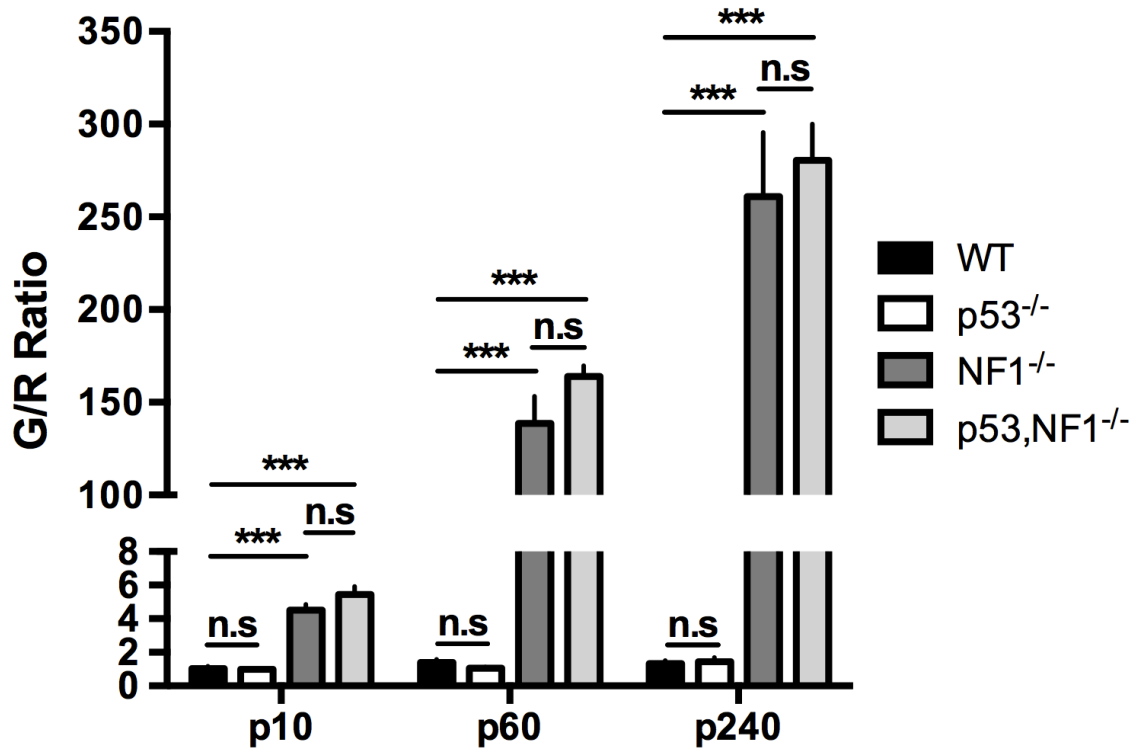
Figure 2.3 Deletion of *NF1* but not *p53* is sufficient for mutant OPC expansion.

GFP+ and RFP+ OPCs were quantified in the aforementioned areas of the brain that were analyzed. Quantification of total GFP+ mutant OPCs/RFP+ WT OPCs at early (P10), pre-transforming (P60), and tumor ages (P240) shows that the deletion of *NF1*, but not *p53* leads to massive over-expansion of mutant OPCs comparable to *p53,NF1-*null OPCs. (n>10) Student *t* Test; Error Bar ± SEM (*** *P* < 0.001)

Figure 2.4 Deletion of *NF1* but not *p53* is sufficient for increased mutant OPC proliferation.
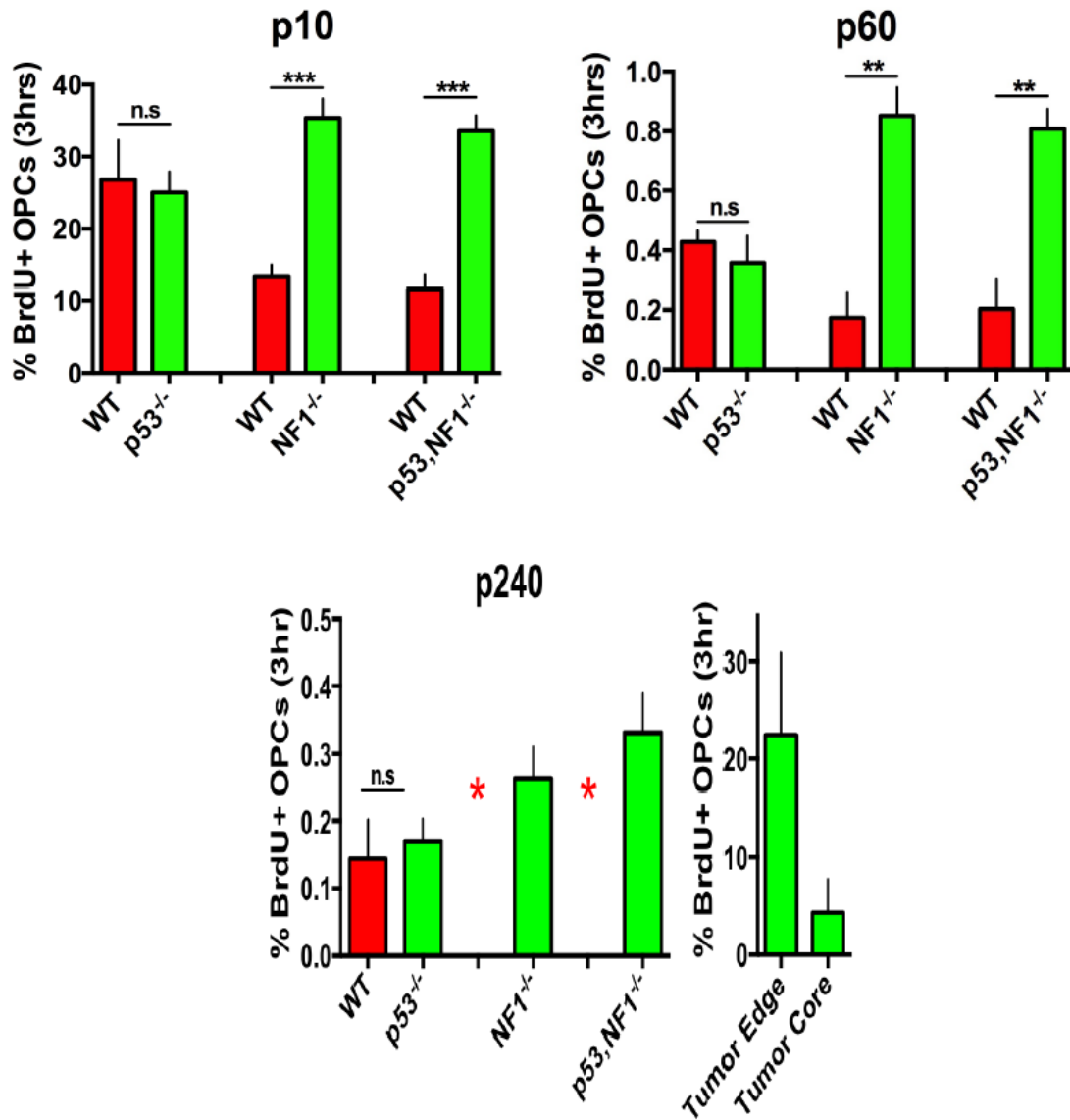
Figure 2.4 Deletion of *NF1* but not *p53* is sufficient for increased mutant OPC proliferation.

The percent of BrdU+, GFP+ OPCs was compared to the percent of BrdU+, RFP+ OPCs following either a 3 hr (P10) or 4 day (P60 and P240) BrdU pulse. At P10 and P60, the deletion of *NF1* but not *p53* leads to a significant increase in the percent of GFP+ OPCs compared to WT OPCs. The proliferative rate is comparable between *NF1*-null and *p53,NF1*-null OPCs, suggesting *NF1* deletion is solely responsible for this phenotype. At P240 WT OPC numbers are too low in MADM-*NF1* and MADM-Tumor models to accurately quantify proliferation rate (marked as red asterisk). Tumor areas show comparable levels of proliferation as perinatal OPCs. (n>10) Student *t* Test; Error Bar ± SEM (** *P* < 0.005, *** *P* < 0.001)

Figure 2.5 Deletion of *NF1* but not *p53* is sufficient for the loss of OPC differentiation.
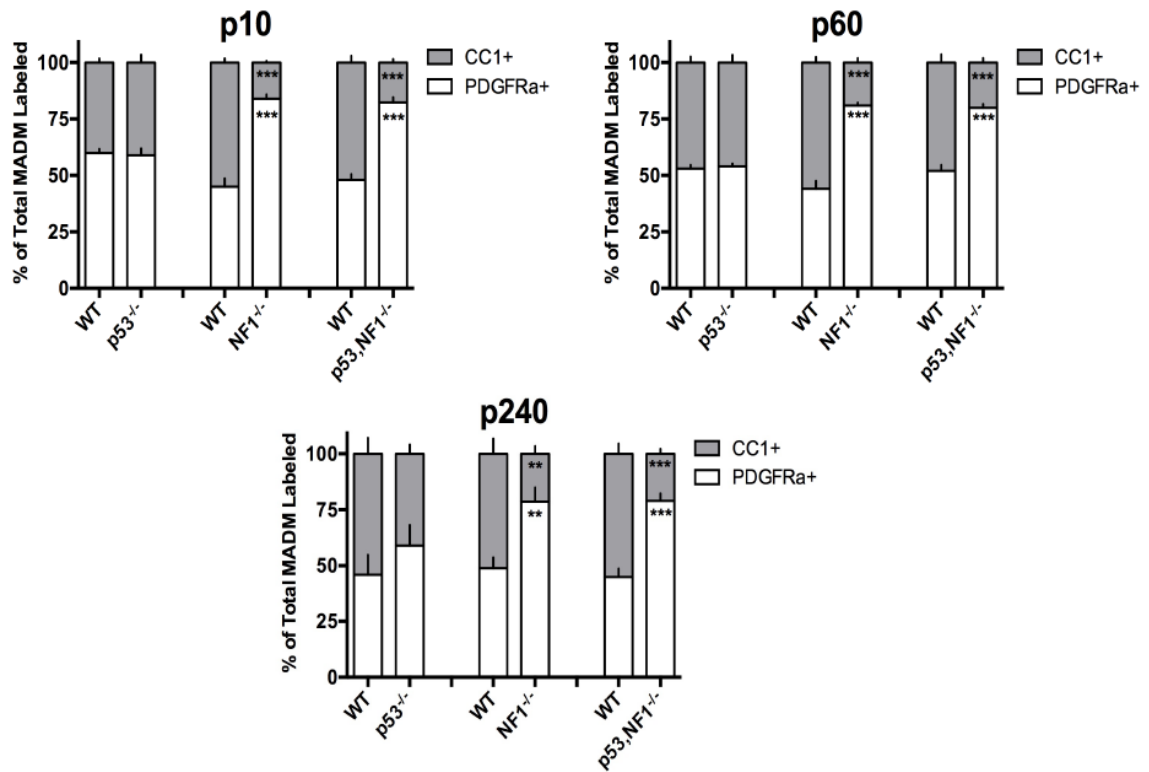
Figure 2.5 Deletion of *NF1* but not *p53* is sufficient for the loss of OPC differentiation.

Brains were analyzed at P10, P60, and P240 for differentiation status using either an OPC (PDGFRα) or an oligodendrocyte (CC1) marker. At all ages, the deletion of *NF1* but not *p53* leads to a significant increase in the percent of GFP+ OPCs while also leading to a significant decrease in GFP+ oligodendrocytes. Differentiation status is comparable between *NF1*-null and *p53,NF1*-null cells, suggesting that *NF1* deletion alone is sufficient for the defects in differentiation. (n>10) Student *t* Test; Error Bar ± SEM (** *P* < 0.005, *** *P* < 0.001)

Figure 2.6 Individual deletions of *NF1* and *p53* is not sufficient for gliomagenesis.
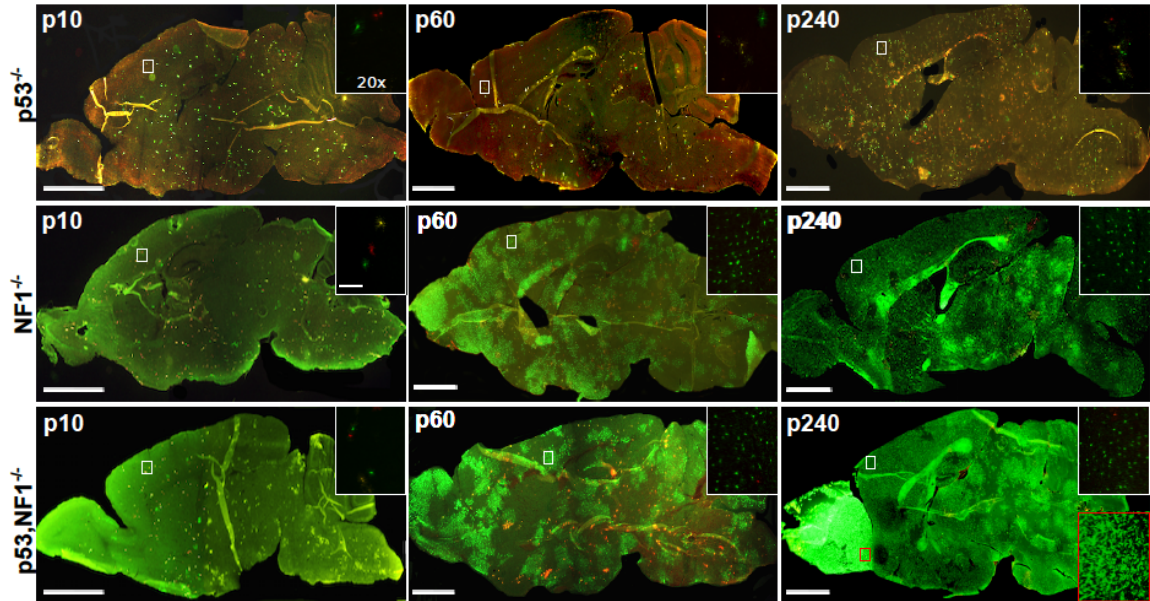
Figure 2.6 Individual deletions of *NF1* and *p53* is not sufficient for gliomagenesis.

Representative whole brain images show that while there is no obvious increase in GFP+ OPCs in MADM-*p53* brains, the deletion of *NF1* leads to a similar increase in GFP+ OPC expansion at P60 and P240. However, the single deletion of either *p53* or *NF1* alone is not sufficient for gliomagenesis despite *NF1* deletion altering cell number, proliferation, and differentiation. Insets show MADM staining in the anterior cortex (n>10) (Scale bar 2 mM; Inset 50 µM)

2.2.5 Deletion of NF1 leads to increased p53 activity in OPCs including senescence in vitro.

Since *p53* deletion didn't lead to any aberrations in OPC proliferation and differentiation but is needed for *NF1*-null OPCs to transform, we hypothesized that *p53* could exert tumor-suppressing activity through promoting apoptosis and/or senescence. To test this hypothesis, we first examined the level of known *p53*-target genes involved in apoptosis and senescence using qRT-PCR to compare purified and cultured *NF1*-null OPCs with *p53,NF1*-null OPCs. We found that *NF1*-null OPCs exhibited significantly higher expression level of *p21*, *Bax*, *PUMA* (Figure 2.7a) Second, we used β-Gal staining to assess cellular senescence in cultured cells and found increased senescence in *NF1*-null OPCs comparison to *p53,NF1*-null OPCs (Figure 2.7b,c) This finding concurs with previous work showing that over-active *Ras* signaling in OPCs leads to *p53*-dependent senescence (Lloyd and Raff, 2001). All these data suggest that loss of *p53* most likely promotes gliomagenesis by allowing OPCs to escape apoptosis and senescence triggered by oncogenic stresses induced by *NF1* deletion.

Figure 2.7 Deletion of *p53* leads to transcriptional activation of *p53* targets and decreased mutant OPC senescence.
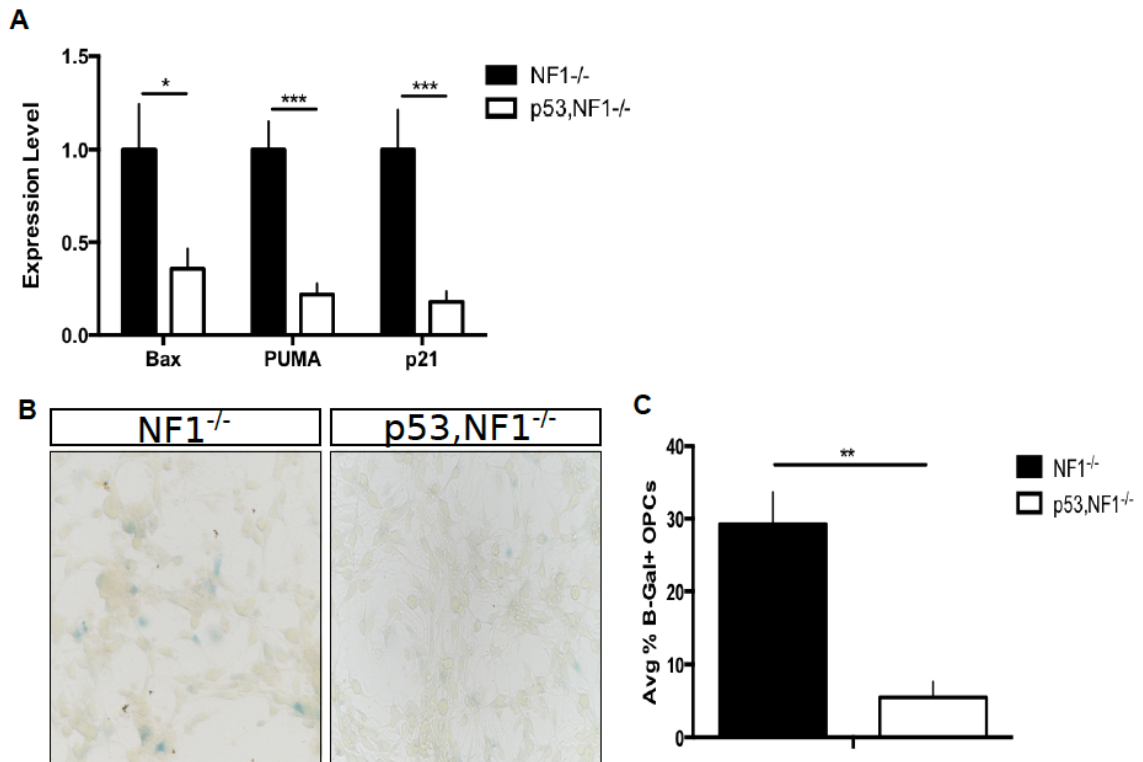
Figure 2.7 Deletion of *p53* leads to transcriptional activation of *p53* targets and decreased mutant OPC senescence

(A) Single *NF1*-null OPCs and double *p53,NF1*-null OPCs were purified and the expression level (RNA) of known *p53* targets *Bax*, *PUMA*, and *p21* were all significantly down-regulated in *p53,NF1*-null OPCs compared to *NF1*-null OPCs.

(B) *NF1*-null OPCs and *p53,NF1*-null OPCs were purified and grown in vitro for 5 days. Following the 5 days, OPCs were stained with β-Galactosidase to determine the percent of senescent OPCs. *NF1*-null OPCs display increased β-Galactosidase expression while cultured *in vitro* compared to *p53,NF1*-null OPCs.

(C) Quantification showing that *NF1*-null OPCs have a significantly increased expression of β-Galactosidase while cultured in vitro compared to *p53,NF1*-null OPCs.

Student *t* Test; Error Bar ± SD (* $P < 0.05$, ** $P < 0.005$, *** $P < 0.001$)

2.3 Restoration of *p53* or *NF1* in Tu-OPCs exerts tumor suppressor functions.

2.3.1 Restoration of p53 in Tu-OPCs is sufficient for Tu-OPC cell cycle arrest and cell death.

While we have shown that the deletion of *p53* is vital for OPC transformation, we next wanted to determine if the restoration of *p53* in Tu-OPCs could have anti-tumor effects. Tu-OPCs were infected with adenovirus expressing GFP, or WT *p53*, or R175H mutant *p53*, respectively. While the infection rate is similar among three types of viruses (Figure 2.8), after 48 hrs, over-expression of WT *p53* led to a 3-fold decrease in the total number of GFP+ infected cells when compared to both GFP and R175H-*p53* infected cells (Figure 2.9a,b) Treatment of R175H-*p53* infected cells with a small molecule PRIMA-1, previously reported to restore DNA binding activity of the R175H-*p53* mutant (Lambert et al., 2009), also led to a significant decrease of cell numbers. These findings suggest that *p53* restoration is sufficient for tumor blockade.

To confirm restoration of *p53* function, we analyzed expression levels of known transcriptional targets of *p53*. 18 hrs post-infection *Bax*, *PUMA*, and *p21* transcript levels significantly increased in cells over-expressing WT *p53* ($p<0.05$) or R175H-*p53*+PRIMA-1 ($p<0.05$) but not those over-expressing GFP or R175H-*p53* (Figure 2.10a). To test whether the decrease in Tu-OPCs infected with WT *p53* was due to cell cycle arrest or cell death, we used FACS to analyze the cell cycle profiles based on DNA content and to quantify apoptotic cells based on Propidium Iodide incorporation. 48 hrs post-infection both WT *p53* and R175H-*p53*+PRIMA-1 infected OPCs showed significant G1 arrest in the cell cycle (Figure 2.10b) as well as increased cell death (Figure 2.10c) in comparison to GFP or R175H-*p53* expressing cells.

Finally, to examine the human relevance of our findings, we repeated the experiments in human glioma cell line, LNZ -308. Cells were infected with GFP, WT *p53*, R175H-*p53*, and R175H-*p53*+PRIMA-1 and assayed for cell survival 48 hrs after infection. Similar to our Tu-OPCs, LNZ-308 cells exhibited a 3-fold increase in cell death in both WT *p53* and R175H-*p53*+PRIMA-1 infected cells but no change in cell death in both GFP and R175H-*p53* infected cells (Figure 2.11). These results along with data from the previous section demonstrate that *p53* is not only a critical blocker for gliomagenesis, but also a promising target for glioma therapy (see Discussion for more details).

Figure 2.8 The rate of infection between Tu-OPCs with GFP, WT *p53*, and R175H
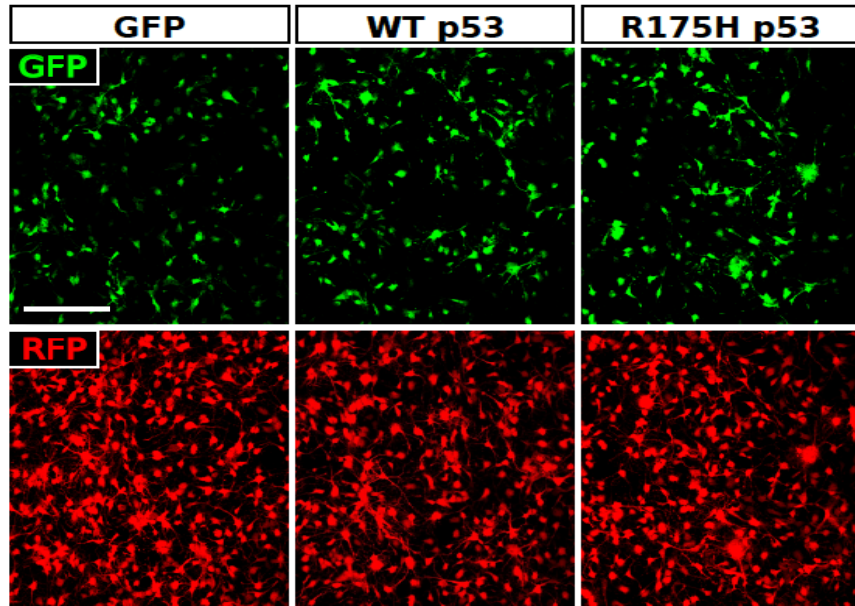
p53 is equal.

Figure 2.8 The rate of infection between Tu-OPCs with GFP, WT *p53*, and R175H *p53* is equal.

Tu-OPCs were infected with GFP, WT *p53*, or R175H *p53* viruses and analyzed for GFP expression 24hrs after infection. The infection rate between all the viruses is equal as seen by the number of GFP+ Tu-OPCs in all three groups. (n=3) (Scale bar 150 µm)

Figure 2.9 Infection of Tu-OPCs with WT *p53* causes a decrease in GFP+ OPCs.
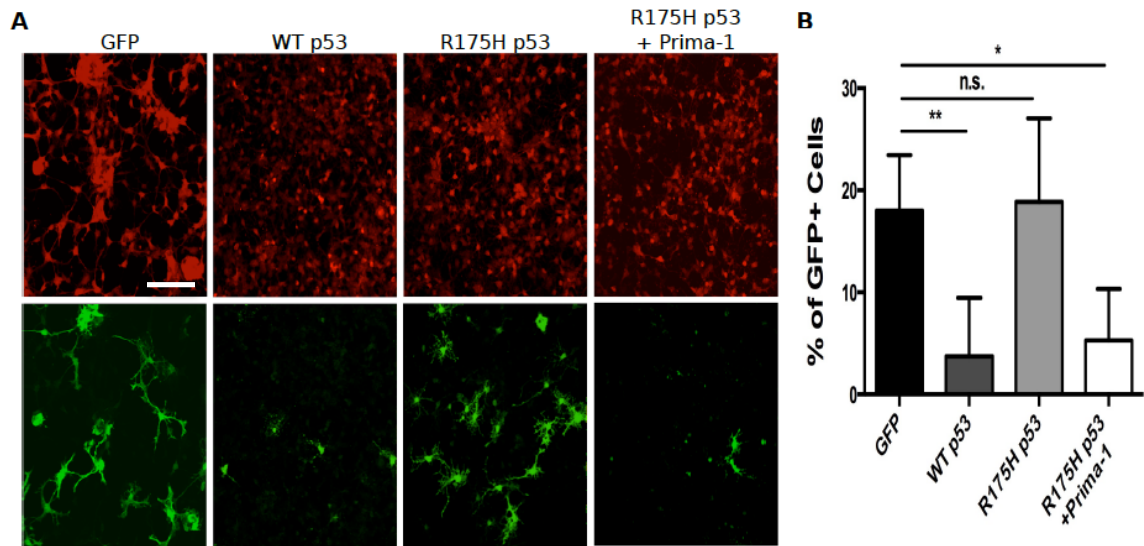
Figure 2.9 Infection of Tu-OPCs with WT *p53* causes a decrease in GFP+ OPCs.

(A) 48hrs after initial infection, the percent of GFP+ Tu-OPCs infected with WT *p53* has significantly decreased compared to GFP control. Following the restoration of R175H *p53* function using Prima-1, the percent of GFP+ Tu-OPCs has also significantly decreased compared to GFP control while R175H p*53* infected Tu-OPCs show no significant change in the percent of GFP+ Tu-OPCs.

(B) Quantification of the decrease in GFP+ Tu-OPCs after WT *p53* or R175H *p53* +Prima-1 restoration compared to GFP control. (n=3) Student *t* Test; Error Bar ± SD (* $P < .05$, ** $P < 0.005$) (Scale bar 150 µm)

Figure 2.10 Restoration of *p53* causes increases in *p53* target gene expression, cell

cycle arrest and cell death in Tu-OPCs.
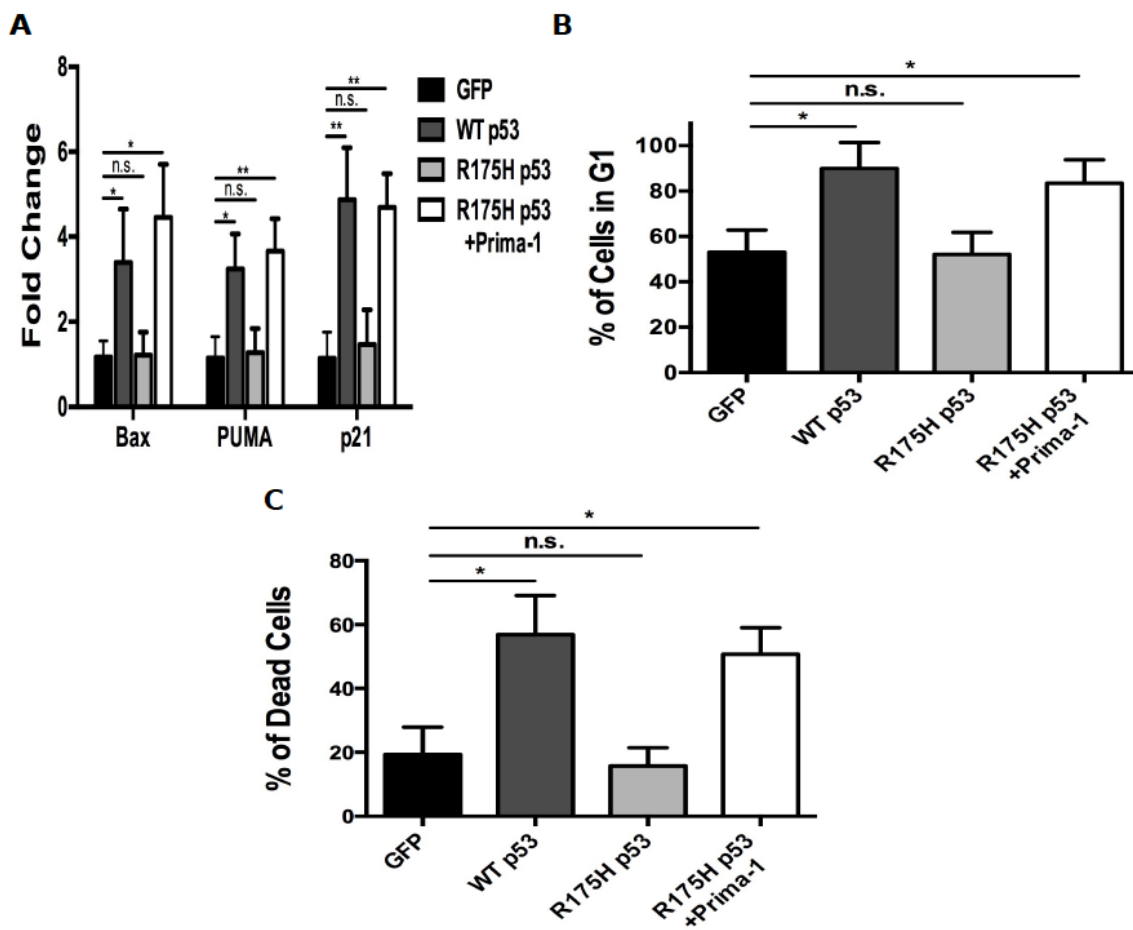
Figure 2.10 Restoration of *p53* is sufficient for increases in *p53* target gene expression, cell cycle arrest and cell death in Tu-OPCs.

(A) 48hrs after infection or treatment with Prima-1, the transcriptional activity of known *p53* targets were analyzed. Following the infection of WT *p53* or the restoration of R175H *p53* with Prima-1, there was significant up regulation of *Bax*, *PUMA*, and *p21* transcripts compared to GFP control. The infection of Tu-OPCs with R175H *p53* alone had no significant effect on transcript levels of all three genes.

(B) 48 hrs after infection, cell-cycle analysis was performed on Tu-OPCs. WT *p53* and R175H p53+Prima-1 infected cells had a significant increase in the percent of cells in G1 compared to GFP control. Tu-OPCs infected with R175H *p53* alone had no significant change in the percent of Tu-OPCs in G1.

(C) 48 hrs after infection, Tu-OPCs were analyzed for cell death. WT *p53* and R175H p53+Prima-1 infected cells had a significant increase in the percent of dead cells compared to GFP control. Tu-OPCs infected with R175H *p53* alone had no significant change in the percent of dead Tu-OPCs. (n=3) Student *t* Test; Error Bar ± SD (* $P < .05$, ** $P < 0.005$)

Figure 2.11 Restoration of *p53* is sufficient for cell death in human glioma cells.
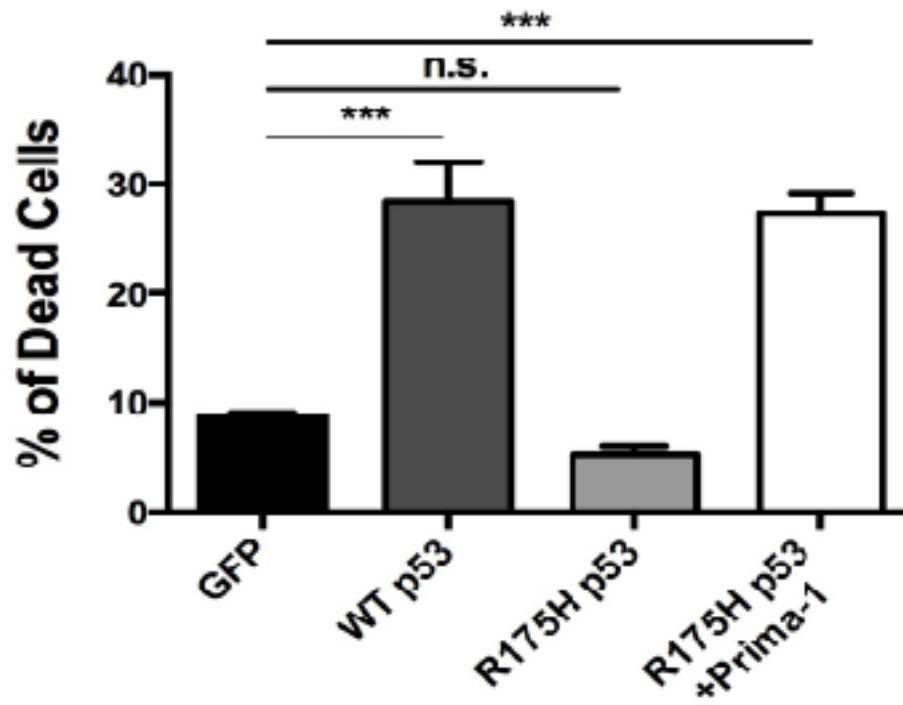
Figure 2.11 Restoration of *p53* is sufficient for cell death in human glioma cells.

LNZ-308 tumor cells, a human glioma cell line, were infected with GFP, WT *p53*, or R175H *p53* viruses and assayed for cell death after 48hrs. R175H *p53* infected tumor cells were also treated with Prima-1 to restore *p53* function in a fourth group. The infection of tumor cells with WT *p53* or R175H p*53*+Prima-1 led to a significant increase in the percent of cell death compared to GFP control or R175H *p53* alone. (n=3) Student *t* Test; Error Bar ± SD (*** *P* < 0.001)

2.3.2 Restoration of the NF1 GAP domain inhibits Tu-OPC proliferation while promoting differentiation.

Since we have shown that the deletion of *NF1* in OPCs leads to increased proliferation and decreased differentiation long before malignant transformation, next we determined whether the restoration of *NF1* could reverse these tumor-initiating activities. Because full-length *NF1* is a large protein that cannot be readily packaged into viral vectors, we focused on the *Ras*-GAP portion of the *NF1* protein since many previous studies have shown that the main function of *NF1* is to act as a GAP to inhibit *Ras* activity. Since tumor-inhibiting activity of *NF1*-GAP could kill infected tumor cells, we constructed lentiviral vectors with a dual-promoter system to allow the visualization of infection rate via GFP expression before the induced expression of NF1-GAP (Figure 2.12a). 48 hrs after infection, OPCs were treated with Doxycycline to induce expression of *NF1*-GAP (Figure 2.12b, time 0) and then assayed 2 days later for proliferation and 5 days later for differentiation (Figure 2.12b).

While the infection rate was equivalent among all control and experimental viruses the abundance of WT *NF1*-GAP infected Tu-OPCs gradually decreased after 2- and 5-days of Dox induction but both mock and mt *NF1*-GAP infected cells remained steady (Figure 2.13). Using EdU labeling as the S phase marker, we found that WT *NF1*-GAP expressing OPCs showed a much lower proliferative rate in comparison to mock and mt *NF1*-GAP infected cells (Figure 2.14a,b). Additionally, when infected OPCs were analyzed after 5 days post induction, while mock and mt *NF1*-GAP infected OPCs had little morphological changes, WT *NF1*-GAP infected OPCs showed greatly increased ramifications, indicative of oligodendrocyte maturation. To confirm this notion, we stained these cells with oligodendrocyte marker MBP and found that restoration of WT *NF1*-GAP

in Tu-OPCs can promote the differentiation of Tu-OPCs into oligodendrocytes (Figure

2.15a,b). Taking together, the restoration of WT *NF1*-GAP is sufficient to inhibit Tu-OPC

proliferation as well as to promote OPC differentiation.

Figure 2.12 Schematic of Lentiviral constructs and timeline for testing the effect of NF1-GAP restoration in Tu-OPCs.

A

B
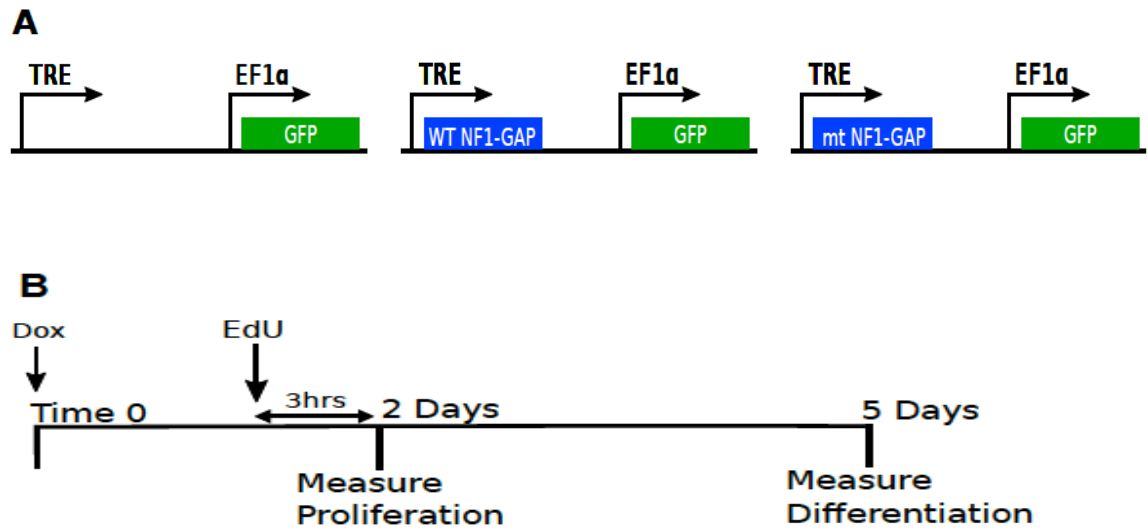
Figure 2.12 Schematic of Lentiviral constructs and timeline for testing the effect of *NF1*-GAP restoration in Tu-OPCs.

(A) Plasmid design of Mock-GFP, WT *NF1*-GAP, and mutant (mt) *NF1*-GAP vectors. GFP expression is controlled independently of NF1-GAP domain expression, which is induced following Doxycycline treatment.

(B) Timeline schematic for determining the effect of *NF1*-GAP restoration in Tu-OPCs. Cells are treated with Doxycycline to induce expression of GAP domain at Time 0. 2 days after the initial Doxycycline treatment, Tu-OPCs are treated with edU for 3 hrs to measure the effect the various plasmids have on Tu-OPC proliferation. Following 5 days of GAP expression, the effect of the GAP domain on Tu-OPC differentiation is determined by immuno-staining cells for *MBP*, a mature oligodendrocyte marker.

Figure 2.13 Restoration of WT *NF1*-GAP is sufficient to cause a gradual decrease in

GFP+ Tu-OPCs after 48 hrs and 5 days.
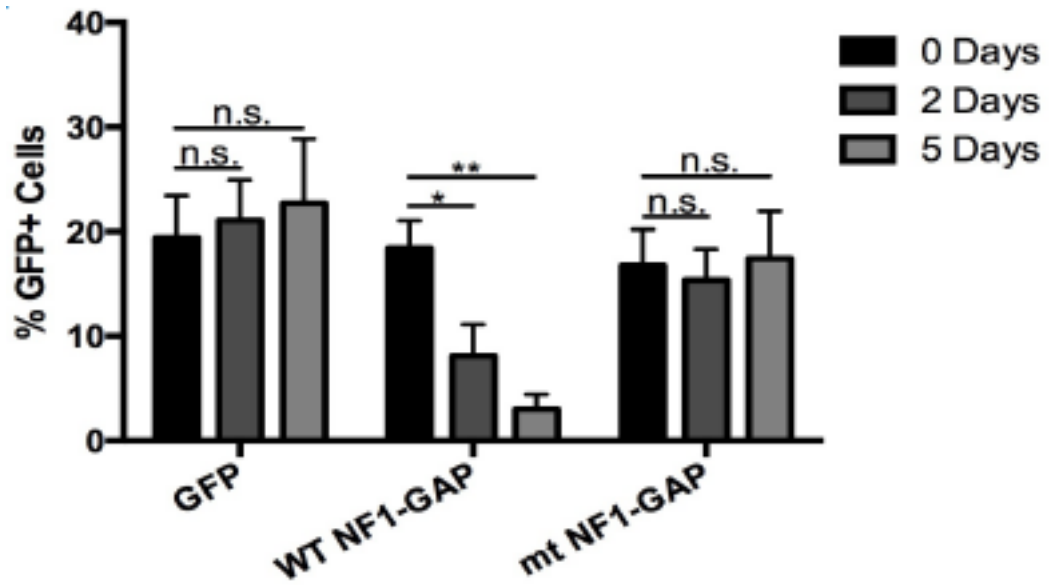
Figure 2.13 Restoration of WT *NF1*-GAP is sufficient to cause a gradual decrease in GFP+ Tu-OPCs after 48 hrs and 5 days.

2 and 5 days after infection of Tu-OPCs with WT *NF1*-GAP, the percent of GFP+ Tu-OPCs significantly decreased at both time points compared to Mock-GFP control infected Tu-OPCs. However, the percent of GFP+ Tu-OPCs infected with mt *NF1*-GAP did not significantly change compared to Mock-GFP control at both time points. (n=3) Student *t* Test; Error Bar ± SD (* P < .05, ** P < 0.005)

Figure 2.14 Restoration of WT *NF1*-GAP is sufficient to cause a decrease in Tu-OPC
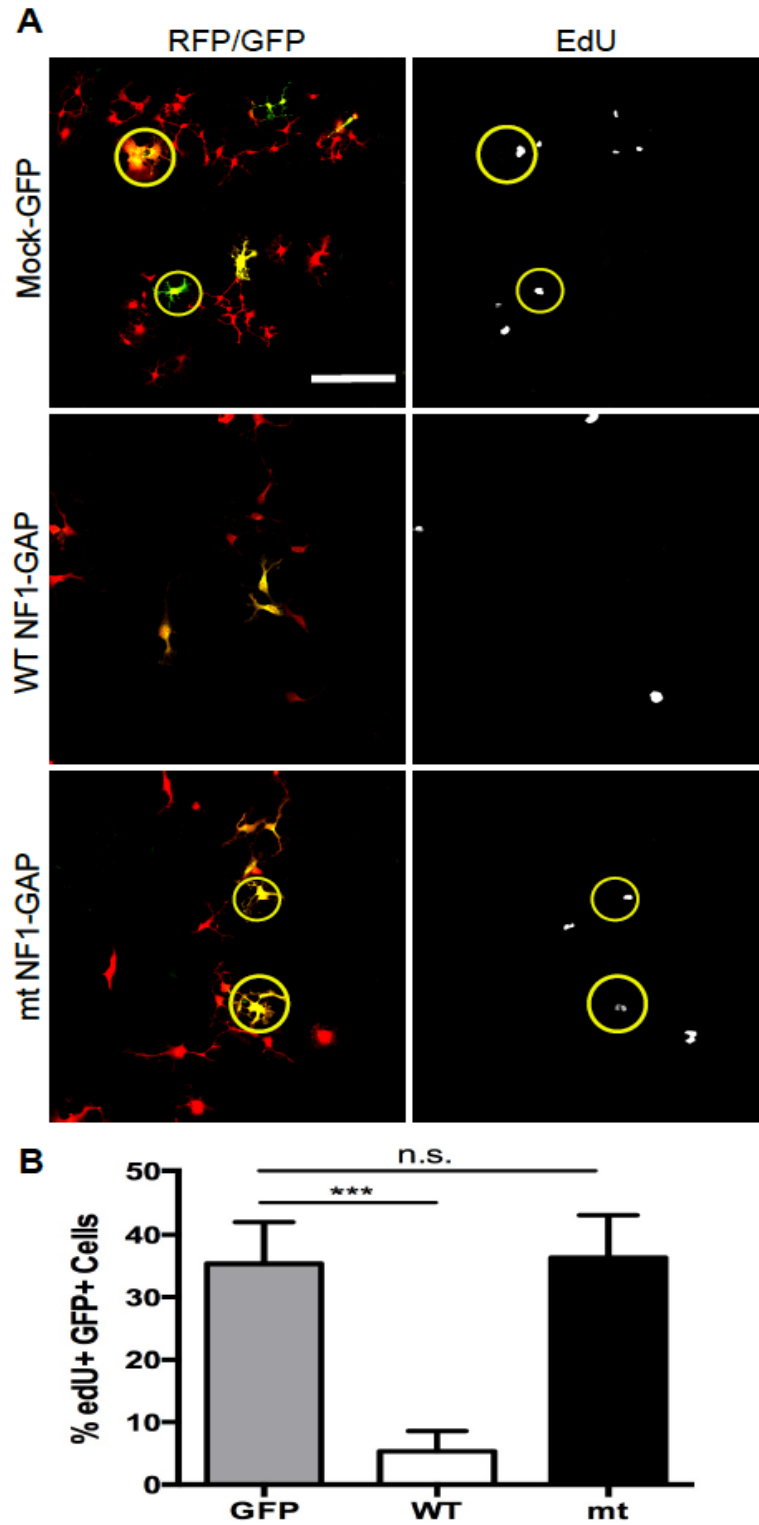
proliferation.

Figure 2.14 Restoration of WT *NF1*-GAP is sufficient to cause a decrease in Tu-OPC proliferation.

(A) Following 2 days of *NF1*-GAP restoration, Tu-OPCs were pulsed with EdU to determine the effect of restoration on Tu-OPC proliferation. While mt *NF1*-GAP infected Tu-OPCs showed no significant change in the amount of EdU+ Tu-OPCs compared to Mock-GFP control, WT *NF*1-GAP infected Tu-OPCs had a significant reduction in the amount of EdU+ Tu-OPCs.

(B) Quantification of the percent of EdU+, GFP+ Tu-OPCs in Mock-GFP, WT NF1-GAP, and mt NF1-GAP infected cells. WT NF1-GAP infected cells had a significantly lower percent of EdU+, GFP+ Tu-OPCs compared to Mock-GFP while mt NF1-GAP infected cells had no significant change in the percent of EdU+, GFP+ Tu-OPCs. Student *t* Test; Error Bar ± SD (*** $P < 0.001$) (Scale bar, 100µM)

Figure 2.15 Restoration of WT *NF1*-GAP is sufficient to cause an increase in Tu-OPC
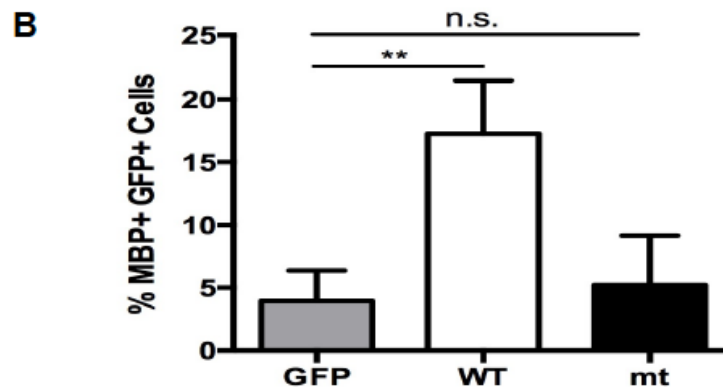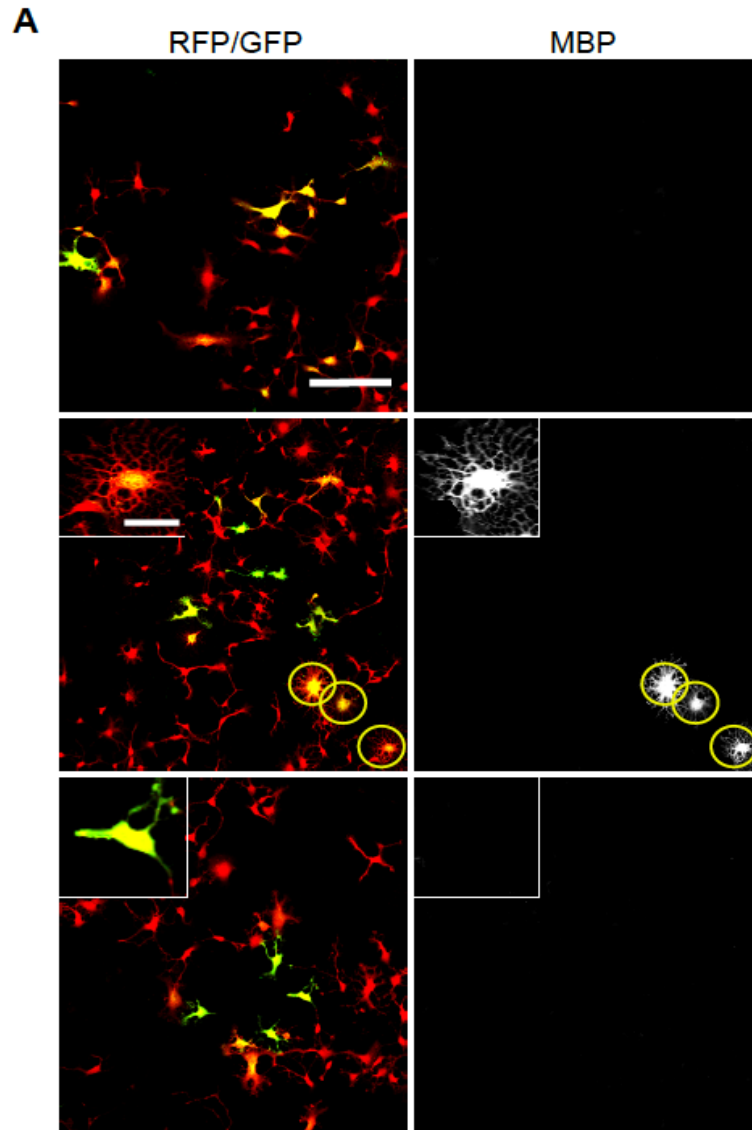
differentiation.

Figure 2.15 Restoration of WT *NF1*-GAP is sufficient to cause an increase in Tu-OPC

differentiation.

(A) 5 days after restoration of WT *NF1*-GAP but not Mock-GFP or mt *NF1*-GAP, Tu-

OPCs have developed oligodendrocyte morphology and started to express MBP, a

known oligodendrocyte marker. Inset shows the morphological differences between WT

and mt *NF1*-GAP expressing cells. Note the ramified processes and web-like

appearance of MBP+ oligodendrocytes.

(B) Quantification of the percent of MBP+, GFP+ Tu-OPCs in Mock-GFP, WT *NF1*-GAP,

and mt *NF1*-GAP infected cells. WT *NF1*-GAP infected cells had a significantly higher

percent of MBP+, GFP+ Tu-OPCs compared to Mock-GFP while mt *NF1*-GAP infected

cells had no significant change in the percent of MBP+, GFP+ Tu-OPCs. Student *t* Test;

Error Bar ± SD (** *P* < 0.005) (Scale bar, 100 µM; inset, 25 µM)

2.4 Signaling analysis reveals *mTOR* is activated in fully transformed but not pre-transforming mutant OPCs.

2.4.1 Following NF1 deletion, mTOR activity remains at basal levels until OPC transformation.

To better understand which signaling pathways may be critical for the initial expansion and malignant transformation of OPCs, we analyzed the signaling transducers in the *Ras* pathway, including *ERK*, *AKT*, and *mTOR* (Figure 2.16). We purified WT, pre-transforming OPCs (PreT-OPCs), and tumor OPCs (Tu-OPCs) by immunopanning and analyzed the levels of phosphorylated (p) ERK, AKT, S6K, and 4EBP1 by western blot. Interestingly, while increased phosphorylation of all effectors was found in Tu-OPCs compared to WT OPCs, moderately increased pERK and pAKT but not pS6K or p4EBP1 was seen in PreT-OPCs. This result suggests that while moderate activation of *ERK* and *AKT* could be responsible for the initial expansion of PreT-OPCs, *mTOR* activation only occurs after the transformation of OPCs (Figure 2.17).

2.4.2 PreT-OPCs have decreased sensitivity to mTOR inhibition.

It should be noted that, because WT OPC control used in this assay were purified from neonatal brains and has baseline *mTOR* activity, the lack of increase of *mTOR* activity in PreT-OPCs does not directly prove that *mTOR* is specifically involved in malignant transformation but not initial expansion. Therefore to test this functionally, we treated PreT-OPCS and Tu-OPCs with mTORC1 inhibitor Temsirolimus to determine

whether they respond differently. *MEK* and *AKT* inhibitors were used as controls since we predict both PreT-OPCS and Tu-OPCs would respond robustly since they had increased activities in both cells. Data from cell viability assays showed that, while the killing curve of PreT-OPCS and Tu-OPCs mostly overlap with *MEK* and *AKT* inhibitors, Tu-OPCs were much more sensitive to Temsirolimus than PreT-OPCs were (Figure 2.18). This further suggests that elevated *mTOR* activity is critical for Tu-OPCs, and its activation may be a driver event for the transformation of PreT-OPCs into Tu-OPCs.

Figure 2.16 Canonical *Ras* signaling pathway.
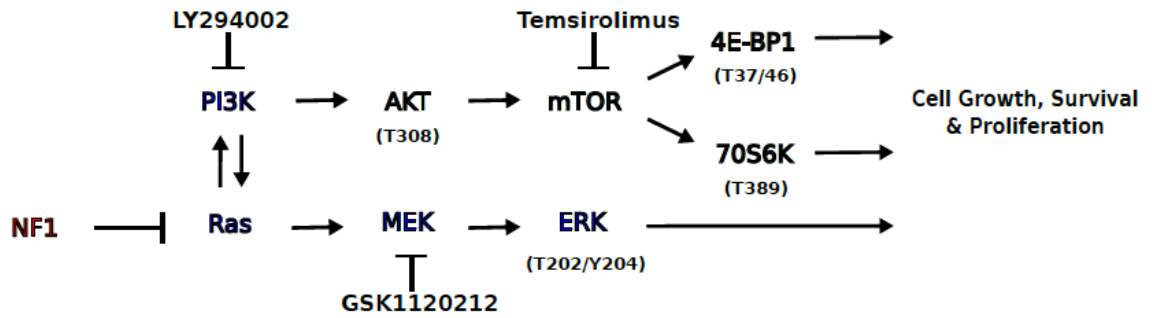
Figure 2.16 Canonical *Ras* signaling pathway.

Ras signaling pathway through *PI3K* and *MAPK*. Phosphorylation sites for activation through specific pathways are shown. Also included are known inhibitors of the Ras signaling pathway including LY294002, a *PI3K* inhibitor, GSK1120212, a *MEK* inhibitor, and Temsirolimus, an *mTOR* inhibitor.

Figure 2.17 *NF1* deletion leads to increased *AKT* and *ERK* activity in PreT-OPCs while *mTOR* activity remains basal until OPC transformation.
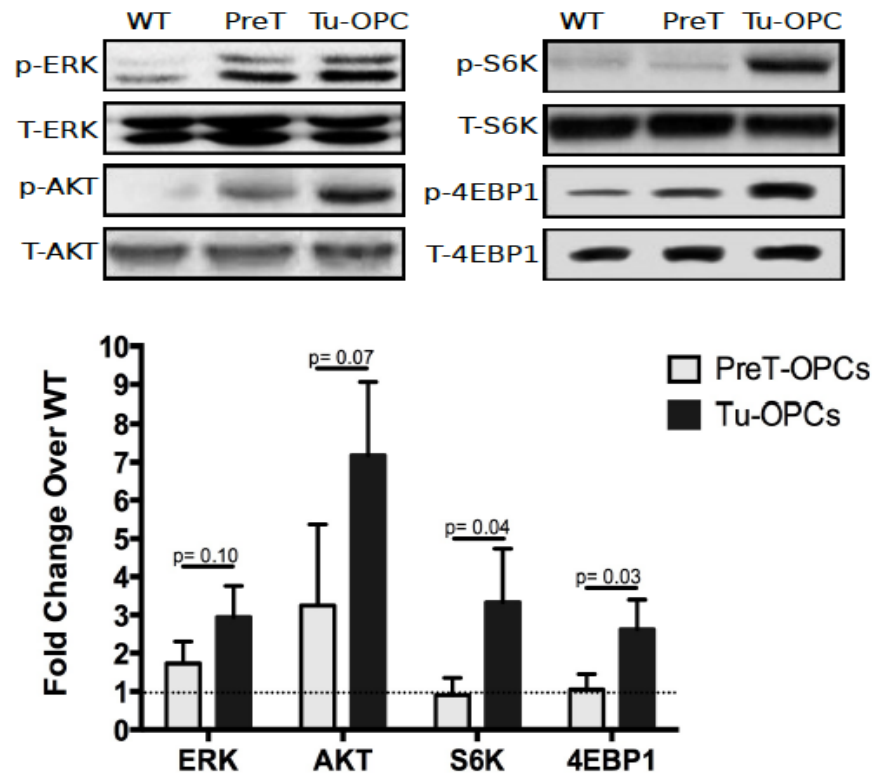
Figure 2.17 *NF1* deletion leads to increased *AKT* and *ERK* activity in PreT-OPCs while *mTOR* activity remains basal until OPC transformation.

Western blots shows that while the deletion of *NF1* leads to increased levels of phosphorylated (p) ERK, pAKT, pS6K, and p4EBP1 in Tu-OPCs, only pERK and pAKT are elevated in PreT-OPCs compared to WT OPCs. pS6K and p4EBP1 show no significant change in their levels between PreT-OPCs and WT OPCs. Bottom graph shows the quantification of the level of pERK, pAKT, pS6K and p4EBP1 in PreT-OPCs compared to Tu-OPCs. While there is no significant difference between PreT-OPCs and Tu-OPCs in the level of pERK and pAKT, there is a significant difference in pS6K and p4EBP1. Dotted line shows the level of phosphorylated proteins in WT OPCs. (n=3) Error Bar ± SD

Figure 2.18 PreT-OPCs have decreased sensitivity to *mTOR* inhibition compared to *ERK* and *AKT* inhibition.
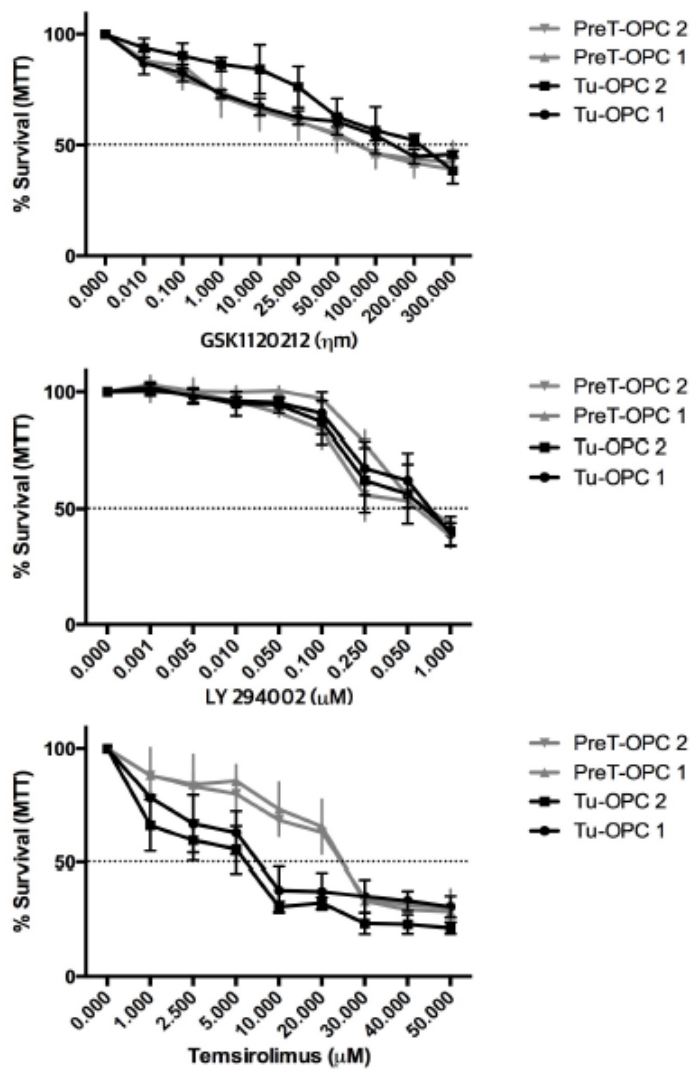
Figure 2.18 PreT-OPCs have decreased sensitivity to *mTOR* inhibition compared to *ERK* and *AKT* inhibition.

PreT-OPCs and Tu-OPCs were treated with a *MEK* (GSK1120212), *PI3K* (LY294002), or *mTOR* (Temsirolimus) inhibitor and assayed 48 hrs later for survival. PreT-OPCs have show a decreased sensitivity to the *mTOR* inhibitor (Temsirolimus) but not *PI3K* (LY294002) or *MEK* (GSK1120212) inhibitor compared to Tu-OPCs. Dashed line represents IC$_{50}$ value. (n=3) Error Bar ± SD

2.5 *mTOR* is critical for the transformation of reactivated Pre-Transforming OPCs

2.5.1 Deletion of mTOR does not affect WT or PreT-OPC proliferation

It is obvious from our data that the deletion of NF1 leads to gradual activation of both *ERK* and *AKT* from pre-malignant stages until tumor stages yet *mTOR* signaling seems to be unaffected until tumor stages. To better understand the necessity of particular signals for OPC transformation, we chose to delete *mTOR* since previous studies have shown that pathways altered at the later stages of tumorigenesis increase malignancy (Fearon and Vogelstein, 1990; Hruban et al., 2000; Schlomm et al., 2008). Our inhibitor data strongly suggests that while *ERK* and *AKT* inhibition have strong effects, PreT-OPCs have relatively little response to *mTOR* inhibition, thus giving us more confidence that *mTOR* deletion will have little affect during PreT-OPC reactivation. Furthermore, recent work has shown that both *AKT* and *ERK* are critical in gliomas and both pathways converge on *mTOR* (Kaul et al., 2015). Thus, while *AKT* and *ERK* deletion could have anti-tumor effects, mTOR deletion should have the combined effect since this node is the common convergence for both *ERK* and *AKT* dependent glioma growth and survival. Therefore, to test whether *mTOR* is critical for the transformation of PreT-OPCs, we need to specifically delete *mTOR* in *p53,NF1*-null OPCs and determine whether this blocks gliomagenesis.

Our early studies demonstrated that OPCs re-enter cell cycle (reactivation) at 12-day post injection (12 dpi) and subsequently transform into glioma at 180 dpi (Galvao et al., 2014). In this study, we further introduced floxed alleles of *mTOR* into the tumor model, which harbors *p53* and *NF1* deletions, to determine the necessity of *mTOR* in

OPC transformation. We first determined whether *mTOR* deletion could prevent the reactivation or eventual transformation of PreT-OPCs (Figure 2.19). Following the daily Tamoxifen administration at P45 for 5 consecutive days, mice were injected with BrdU for 7 days to label proliferating cells. In WT animals, the deletion of *mTOR* had no significant effect on OPC proliferation compared to control brains, suggesting that *mTOR* is not critical for adult OPC proliferation at this age (Figure 2.20). Additionally, the deletion of *mTOR* in PreT-OPCs had no significant effect on PreT-OPC proliferation compared to controls (Figure 2.20) indicating that *mTOR* activity is not necessary for the reactivation of PreT-OPCs.

2.5.2 mTOR is necessary for the transformation of PreT-OPCs.

To determine the effect of *mTOR* deletion on OPC transformation, mice were examined at 180 dpi for both tumor penetrance and tumor size. Compared to control mice that normally form medium-large tumors by 180 dpi, *mTOR*-null mice rarely had tumors (2/10) and all tumors that formed were small lesions (Figure 2.21a,b). Furthermore, after we purified Tu-OPCs using immuno-panning from two small tumors in *mTOR*-null mice, genotyping result showed that one of the floxed *mTOR* alleles was still intact, suggesting that they are "escaper cells" due to the inefficiency of NG2-CreER (Figure 2.22). Interestingly, compared to the control CKO brains at 180 dpi, mTOR-null brains contained a decent (roughly 15-20%) proportion of cells that had morphological characteristics of oligodendrocytes (Figure 2.23). While these cells failed to stain positive for CC1, mainly due to technical limitations, they most likely are differentiated oligodendrocytes, suggesting that mTOR may be responsible for maintaining an OPC-state. The fact that Tu-OPCs in *mTOR* KO mice retain one copy of *mTOR* further

demonstrates the absolute requirement of *mTOR* activity for malignant transformation. In summary, these data suggest that, while *mTOR* is not necessary for initial reactivation of PreT-OPCs, it is critical for their final transformation, making it an effective target for glioma treatment as long as its activity can be inhibited completely.

Figure 2.19 Schematic for determining the necessity of *mTOR* during OPC

reactivation and transformation.
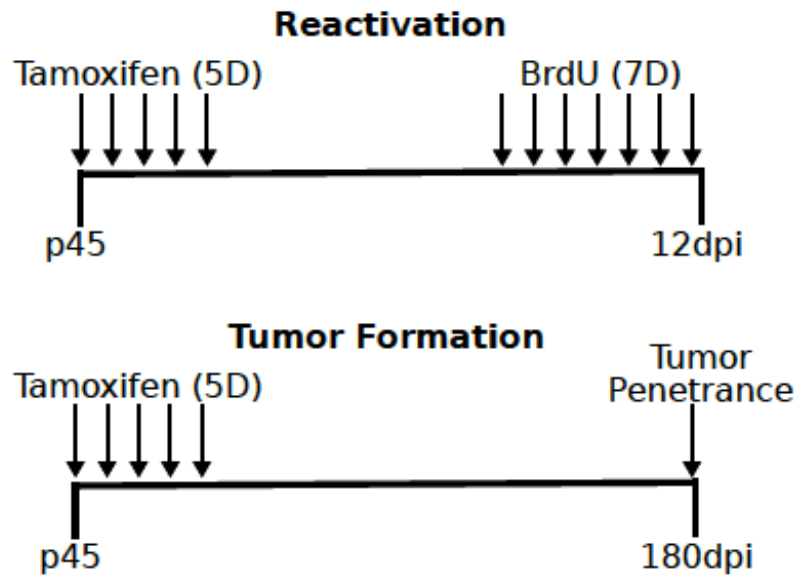
Figure 2.19 Schematic for determining the necessity of *mTOR* during OPC reactivation and transformation.

Top schematic shows the experimental design for testing the effect of *mTOR* deletion on PreT-OPC reactivation. Mice are treated for 5 days with Tamoxifen to induce cre-mediated recombination and then treated for 7 days with BrdU to label dividing OPCs. Bottom schematic shows the experimental design for testing the effect of *mTOR* deletion on PreT-OPC tumor formation. Following 5 days of Tamoxifen treatment, mice are kept for 180 days to determine the tumor penetrance following *mTOR* deletion.

Figure 2.20 Deletion of *mTOR* has no effect on WT proliferation and PreT-OPC reactivation.
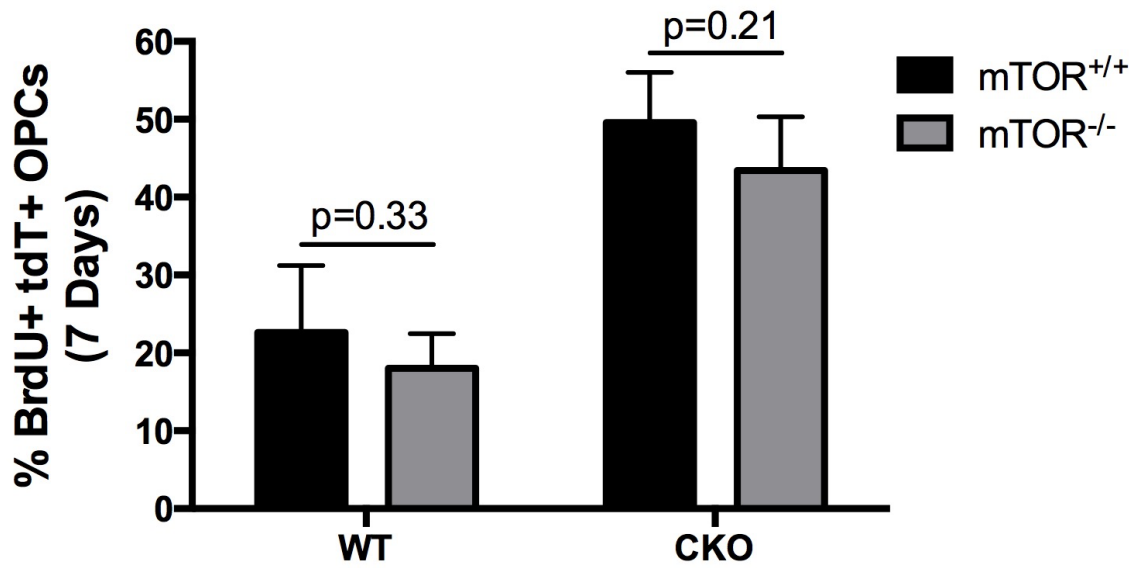
Figure 2.20 Deletion of *mTOR* has no effect on WT proliferation and PreT-OPC reactivation.

Following 7 days of BrdU injections, both WT mice and CKO mice were examined for the percent of dividing OPCs following *mTOR* deletion. Both WT and CKO mice had no significant difference in the percent of dividing OPCs that were either *mTOR*-WT or *mTOR*-null. (n=4 WT, n=5 CKO) Student *t* Test; Error Bar ± SD

Figure 2.21 Deletion of *mTOR* leads to a decrease in OPC transformation.
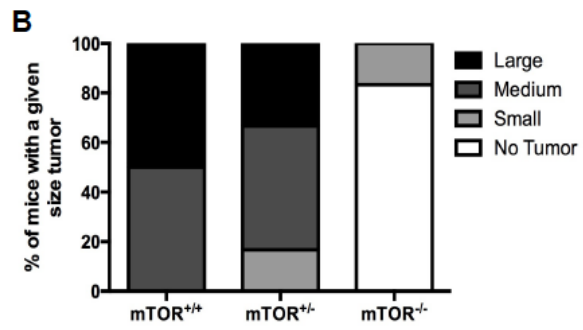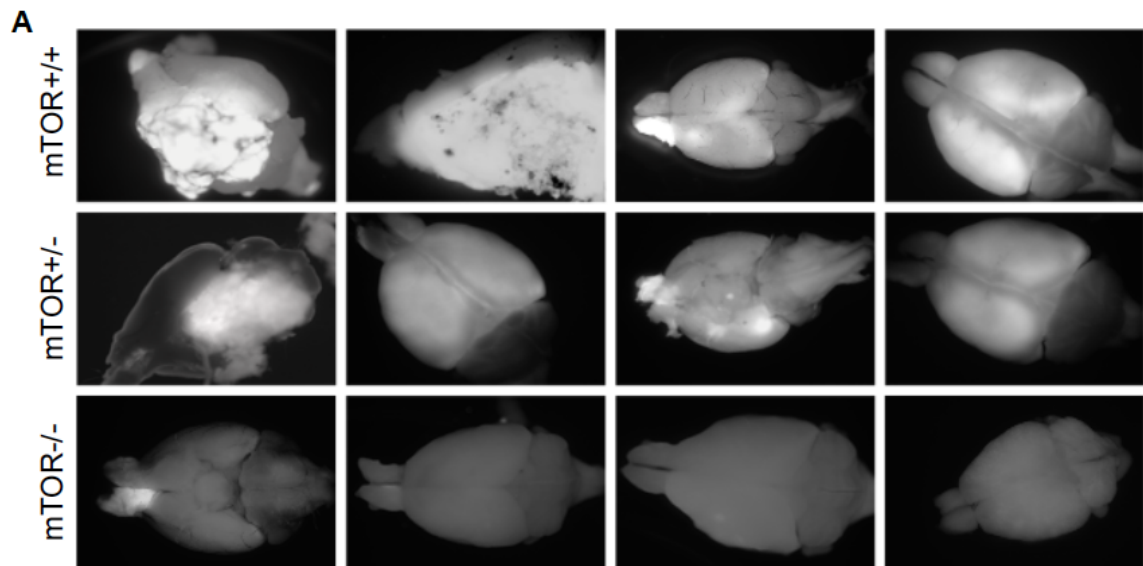
Figure 2.21 Deletion of *mTOR* leads to a decrease in OPC transformation.

(A) Glioma-CKO mice (*p53,NF1*-null) with either *mTOR*-WT, *mTOR*-het, and *mTOR*-null status were dissected at P240, to determine the rate of penetrance following mTOR deletion. While *mTOR*-WT CKO mice normally had large tumors, *mTOR*-null CKO mice rarely had tumors and when they did occur, they were small. The images are representative of the average tumor size in *mTOR*-WT, *mTOR*-het, and *mTOR*-null glioma mice.

(B) Deletion of *mTOR* leads to a near complete block of tumor penetrance and a decrease in tumor size. *mTOR*-het mice show no obvious change in both tumor penetrance or tumor size compared to littermate controls. (n≥10 for tumor experiments)

Figure 2.22 Tumors from *mTOR*-null mice formed from OPCs with incomplete *mTOR*
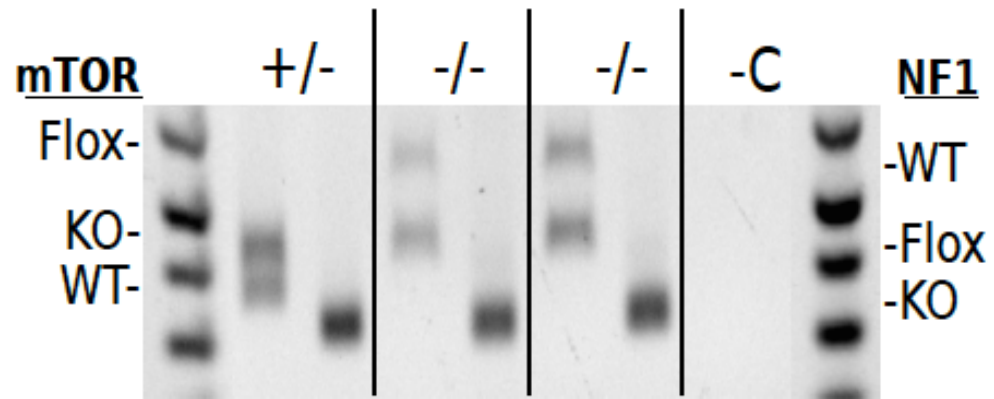
knockout.

Figure 2.22 Tumors from *mTOR*-null mice formed from OPCs with incomplete *mTOR* knockout.

Tumors from *mTOR*-null brains were isolated and purified to allow for precise genotyping. Following purification, cells were lysed and the status of *mTOR* deletion was determined using PCR. Tumors that formed in *mTOR*-null brains were OPCs that had incomplete recombination of both *mTOR* alleles. Purified cells were lysed for genomic DNA and stained for PDGFRα to confirm OPC purity following purification. (n≥10 for tumor experiments)

Figure 2.23 *mTOR* deletion leads to an increase in oligodendrocyte-like cells in CKO
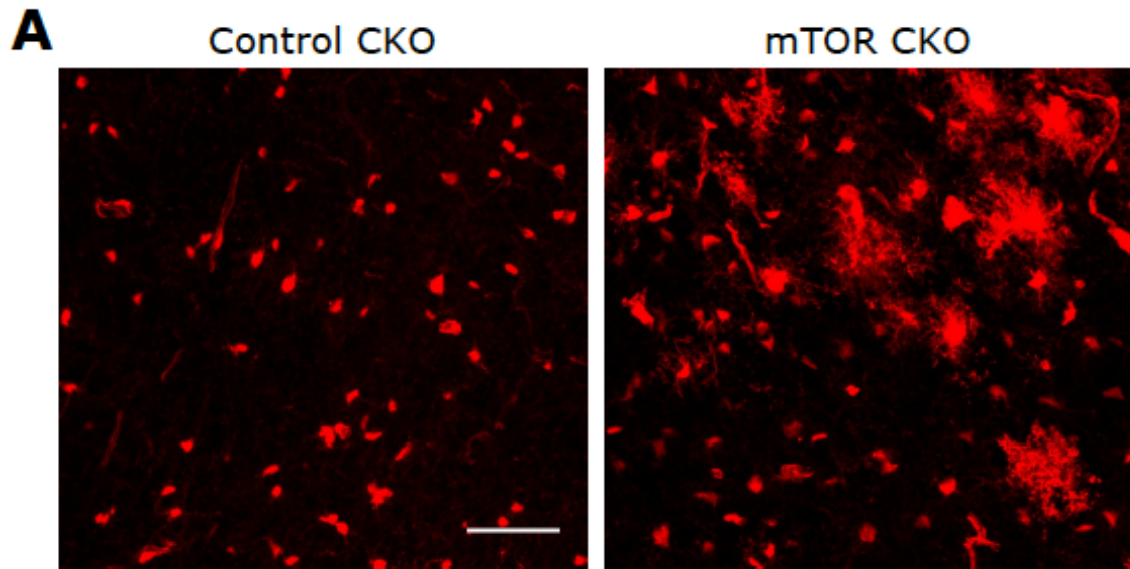
model.

Figure 2.23 *mTOR* deletion leads to an increase in oligodendrocyte-like cells in CKO

model.

mTOR-WT CKO tumor age mice (180 dpi) have tdT+ cells with typical OPC

characteristics, left panel. However upon examination of brains of *mTOR*-null CKO mice,

tdT+ cells show a characteristic oligodendrocyte-like morphology. Note the ramified

processes and large cell bodies, both characteristics of mature oligodendrocytes.

Discussion

Most, if not all, current mouse cancer models employ multiple genetic mutations to drive tumor formation, with the focus on studying malignant cells (Dunn et al., 2012; Zong et al., 2012, 2015). However, we could gain more insights into therapeutic interventions by dissecting out the transformation process in greater details. On one hand, the impact of individual genetic changes on biological aberrations of the cell of origin of a given tumor type should be distinct from each other. While restoring tumor suppressor gene (TSG) activity remains challenging, one could correct biological aberrations by targeting the entire regulatory axis. On the other hand, thorough assessment of alterations of cellular behaviors at pre-malignant stages could guide one to devise cancer prevention strategies. While these studies are highly important, the main hurdle is the lack of a suitable model to study these problems because pre-malignant mutant cells are invisible in most mouse models. Here we employed our MADM system to dissect apart the roles of *p53* and *NF1* in suppressing OPC transformation and also the alterations that are necessary at pre-transforming stages for OPC transformation.

D2.1 Individual Roles of p53 and NF1 during the progression towards transformation in OPCs.

Because we and others have previously shown OPCs to be the cell of origin in a *p53/NF1* deletion model, we are able to directly assess functional roles of TSGs in this particular cell type. While studies have previously shown *p53* and *NF1*'s important roles in tumorigenesis, our study is the first to look at consequences of these deletions in OPCs at pre-malignant stages (Schwartzbaum et al., 2006; Shchors et al., 2013; Zhu

and Parada, 2002). While *NF1* controls the expansion, proliferation, and differentiation of OPCs early on, *p53* clearly plays a later but vital role in preventing OPC transformation since *NF1*-null OPCs never transform despite their overwhelming expansion in the brain parenchyma. It is plausible that *p53* deletion allows a further accumulation of necessary mutations that allow cells to transform that has been shown in several tumor types (Levine, 1997; Weiss et al., 2010; Young et al., 2011). However recent reports have shown that *p53* may exert its tumor suppressor functions independently of DNA-damage, cell-cycle arrest, and apoptosis (Li et al., 2012; Valente et al., 2013b). Regardless of which pathway *p53* exerts its tumor suppressor function, it is clear that *p5*3 deletion is needed for the transformation of *NF1*-null OPCs. Perhaps the role of p53 in suppressing NF1-null OPC transformation is to maintain genome stability, which does not allow for the additional mutations needed during gliomagenesis.

D2.2 Restoration of p53 and NF1 have strong anti-tumor effects.

While traditional studies look at how inhibitors of different overactive pathways can affect tumor cell survival, we chose to restore the lost regulators of these pathways to determine therapeutic efficacy. Such an approach aims at thoroughly testing therapeutic targets without the concern of off-target effect and other complications with pharmacological inhibitors, thereby helping the focus of drug discovery efforts. The restoration of *p53* has strong anti-tumor effects in Tu-OPCs and human glioma cells suggest that targeting *p53* in glioma may prove useful in the clinic. Our findings are in line with recent work demonstrating that p53 restoration is efficacious for astrocytomas (Shchors et al., 2013). Furthermore, of the 20% of glioma patients harboring p53 mutations, nearly half of these mutations are common mutations and there are drugs

designed to restore p53 function (Khoo et al., 2014; Lehmann and Pietenpol, 2012).

Specifically, PRIMA-1, STIMA-1, MIRA-1, and SCH529074 are all either in preclinical or

clinical trials(Lehmann and Pietenpol, 2012). Additionally, several classes of MDM2

inhibitors have been discovered that lead to increased p53 activity through disruption of

the MDM2-p53 interaction (Ramirez et al., 2013). Both sets of drugs have the potential

to decrease tumor cell survival to help glioma patients harboring either p53 mutations or

MDM2 activation. In addition, while *NF1* is known as a Ras-GAP, we clearly show that

restoration of the NF1-GAP domain has an additional function outside of proliferation

(Corral et al., 2003; Ismat et al., 2006). Our data demonstrate that restoration of the

NF1-GAP promotes differentiation in addition to halting proliferation, suggesting that

targeting Ras effectors could terminally differentiate cells, which may be missed in a

conventional survival assay. Thus, failure of certain drugs, such as *mTOR* inhibitors,

may have been due to not analyzing all the phenotypes that could result from treatment

including OPC differentiation.

D2.3 Pre-malignant stage analysis reveals unique activation of downstream Ras targets.

Furthermore, since most alterations necessary for transformation occur during

the premalignant stage, when malignancies are undetectable, we chose to examine

changes in downstream *Ras* effectors to uncover potential targets. While traditionally

models can uncover increased activity of targets at the tumor stage our model allowed

us to show that both *ERK* and *AKT* undergo gradual activation, compared to Tu-OPCs,

following *NF1* deletion (Kaul et al., 2015; Lee et al., 2010). However to our surprise

mTOR remains at basal levels and only becomes activated following OPC

transformation. This suggests that *mTOR* activation is critical for Tu-OPC transformation while it may be inconsequential for early progression. Additionally, the significant change in PreT-OPC response to *mTOR* inhibitors compared to Tu-OPCs further supports the idea that *mTOR* is more critical in Tu-OPCs compared to PreT-OPCs.

D2.4 mTOR is necessary for transformation of OPCs but is not necessary for the reactivation of OPCs.

Recent studies have shown that inhibition of multiple pathways is more beneficial for glioma patients, suggesting that dual inhibition will be necessary for future therapeutics in glioma patients (Chipuk, 2015; Haar et al., 2012; Ramirez et al., 2013).. Given that *ERK* and *AKT* activation is not unique to PreT-OPCs compared to Tu-OPCs, yet *mTOR* is uniquely activated in the latter, we chose to target *mTOR* to prove whether this signaling node is critical for OPC transformation. Following mTOR deletion, PreT-OPC reactivation is unaffected but surprisingly OPC transformation is completely blocked. This suggests that while *mTOR* is not critical for the early stages it is necessary for OPC malignancy and thus may make a great therapeutic target. Additionally, this suggests while dual inhibition may be beneficial, complete inhibition of a critical node such as *mTOR* may be sufficient to block glioma cells. While past trials with *mTOR* inhibitors have failed, most of these failures are due to the inability of the drugs to effectively penetrate the blood-brain barrier and adequately inhibit their targets (Cloughesy et al., 2008; Rodrik-Outmezguine et al., 2016). Our results should give clinicians more hope for *mTOR* inhibitors, since we blocked gliomagenesis by complete

ablation of *mTOR* and the effects of *mTOR* inhibitors on mutant, non-transformed cells is minimal, suggesting minimal side effects and most likely less acquired resistance.

In summary, our current study teases apart the role of individual TSGs in promoting the cell of origin of glioma and fundamentally addresses the efficacy of targeting these pathways by directly restoring both genes. These data provide hope for future targeted therapies as well as begs more questions. What critical step is *p53* preventing in *NF1*-null OPCs that does not allow malignant transformation? What triggers the transition from mutant to tumor OPCs? Why is *mTOR* only up regulated specifically in tumor OPCs? These answers and others will help us further understand the path to malignancy and the mechanisms needed to treat patients.

Chapter 3 Critical role of OPC competition in physiological homeostasis and glioma initiation and progression

Introduction

The importance and challenges of studying premalignant progression of mutant cells

Malignant brain tumors remain one of the most deadly cancers due to their rapid onset and the limited effectiveness of therapies (De Bonis et al., 2013; Haar et al., 2012; Ramirez et al., 2013). Glioblastoma multiforme (GBM) is the most common primary brain tumor with an average survival time of 12-15 months post-diagnosis (Lote et al., 1997; Stupp et al., 2005). Poor outcomes for glioma patients can be attributed to current therapeutic efficacy, limited resection capabilities, and eventual relapse of tumor cells with a reduced response to therapies (Chipuk, 2015; Haar et al., 2012; Lawrence et al., 2012). Even patients diagnosed with low-grade gliomas (LGG) have a grim outlook, as a majority of LGGs progress to malignant gliomas (Kleihues and Ohgaki, 1999; Ohgaki and Kleihues, 2007, 2013; Sanai et al., 2011). Therefore, investigating pre-malignant progression could lead to mechanistic insights that shed light on preventative treatment. However, analysis of pre-malignant progression is extremely difficult, if at all possible, because even the smallest detectable tumors contain tens of thousands to millions of cells, which may have already transformed (Rhiner and Moreno, 2009). The difficulty lies in the absence of histopathologically detectable features of pre-malignant cells. Because of this, the cellular and molecular events in precancerous lesions remain unknown.

During the normal development of an organism, tissue specification is tightly controlled by a variety of signals that control cell specification in order to maintain tissue integrity. This process is thoroughly controlled so that tissue integrity, a fundamental feature of a healthy tissue, remains intact both during development and during the life of the organism (Simons and Clevers, 2011) . The loss of tissue integrity leads to malignancies that can ultimately lead to organismal death (Biteau et al., 2011). However, how cells within a tissue differentiate between normal, healthy cells and unhealthy cells and how unhealthy cells are eliminated are not fully understood. One tantalizing mechanism emerging from the literature is known as cell competition.

Cell competition is a process defined as the system by which cells that are normally viable on their own are eliminated in the presence of a more competitive cell. This process is important during development and aging to ensure the elimination of damaged cells to preserve issue integrity. Recent work in *Drosophila* development has revealed that this mechanism also allows for an accumulation of non-WT cells, typically cells containing mutations which augment their ability to proliferate, within a tissue without altering tissue structure, which is termed "super-competition" (Rhiner and Moreno, 2009). During development, cells with different genotypes compete with one another for space within a tissue, resulting in the elimination of "unfit" cells to ensure tissue integrity (Bondar and Medzhitov, 2010; Clavería et al., 2013; Snippert et al., 2010, 2014).

However, the relevance of cell competition to cancer has only recently been explored (Johnston, 2009). Cell competition, when in favor of cells with oncogenic mutations, will promote cancer evolution and tumor progression (Baker and Li, 2008).

Furthermore, genes/pathways that have been shown to regulate cell competition are also commonly involved in a variety of tumors. During hematopoietic stem cell development, cells with higher levels of *p53* are out-competed in a non-cell-autonomous manner by induction of growth arrest and senescence-related gene expression (Bondar and Medzhitov). Cell competition orchestrated by multiple oncogenic mutations has been found to promote tumor progression, nicely explaining the multi-hit model for most cancer types. For example, in a Drosophila model, it was found that while cells containing *lgl* mutations had significant growth advantages and could outcompete WT cells, they rarely formed tumors. However, upon Ras activation, these mutant cells were able to form tumors due to inactivation of several downstream targets, resulting in increased cell competition of the mutant cells (Menendez 2010, Brumby 2003).

Many competition genes were identified in the Drosophila model system. The Hippo pathway has previously been shown to be a tumor suppressor, which negatively regulates YAP. Cells with lower levels of YAP were outcompeted by cells with higher levels (Tyler 2007, Neto-Silva 2010, Ziosi 2010). SPARC, a gene known to play a role in tumorigenesis has also recently been shown to be involved in cell competition. It has been shown that SPARC is up regulated in loser cells in Drosophila but that this up regulation counteracts the typical cell death outcome of cell competition (Portela 2010). Rather, these cells are able to evade the elimination caused by more competitive cells. Interestingly, this phenomenon was also seen in several human tumor types, suggesting that this pathway may be a highly relevant cell competition pathway involved in human malignancies (Petrova et al., 2012). The most well studied gene in cell competition and one of the most highly mutated genes in tumors is Myc. Several studies have shown that mutations in Myc, resulting in increased Myc levels, cause an increase in competitive fitness and have gone on to show that varying levels of Myc cause varying levels of

competition (Claveria; De La Cova; Johnston 1999; Moreno 2004). Thus, it should come as no surprise that recent work in *Drosophila* has shown that the progression towards malignancy can be regulated by cell competition (Eichenlaub and Cohen, 2016; Froldi et al., 2010; Hogan et al., 2011; Kucinski et al., 2016). However, whether cell competition plays a role in mammalian systems has been studied minimally (Petrova et al., 2012).

OPCs maintain homeostasis through repulsive homotypic cell-cell interactions

For OPCs and other neuroglial cells, it is important to sense one another and to reach the optimal density since the space within a skull is limited. Previous work in mice has shown that OPCs are highly dynamic and they sense one another through a touch and repulsion mechanism to maintain homeostasis (Hughes et al., 2013b). It was shown that OPCs normally sense their local environment through the extension and retraction of dynamic filopodia. Upon the elimination of an OPC, adjacent OPCs respond by quickly proliferating and replacing the lost OPC similar to neutral drift towards clonality previously described in the intestinal crypts (Snippert 2010). While this does not seem surprising, this response could have dire effects for cancer therapies directed towards tumor OPCs. If, following radiation or chemotherapy, tumor OPCs are still present in the brain, they may quickly respond to the loss of surrounding OPCs, whether tumor or normal. This response may be one reason why GBM patients are susceptible to relapse. However, whether the responses of OPCs to these types of insults are OPC specific or tumor specific is unclear.

Summary of our findings on the role of OPC competition in gliomagenesis and homeostasis.

Using a mosaic mouse genetic tool termed MADM, mosaic analysis with double markers, our lab recently showed that oligodendrocyte progenitor cells (OPCs), could serve as the cell of origin in glioma. Interestingly, because MADM generates a RFP+ WT cell at the same time as a GFP+ mutant cell, we found that during the pre-malignant phase, Pre-Transforming (*p53,NF1*-null) OPCs dramatically expand over 150-fold compare to WT cells. Yet, these animals remain asymptomatic, including having no easily identifiable change in brain size, until tumors form at 8 months of age. This suggested to us that despite the overwhelming increase of *p53,NF1*-null OPCs in these mice, the total number of OPCs must not change that dramatically since the brains remained largely the same size as WT mice. Yet whether this truly happens and how this happens remained unknown. In this chapter we set out to determine how *p53,NF1*-null OPCs expand in the brain and if this expansion affects WT OPCs. We followed the progression from the initial expansion of *p53,NF1*-null OPCs until P60 and found that *p53,NF1*-null OPCs expand at the expense of WT OPCs. We also found that the competitive fitness of *p53,NF1*-null OPCs is controlled through the GAP function of *NF1* since the elimination of GAP function leads to increased competitive fitness. Finally and most surprisingly, we found that we can completely block gliomagenesis by decreasing the competitive advantage that *p53,NF1*-null OPCs gain following *NF1* deletion. Thus, cell competition is a critical component of the gliomagenic process.

Furthermore, we then tested the response of OPCs to radiation, a common GBM therapy. Using WT mice, we treated the brain with high doses of radiation and determined if normal OPCs can be eliminated or whether they respond to large insults in

the same way that they respond to local OPC death. Following radiation, there was massive OPC death followed by a sharp increase in OPC proliferation. This response led to a gradual increase in OPC density such that OPC density returned to normal within 4 weeks of radiation. Additionally, we performed lineage tracing using an OPC reporter and found that all OPCs that repopulate the brain after radiation are derived from OPCs labeled before the treatment. Thus, OPCs have a robust mechanism in place that allows them to respond to severe insults by increased proliferation of surviving OPCs that eventually leads to normalization of OPC density.

Results

3.1 *p53,NF1*-null OPCs expand at the expense of WT OPCs

3.1.1 OPC density changes only 1.5-fold between MADM-WT and MADM-Tumor brains.

Previously we have shown that from P10 to P60, there is a dramatic increase in the ratio between mutant Pre-transforming OPCs (*p53,NF1*-null OPCs) and WT OPCs. By P60, the mutant:WT (G/R) ratio has increased to roughly 150-fold, demonstrating drastic over-expansion of *p53,NF1*-null OPCs. To assess how such expansion of mutant OPCs affects the overall density of OPCs, we stained both MADM-WT and MADM-Tumor brains with the OPC marker PDGFRα at P10 to P60 and systematically sampled throughout the brain (Figure 3.1b). Surprisingly, despite the huge increase in G/R ratio, the overall density of OPC only increased marginally in MADM-Tumor brains when compared to MADM-WT brains (less then 2-fold at P60, similar to what was previously reported, Figure 3.1c,d) (Bennett et al., 2003), suggesting that the expansion of mutant OPCs occurred at the expense of surrounding non-mutant OPCs (Figure 3.1a).

3.1.2 p53,NF1-null OPCs grow at the expense of other OPCs.

It seems paradoxical that *p53,NF1*-null OPCs can expand 150-fold yet the overall OPC only increases slightly. However, one explanation is that the *p53,NF1*-null OPCs expand while at the same time both WT and heterozygous uncolored/yellow OPCs decrease, thus providing an environment where total OPC numbers are not altered radically. To determine if this was indeed the case, we quantified the relative proportion

of WT, heterozygous, and *p53,NF1*-null OPCs within the total OPC population. At P10 a majority (>95%) of all the OPCs are heterozygous OPCs while WT and *p53,NF1*-null OPCs make up less then 2% each (Figure 3.2a,b left side). However, by P60, nearly 75% of all the OPCs within the brain are *p53,NF1*-null OPCs while WT OPCs have all but disappeared (Figure 3.2a,b right side).

Furthermore, the total population of either GFP+ or other OPCs in MADM-WT and MADM-Tumor brains were quantified at P20, P40, P60, and P120. Not surprisingly, in MADM-WT brains there was an overall decrease in total OPC population over time with no significant change in the total OPC population of GFP+, RFP+, or uncolored OPCs (Figure 3.3a). However, in MADM-Tumor brains, the total OPC population increases over this same time but more importantly, the population of GFP+ OPCs (*p53,NF1*-null) grows significantly while the total population of all other OPCs significantly decreases (Figure 3.3b). Thus this suggests that the concurrent deletion of *p53* and *NF1* in OPCs leads to an increase in *p53,NF1*-null OPC numbers at the expense of all other OPCs.

We also made two interesting observations in P60 MADM-tumor brains. First, *p53,NF1*-null OPCs form distinctive patches that are free of WT OPCs, suggesting that mutant OPCs most likely outcompete WT OPCs through contact-mediated clonal expansion. Second, the density of OPCs in the green patches is higher than in the non-patchy regions, suggesting mutant OPCs could tolerate closer contact with each other than WT OPCs do.

Figure 3.1 OPC density changes only 1.5-fold between MADM-WT and MADM-Tumor brains.
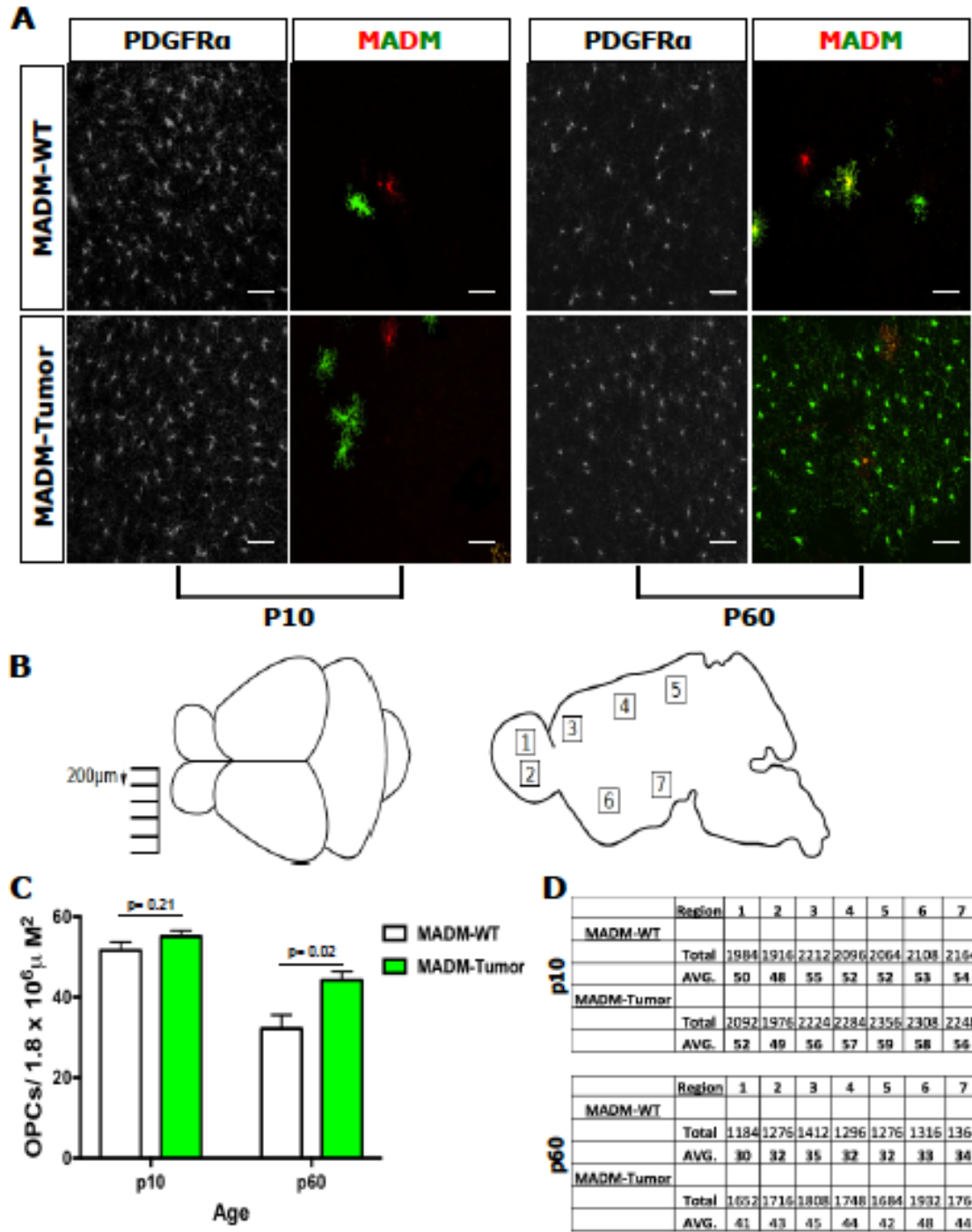
Figure 3.1 OPC density changes only 1.5-fold between MADM-WT and MADM-Tumor brains.

(A) MADM-WT and MADM-Tumor brains were stained with GFP, RFP, and PDGFRα at P10 and P60. At P10, OPC density remains largely unchanged with very few MADM labeled cells found throughout the brain in both genotypes. However, by P60, there is an obvious increase in OPC density in the MADM-Tumor brains, most of which are GFP+ OPCs. (Scale bar 50 μM)

(B) Quantification scheme for sampling OPC density throughout the brain. Brains were sliced medial-lateral, collecting a slice every 200 μm. Within each brain slice, 7 areas were quantified to sample throughout the brain to adjust for regional differences.

(C) Quantification of the overall OPC density, regardless of MADM labeling. At P10, there is no significant change in the overall OPC density between MADM-WT and MADM-Tumor brains. However, by P60, there is a significant (p=0.02) increase in OPC density in MADM-Tumor brains compared to MADM-WT brains. (p10 n≥5, p60 n>10) Student *t* Test; Error Bar ± SEM

(D) Region-specific breakdown of total and average numbers of OPCs throughout the brain. There was no significant difference in OPC density in any brain area examined.

Figure 3.2 *p53,NF1*-null OPCs take over the OPC population by P60.
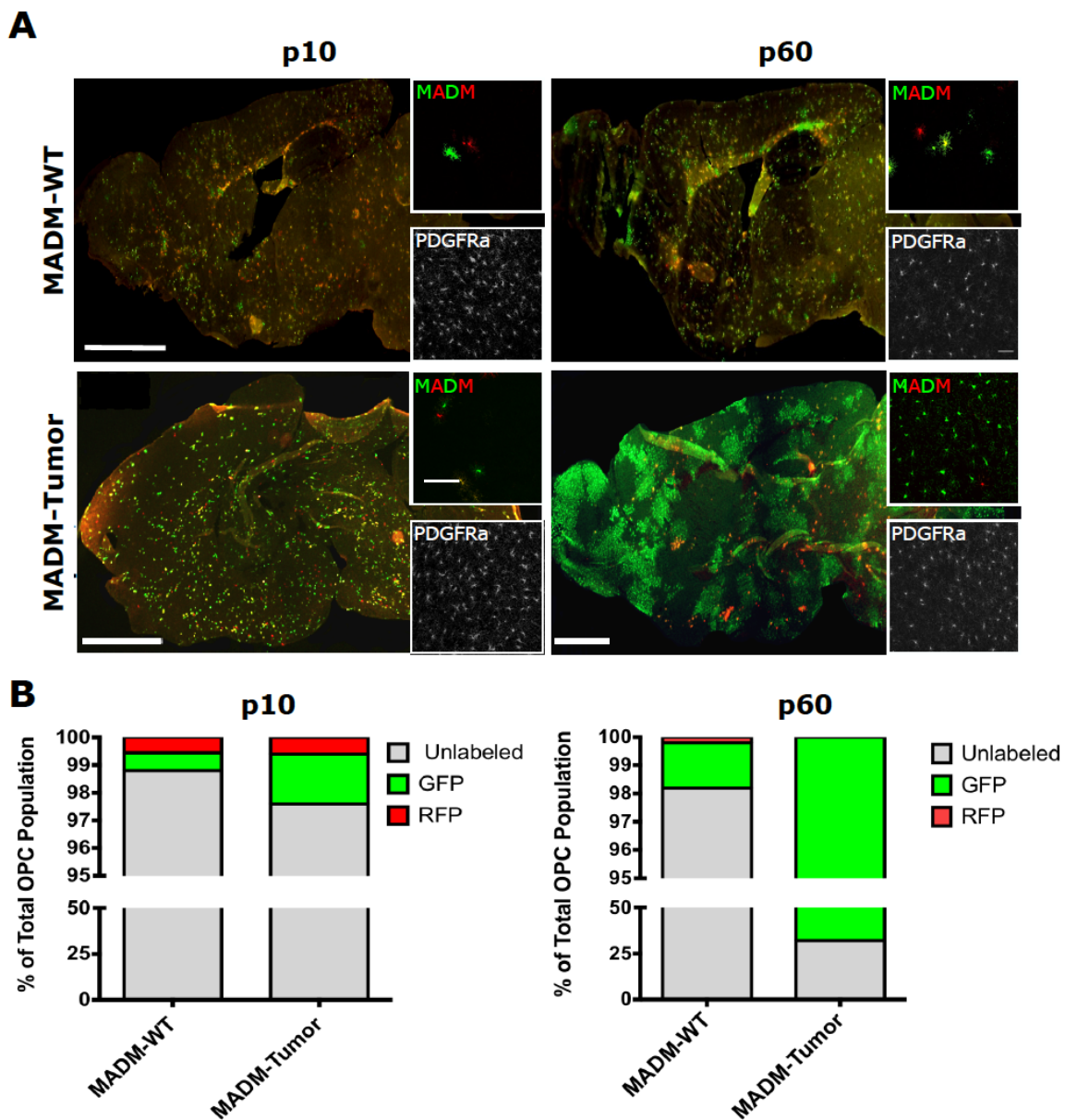
Figure 3.2 *p53,NF1*-null OPCs take over the OPC population by P60.

(A) Representative images to show the relative distribution of various OPCs throughout the brain in both MADM-WT and MADM-Tumor brains at both P10 and P60. While MADM-WT brains have relatively little change in MADM labeling between P10 and P60, MADM-Tumor brains show a sharp increase in GFP+ OPCs between P10 and P60. Insets show MADM labeling (top) and OPC labeling (bottom). All insets are taken from the anterior cortex. (Scale bar 2 mM; Inset 50 µM)

(B) At P10 and P60, MADM-WT and MADM-Tumor brains were analyzed for the relative distribution of GFP+, RFP+, or YFP/Unlabeled OPCs within the total OPC population. At P10 a majority (>95%) of all OPCs are YFP+/uncolored in both genotypes. By P60 MADM-WT brains still have a majority of YFP/Uncolored OPCs making up over 95% of the total OPC population. In contrast, a majority (75%) of all OPCs in MADM-Tumor brains are GFP+ *p53,NF1*-null OPCs while at the same time there is an overall decrease in RFP+ and YFP/Uncolored OPCs. (n>10)

Figure 3.3 p53,NF1-null OPCs grow at the expense of all other OPCs.
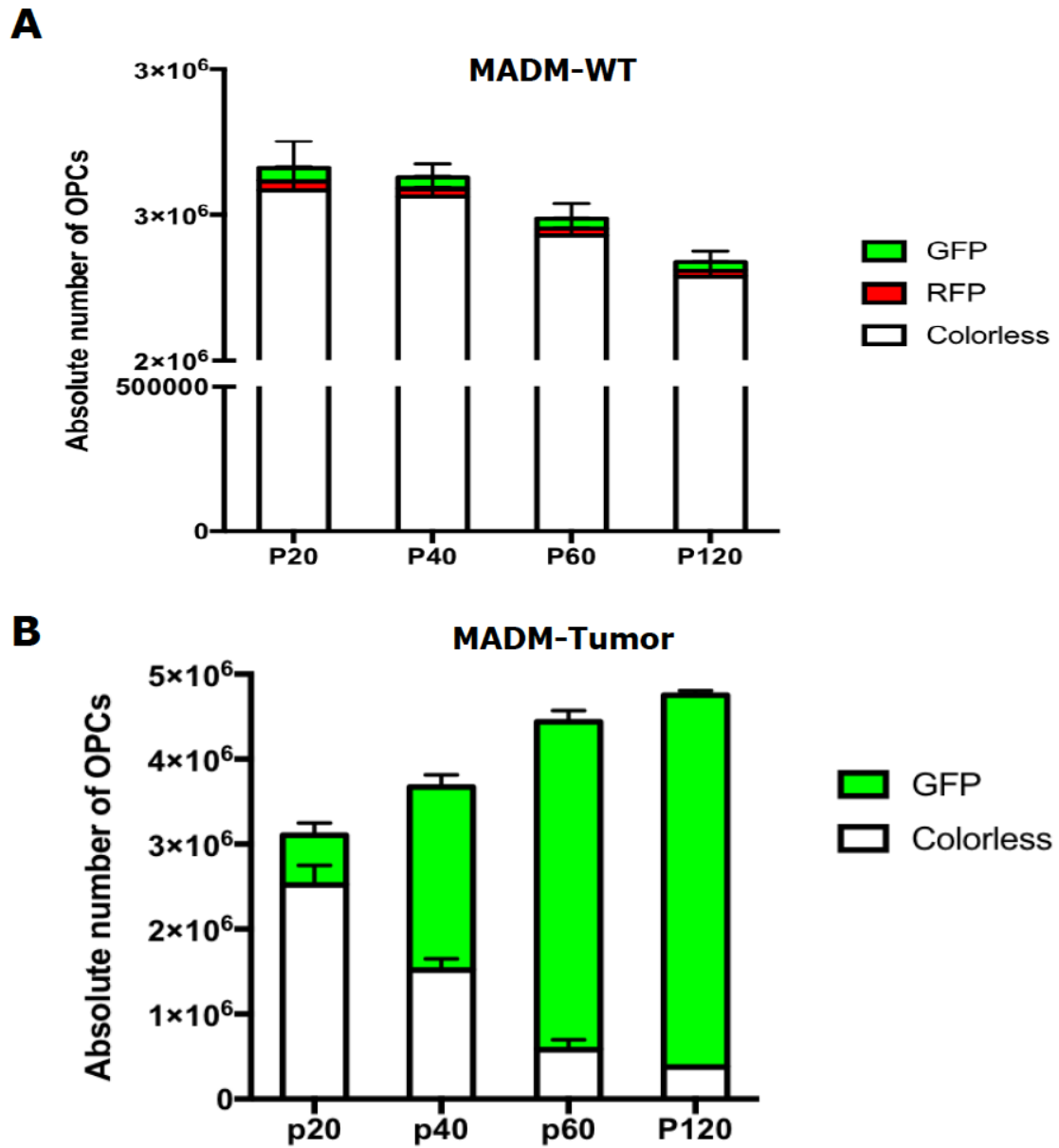
Figure 3.3 *p53,NF1*-null OPCs grow at the expense of all other OPCs.

(A) MADM-WT brains were quantified at P20, P40, P60, and P120 to determine the overall OPC population. While the total OPC population declines over time, there is no significant change in the population of GFP+, RFP+, and Colorless OPCs in MADM-WT brains at all ages.

(B) MADM-Tumor brains were quantified at P20, P40, P60, and P120 to determine the effect of *p53* and *NF1* deletion on overall OPC population. Unlike MADM-WT brains, MADM-Tumor brains had an increase in total OPC population across all ages. Importantly, the population of GFP+ OPCs grows substantially across all time points while the population of all other OPCs declines over time.

3.2 *NF1* deletion is sufficient for OPC competition.

3.2.1 Single deletion of NF1 is sufficient for an increase in OPC competition but is not sufficient for gliomagenesis.

It is clear that the concurrent deletion of *p53* and *NF1* leads to an increase in *p53,NF1*-null OPC competiveness. However, it is still unclear whether one of these or both gene mutations lead to an increase in competitive fitness. To address this, we established MADM-*p53* and MADM-*NF1*, in which only one TSG is mutated by the MADM system. Then we analyzed mutant OPC expansion in these brains, in comparison to the MADM-Tumor brains. At P10, all three models showed similar proportions of WT, heterozygous, and mutant OPC numbers within the total OPC population (Figure 3.4a left side; Figure 3.5a,b left side). However, by P60, MADM-*p53* brains had no expansion of *p53*-null OPCs while *NF1*-null OPCs brains phenocopied *p53,NF1*-null OPC competition (Figure 3.4a right side; Figure 3.5a,b right side). Therefore, *NF1* loss but not *p53* loss is responsible for the increased competitive fitness of *p53,NF1*-null OPCs. It is important to note that both MADM-Tumor and MADM-NF1 brains contain patches of GFP+ mutant OPCs.

3.2.2 GAP domain of NF1 is critical for OPC competition.

Our previous data demonstrate that the complete deletion of *NF1* is sufficient for an increase in OPC competitive fitness. However, NF1 is a large 280 kDa protein with many domains, one of which is RasGAP. It would be important to investigate whether the ability to increase OPC competitive fitness is related to NF1's RasGAP activity or activities outside this function. To address this we established a MADM-GAP-Inactive model (MADM-GAP-Dead), in which we incorporated a new mutant *NF1* allele that carries a single Arginine to Proline change at amino acid 1276 in the GAP catalytic site (Figure 3.6a). This single mutation leads to a complete loss of GAP function with normal levels of NF1 protein still present in the cell (John Epstein lab, unpublished). Using this new MADM mouse (MADM-GAP-Dead), we then evaluated the expansion of mutant OPCs and the penetrance of gliomagenesis. Interestingly, while the MADM-Tumor mice have >75% of GFP+ OPCs at P60, only 50% of OPCs in MADM-GAP-Dead mice are GFP+ (Figure 3.6b,c). Additionally, while OPCs with *NF1* deletion have a 4-day proliferation rate near 25%, OPCs with the *NF1*-GAP-Dead allele, have a proliferation rate of 11.8% ± 2.89 (Figure 3.6d). Taken together, these data suggest that the loss of GAP activity only partially recapitulates the complete deletion of *NF1*.

However, despite the fact that the *NF1*-GAP-dead allele does not fully recapitulate *NF1* deletion, these mice may still form tumors since there still seems to be competition. Therefore, mice were kept until P240, the latency age for tumor formation in our MADM-Tumor model and analyzed for tumor formation. While MADM-GAP-dead mice did form tumors, it was at a much lower penetrance (5/11) compared to MADM-Tumor mice (10/10). The tumors that did form were smaller than MADM-Tumor brains (Figure 3.7a,b). Thus, while the competition between *p53,NF1*-null OPCs and other

OPCs is less than our original model, these OPCs still compete and do form tumors. This suggests that the critical component of the *NF1* gene necessary for competition is the GAP domain. However, because the GAP-dead OPCs still retain some increased competitive fitness and some malignancy, this suggests that the allele is either not completely dead or other domains may contribute to the tumor suppressing activity of *NF1*.

Figure 3.4 Single deletion of *NF1* is sufficient for an increase in OPC competition.
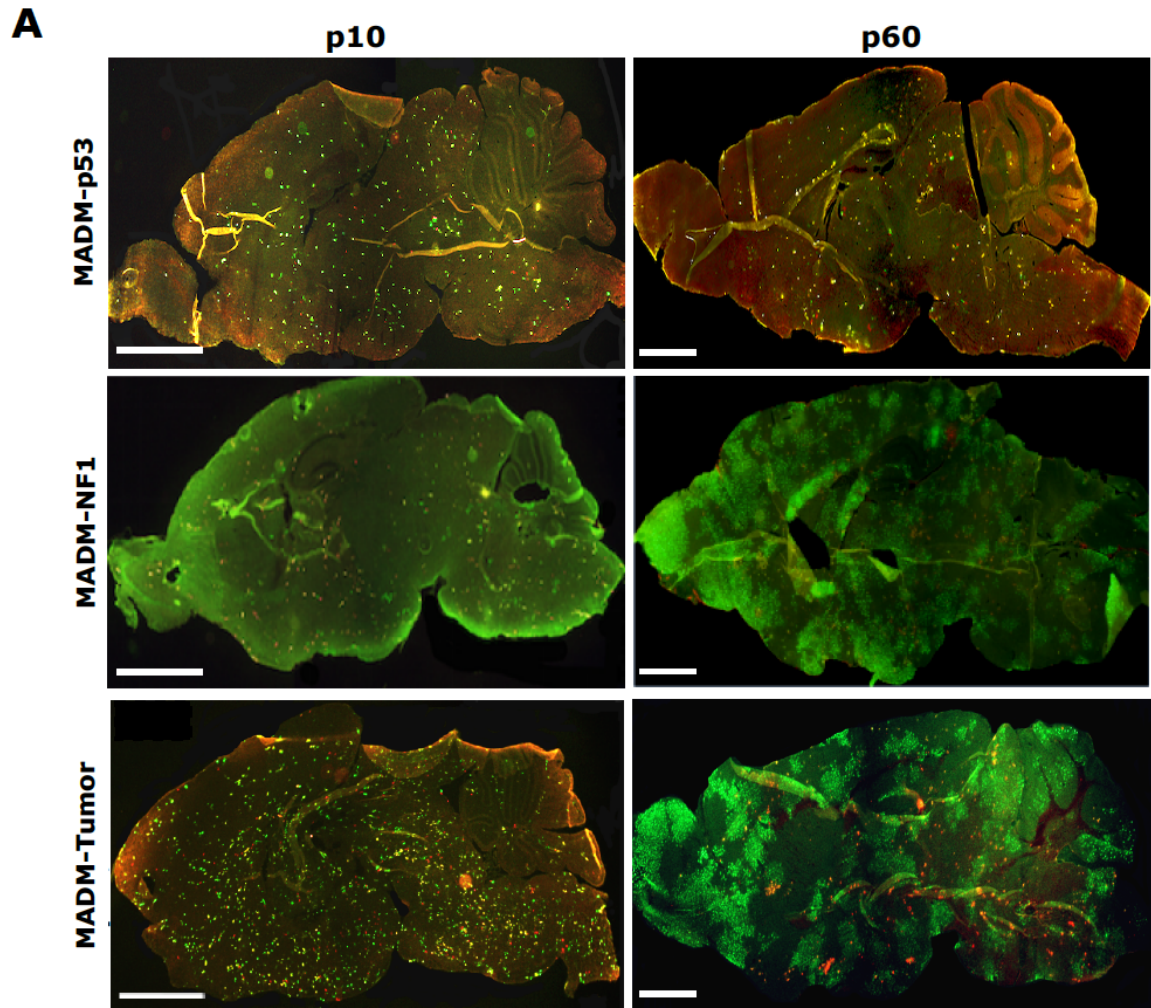
Figure 3.4 Single deletion of *NF1* is sufficient for an increase in OPC competition.

(A) Representative images to show the relative distribution of various OPCs throughout the brain in MADM-*p53*, MADM-*NF1*, and MADM-Tumor brains at both P10 and P60. While MADM-*p53* brains have relatively little change in MADM labeling between P10 and P60 (top), MADM-*NF1* brains (middle) show a sharp increase in GFP+ OPCs between P10 and P60, similar to what is seen in MADM-Tumor brains (bottom). (Scale bar 2 mM)

Figure 3.5 Deletion of *NF1* leads to an increase in the percent of GFP+ OPCs by P60.
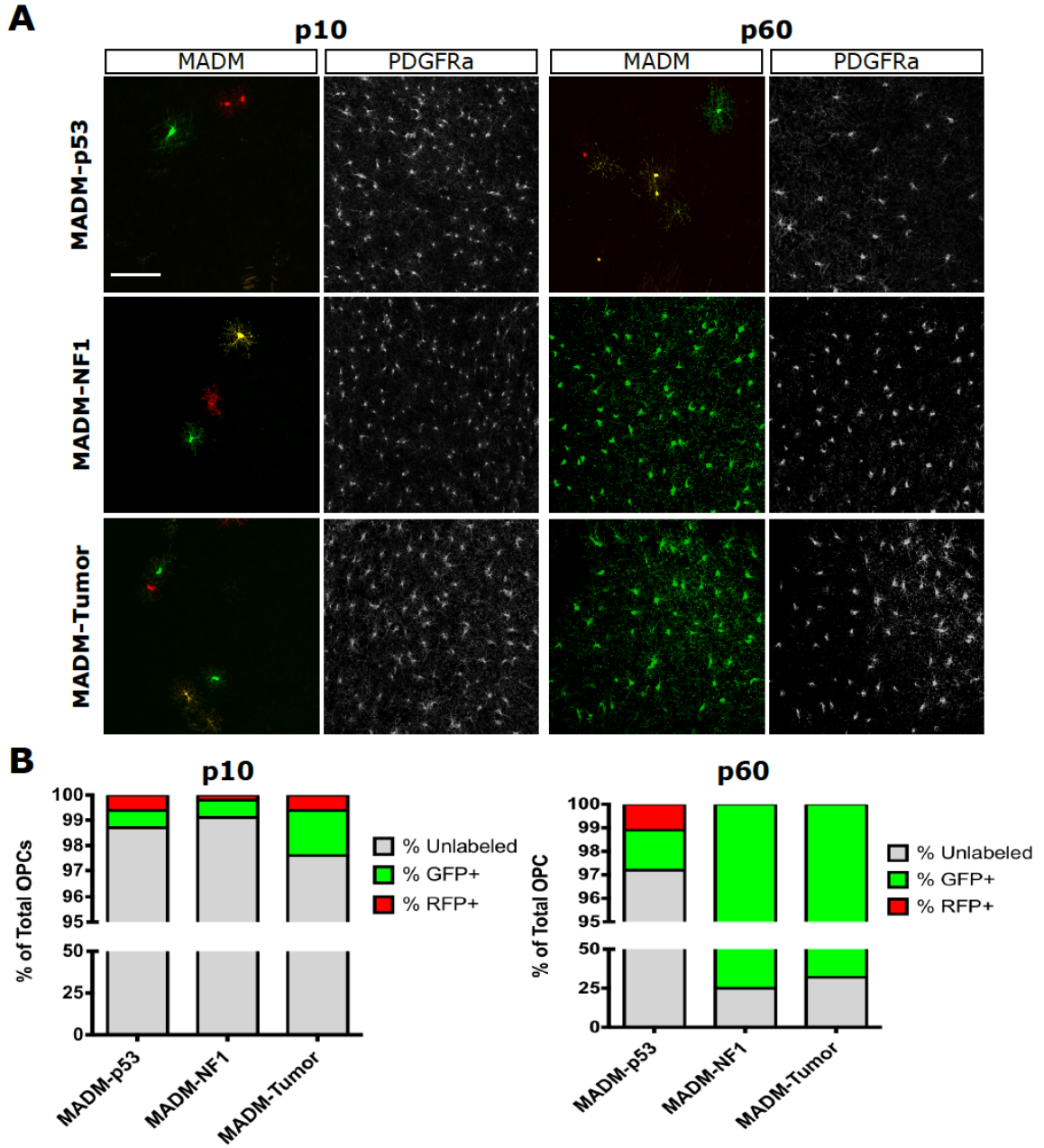
Figure 3.5 Deletion of *NF1* leads to an increase in the percent of GFP+ OPCs by P60.

(A) Representative images to show the relative MADM labeling in the brain at different ages. At P10, MADM-*p53*, MADM-*NF1*, and MADM-Tumor brains have similar levels of MADM labeled cells, and similar numbers of OPCs in the brain. However, by P60, MADM-*p53* brains show little change in the level of MADM labeled cells while MADM-*NF1* brains show similar levels of MADM labeled cells; a majority of these cells are GFP+. Additionally, OPC density has increased in both MADM-*NF1* and MADM-Tumor but not MADM-*p53* brains. All pictures are taken from the anterior cortex. (Scale bar 50 μM)

(B) At P10, MADM-*p53*, MADM-*NF1*, and MADM-Tumor brains were analyzed for the relative distribution of GFP+, RFP+, or YFP/Unlabeled OPCs within the total OPC population. In MADM-*p53*, MADM-*NF1*, and MADM-Tumor brains, less than 4% of the total OPC population was MADM labeled. By P60 (bottom right), MADM-*p53* brains still had a majority (>95%) of non-MADM labeled OPCs in the brain. In contrast, MADM-*NF1* brains had nearly 75% GFP+ OPCs within the total OPC population, similar to MADM-Tumor brains. (n>10)

Figure 3.6 GAP activity is required for inhibiting increased OPC competitive fitness.
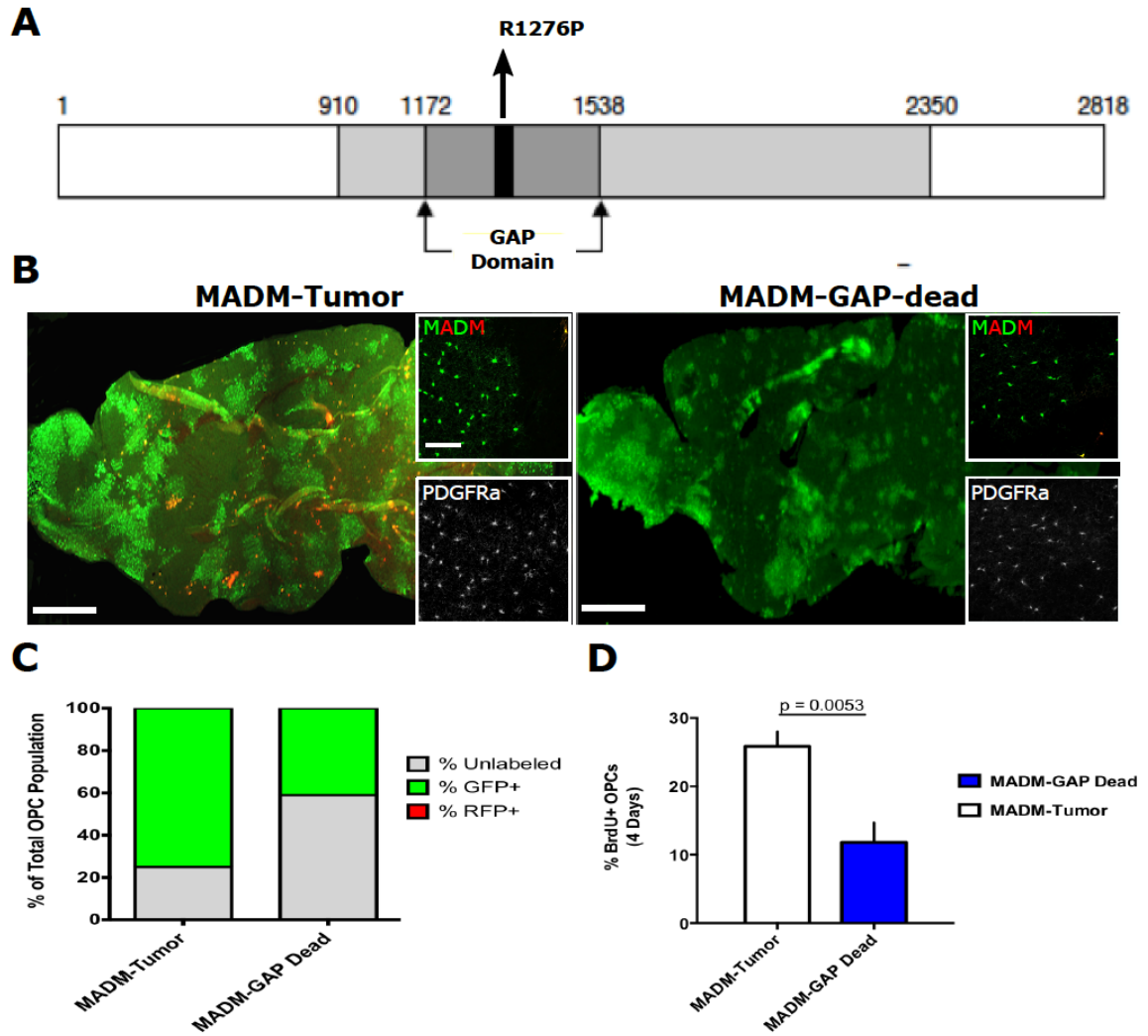
Figure 3.6 GAP activity is required for inhibiting increased OPC competitive fitness

(A) Diagram of the full length NF1 protein, including the GAP domain with the Arginine to Proline mutation at 1276 indicated within the catalytic domain.

(B) Representative images to show the difference in GFP+ clones between MADM-Tumor brains and MADM-GAP-dead brains at P60. While MADM-GAP-dead brains show GFP+ clones, a majority of the clones are smaller in size compared to MADM-Tumor brains. Insets show GFP+ areas (top) and OPC distribution (bottom), all taken from the anterior cortex. (Scale bar 2 mM; Inset 50 µM)

(C) Quantification of the distribution of MADM labeled cells within the total OPC population. While 75% of the OPCs in MADM-Tumor mice are GFP+ OPCs, in MADM-GAP Dead mice, only 50% of all OPCs are GFP+ OPCs at P60, suggesting that GAP-Dead OPCs have slightly lower competitive fitness than *NF1*-null OPCs.

(D) Quantification of the proliferation rate of GFP+ OPCs in both MADM-GAP-dead and MADM-Tumor mice. The proliferation rate of OPCs in MADM-Tumor brains is significantly (p=0.0053) higher than GAP-Dead OPCs. (n>5) Student *t* Test; Error Bar ± SEM

Figure 3.7 GAP activity is required for full tumor suppressing activities
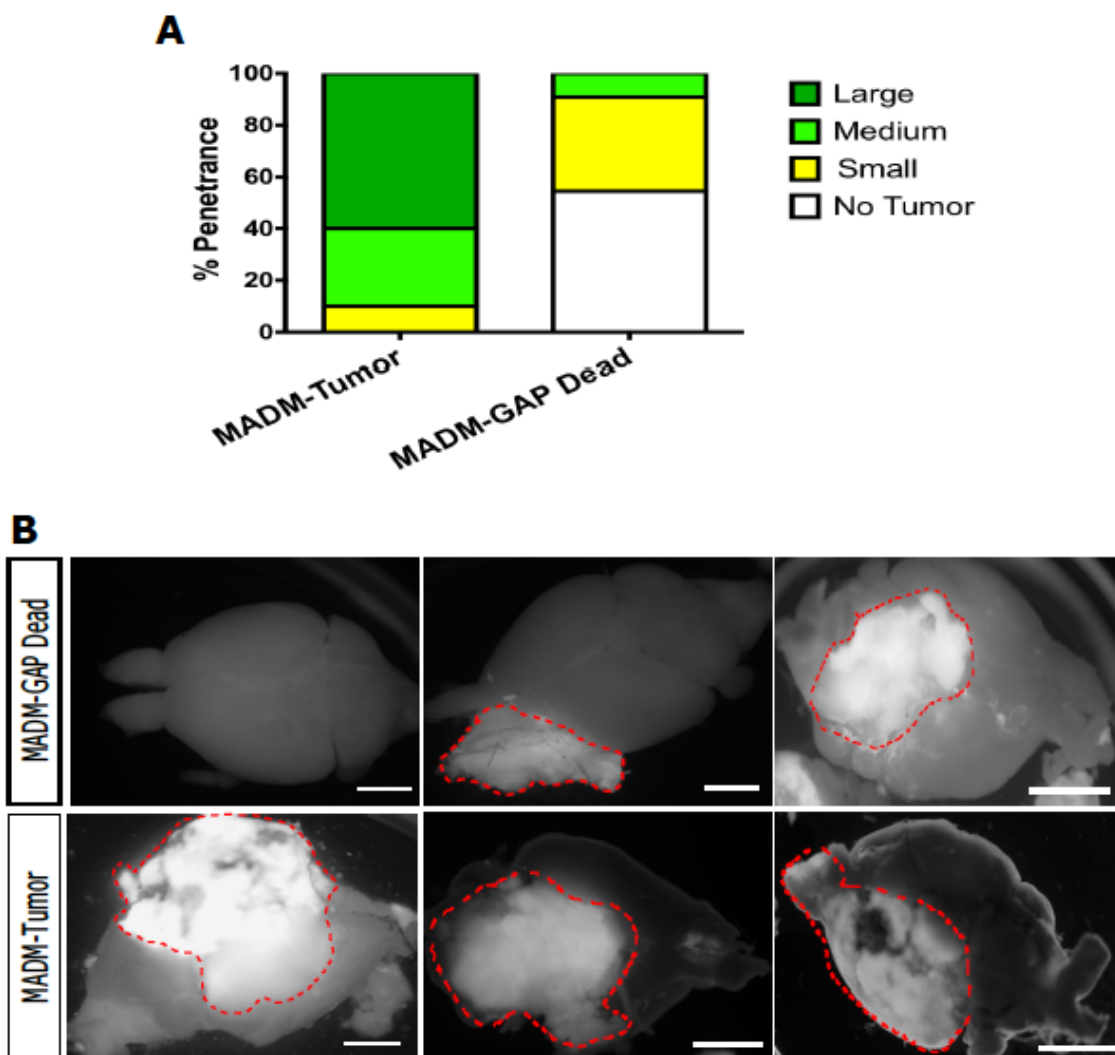
Figure 3.7 GAP activity is required for full tumor suppressing activities

(A) Quantification of the tumors that develop in both MADM-GAP-dead and MADM-Tumor mice. Small represents a tumor roughly the size of a mouse olfactory bulb, medium represents a tumor half the size of one mouse brain hemisphere, and large represents anything that is roughly the size of half of the mouse brain. (n>10)

(B) Representative images showing the average difference in tumor size between the MADM-GAP-dead and MADM-Tumor mice. Tumor boundary is outlined in red. (Scale bar 2 mM)

3.3 Competition is necessary for gliomagenesis.

3.3.1 Design of new MADM system to increase the competitive fitness of non-GFP+ OPCs

It is clear from the previous data that during the initial pre-transforming stages, *p53,NF1*-null OPCs have increased competitive fitness and gradually eliminate other OPCs to take over the brain. However, one critical question is whether or not this competition is necessary for OPC transformation. To address this we needed to designed a new MADM system, in which the competitive fitness of non-GFP+ OPCs could be increased. Because *NF1* deletion leads to the same competition as seen in the MADM-Tumor model while MADM-*NF1* mice never form tumors, we decided to incorporate an additional mutant *NF1* allele in our MADM system (Figure 3.7). We call this model MADM-AC (anti-competition) because all OPCs are *NF1*-null while green OPCs are *p53,NF1*-null, which were predicted to have similar competitive fitness due to the equal *NF1* status (Figure 3.8).

3.3.2 Increasing the competitive fitness of non-GFP+ OPCs blocks gliomagenesis.

First we examined G/R ratio at P10, P60, and P240 in MADM-AC to see if competition is truly eliminated. While MADM-Tumor mice at P10 have already expanded 5-fold over WT OPCs, MADM-AC mice have a G/R ratio of 1 similar to MADM-WT (Figure 3.9a,b left images and left-most bars). By P60, MADM-Tumor mice have a G/R ratio near 150 while MADM-AC again still retain a G/R ratio of 1 (Figure 3.9a,b, middle

images and middle bars). By P240 this ratio remains steady while MADM-Tumor mice have now expanded nearly 300-fold over WT OPCs (Figure 3.9a,b, right images and right-most bars). Thus, the introduction of *NF1* deletion into non GFP+ OPCs blocks the ability of these double-null OPCs to expand over RFP+ OPCs.

However, despite the lack of expansion of *p53,NF1*-null OPCs, because of the deletion of *NF1* globally, the number of OPCs in the brain may have increased substantially compared to both MADM-WT and MADM-Tumor mice. Additionally, if there was an increase in OPC density, the proportion of GFP+, RFP+, and YFP+/Uncolored OPCs could have changed also. To determine this, brains from MADM-WT, MADM-Tumor, and MADM-AC were stained for PDGFRα and the density of total OPCs was quantified. At P10, all three genotypes had similar densities of OPCs, which was not significantly different from one another (Figure 3.10a, left bars). However, at P60, both MADM-Tumor and MADM-AC brains had similar (p=0.36) OPC densities, both of which were significantly higher then MADM-WT brains (p=0.02 & p=0.008, respectively) (Figure 3.10a, right bars). However, the overall increase in OPC numbers is less than 2-fold despite the complete take-over of the OPC population by PreT-OPCs.

Next, we determined the relative proportion of GFP+, RFP+, and YFP+/Uncolored OPCs in these brains. At P10, there was obvious difference in the relative proportions of any of these populations within the total OPC population (Figure 3.10a left most images and 3.10b,c left-most bars). However, at P60 the proportion of GFP+ and RFP+ OPCs in the MADM-AC brain, made up less than 5% of the total OPC population, similar to MADM-WT while a majority (>95%) of the OPCs were still YFP+/Uncolored (Figure 3.10a right images and Figure 3.10b,d middle bars). This is in sharp contrast to MADM-Tumor brains in which a majority (>75%) of all OPCs are p53,NF1-null GFP+ OPCs. This data demonstrates that the deletion of *NF1* in all OPCs

slightly increases OPC density but does not allow for *p53,NF1*-null OPCs to out-compete any other OPCs.

Next we investigated whether GFP+ OPCs could transform into glioma since they still carry *p53* and *NF1* deletions. To examine this, we kept MADM-AC mice until P240, the latency age for the MADM-Tumor model. Of the 15+ mice examined, none of the mice formed tumors while MADM-Tumor mice form tumors at 100% penetrance at this age (Figure 3.11). Thus, these data demonstrate that the expansion of *p53,NF1*-null OPCs is necessary for transformation. It seems likely that the probability of an OPC transforming goes up significantly since the entire OPC population consists almost entirely of *p53,NF1*-null OPCs, thus increasing the pool of cells that have the ability to form a tumor. These data also demonstrate that by blocking the ability of *p53,NF1*-null OPCs to expand, we likely decreased the chance of a cell acquiring the necessary mutations for transformation.

3.3.3 mTOR is critical for expansion of p53,NF1-null OPCs

Because the global deletion of *NF1* led to an inhibition of *p53,NF1*-null OPC competition, we wondered if this competition was mediated through mTOR since mTOR deletion blocked OPC gliomagenesis. To test this we first quantified the G/R ratio of PreT-OPCs at P10, P20, and P60 to determine the range of G/R expansions. Between P10 and P20 the G/R ratio increases nearly 8-fold compared to only a 3-fold increase between P20 and P60 (Figure 3.12a). To maximize *mTOR* inhibition we treated mice starting at P10 every other day until P15 when we treated mice daily with 50mg/kg Temsirolimus (Figure 3.12b, top). To verify that the inhibitor was effective in blocking *mTOR* we examined the levels of phosphorylated-S6 at P12, P14, and P20. Compared

to control, treated animals at all time points had no detectable levels of p-S6 (Figure

3.12b, bottom). When we examined the brains of these mice, Temsirolimus-treated mice

had significantly smaller GFP+ clones compared to control animals (Figure 3.12c).

Additionally, Temsirolimus-treated mice had nearly the same G/R ratio as P10 mice,

which was significantly smaller than P20 control mice (Figure 3.12d). Thus, not only

does the global deletion of *NF1* block *p53,NF1*-null OPC competition, but it appears to

be an *mTOR*-dependent mechanism.

3.8 Design of MADM-Anti Competition (MADM-AC) mouse.
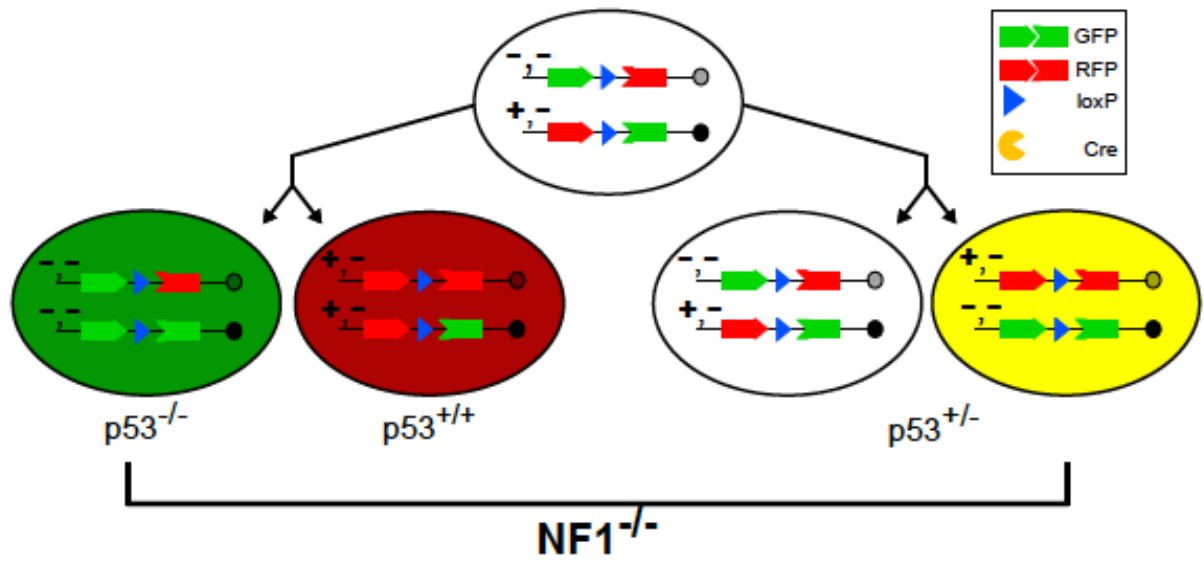
3.8 Design of MADM-Anti Competition (MADM-AC) mouse.

The traditional MADM mouse has one half of the MADM cassette with *p53* and *NF1* mutant alleles while the second half of the MADM cassette is WT for both genes. In the MADM-AC design, one half of the MADM cassette carries the *p53* and *NF1* mutant alleles while the second half of the MADM cassette carries another copy of the NF1 mutant allele. During mitotic recombination and segregation, GFP+ cells will be *p53, NF1*-double null while RFP+ cells will be *NF1*-null. Importantly, the vast majority of cells, which are YFP+/Uncolored initially, will also be *NF1*-null and *p53*-heterozygous.

Figure 3.9 Global deletion of *NF1* in all OPCs leads to a reduction in *p53,NF1*-null

OPC expansion ability.
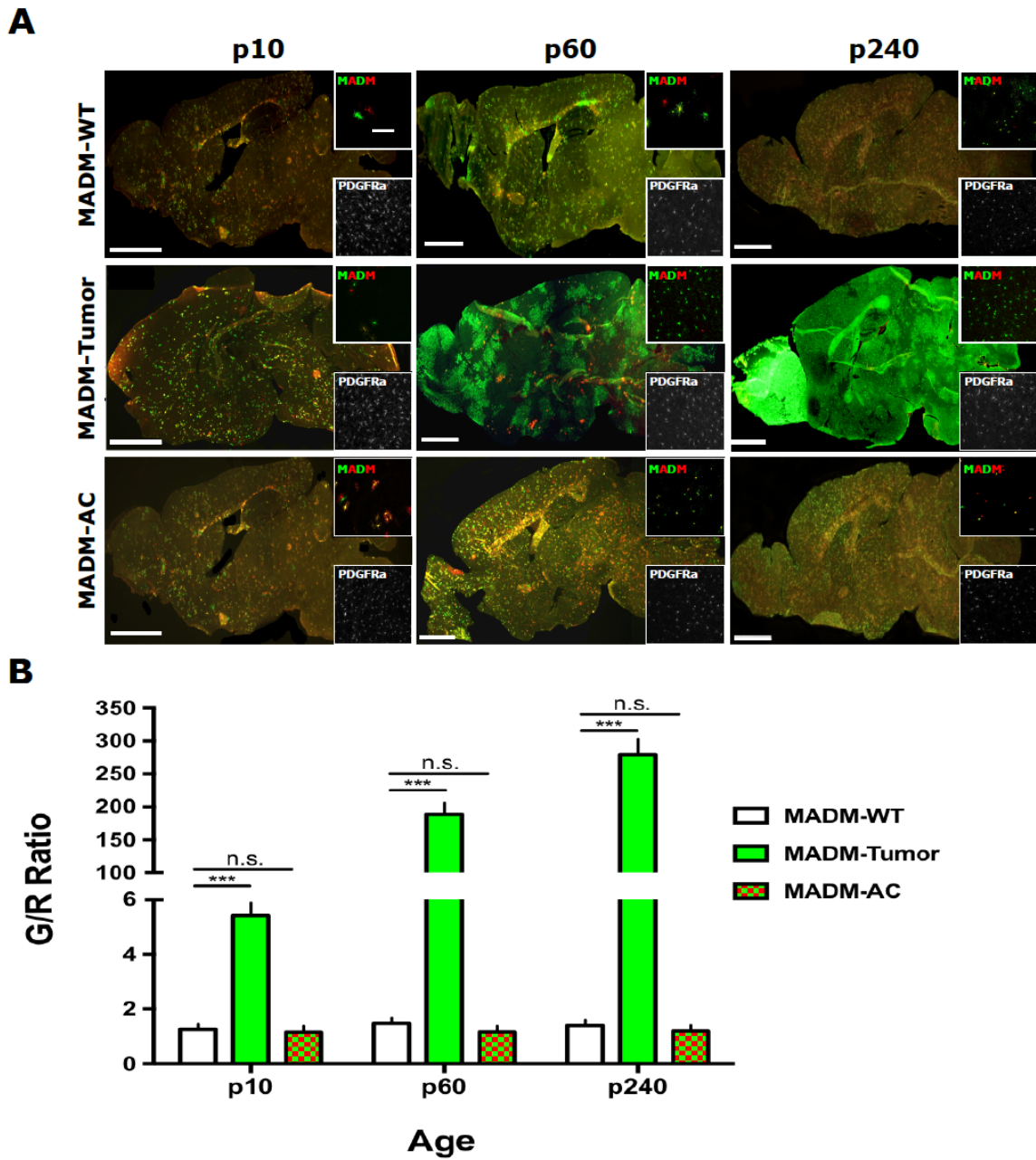
Figure 3.9 Global deletion of *NF1* in all OPCs leads to a reduction in *p53,NF1*-null

OPC expansion ability.

(A) Representative images to show overall MADM distribution throughout the brain.

While MADM-WT brains have relatively little change in MADM labeled cells from P10-

P240, MADM-Tumor brains show a substantial increase in GFP+ cells across this time.

However, MADM-AC brains have similar MADM labeling as MADM-WT brains. Insets

show 20x magnification of MADM (top) and PDGFRα (bottom) staining in anterior cortex.

(Scale bar 2mM; Inset 50µM)

(B) G/R ratios of MADM-WT, MADM-Tumor, and MADM-AC mice were quantified at

P10, P60, and P240. While MADM-Tumor brains showed significant increases in G/R

ratio at all ages, MADM-AC brains had similar G/R ratios to MADM-WT at all ages

examined. (n>10) Student *t* Test; Error Bar ± SEM (*** $P < 0.001$)

Figure 3.10 Global deletion of *NF1* in OPCs leads to an increase in OPC density but a decrease in the percent of OPCs that are *p53,NF1*-null.
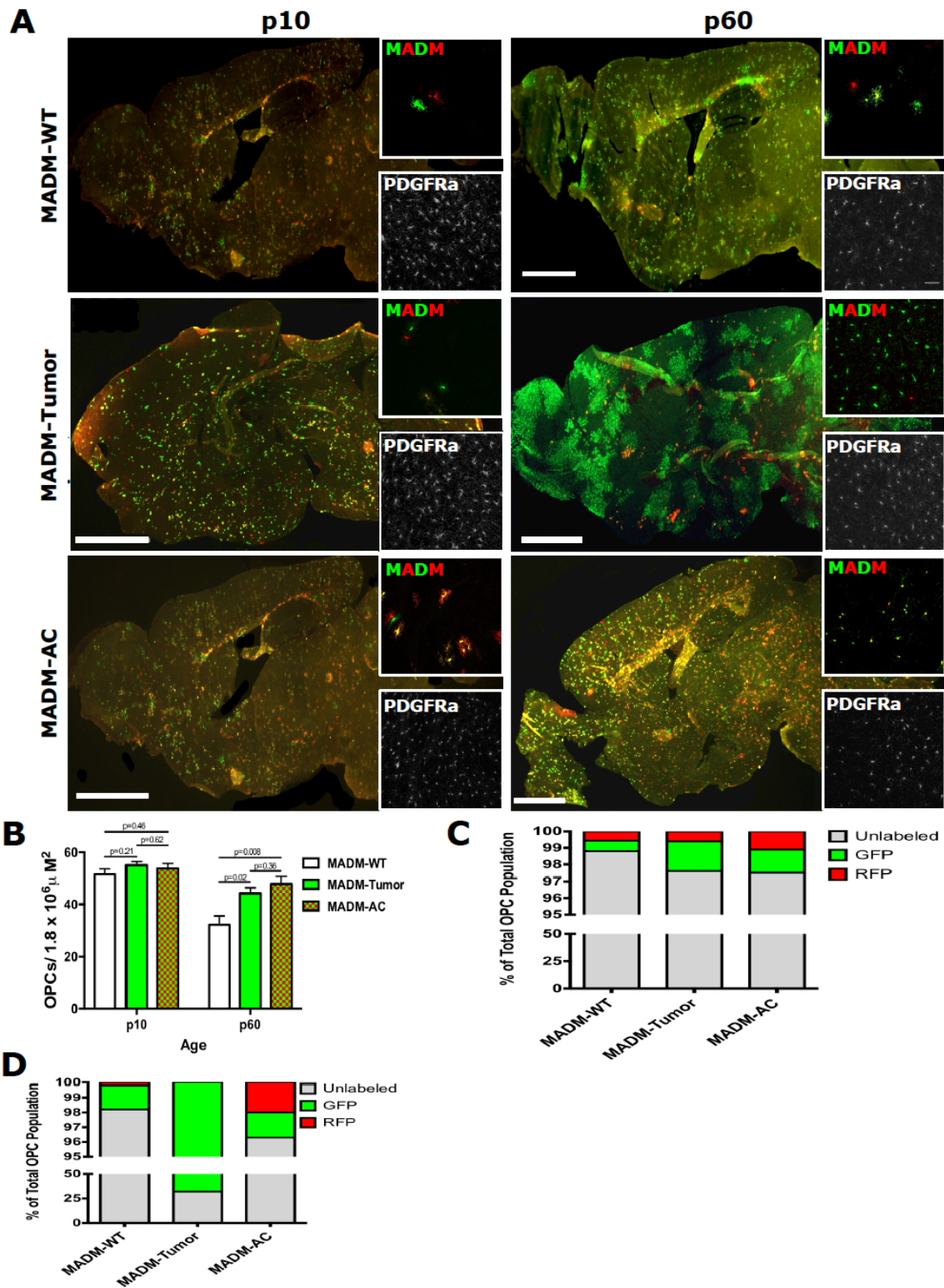
Figure 3.10 Global deletion of *NF1* in OPCs leads to an increase in OPC density but a decrease in the percent of OPCs that are *p53,NF1*-null.

(A) Representative images to show overall MADM distribution throughout the brain. While MADM-Tumor brains show a sharp increase in GFP+ cells from P10 to P60, MADM-AC brains show a similar level of MADM labeling between P10 and P60, similar to MADM-WT brains. Insets show 20x magnification of anterior cortex. Top inset shows MADM labeling (top) while the bottom inset shows OPC labeling (bottom). (Scale bar 2 mM; Inset 50 µM)

(B) Quantification of OPC density at both P10 and P60. At P10, there is no significant difference in OPC density between all three genotypes. By P60, both MADM-Tumor and MADM-AC have a significant increase in OPC density compared to MADM-WT brains. However, there is no significant difference in OPC density between MADM-Tumor and MADM-AC brains. Student *t* Test; Error Bar ± SEM (n>10)

(C) At P10, MADM-WT, MADM-AC, and MADM-Tumor brains were analyzed for the relative distribution of GFP+, RFP+, or YFP/Unlabeled OPCs within the total OPC population. In MADM-WT, MADM-AC, and MADM-Tumor brains, less than 4% of the total OPC population was MADM labeled.

(D) At P60, while MADM-Tumor brains have a majority of GFP+ OPCs (75%), MADM-AC and MADM-WT maintain a low level (>4%) of MADM-labeled OPCs within the total OPC population. This suggests that the increased competitive fitness of non-GFP+ OPCs blocks the expansion ability of GFP+ OPCs.

Figure 3.11 Increasing the competitive fitness of non-GFP+ OPC blocks gliomagenesis.
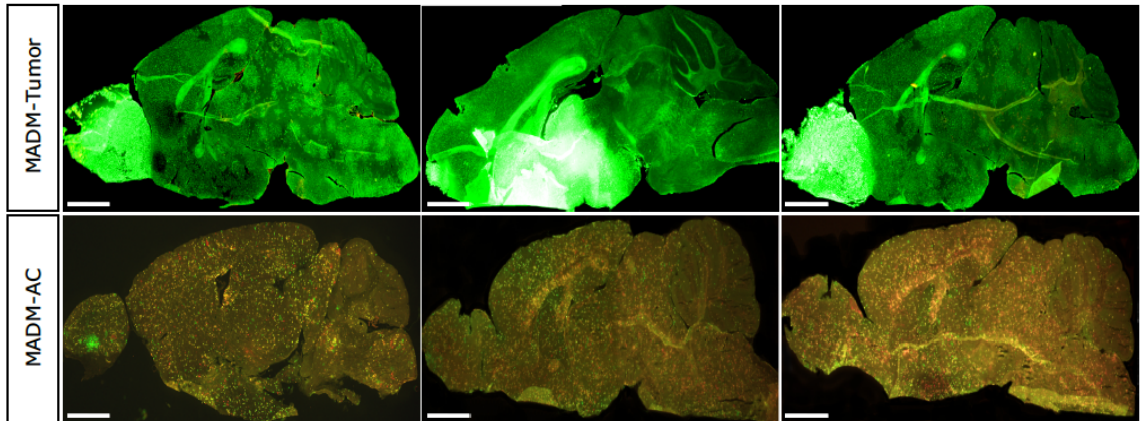
Figure 3.11 Increasing the competitive fitness of non-GFP+ OPC blocks gliomagenesis.

Representative images to show that increasing the competitive fitness of non-GFP+ OPCs, blocks GFP+ OPC expansion. While MADM-Tumor brains have 100% penetrance at P240, MADM-AC brains never form tumors. Thus, the increased competitive fitness of non-GFP+ OPCs blocks tumor formation. Inset shows MADM density at 20x magnification. (n>10) (Scale bar 2 mM).

Figure 3.12 *mTOR* inhibition blocks PreT-OPC competition.
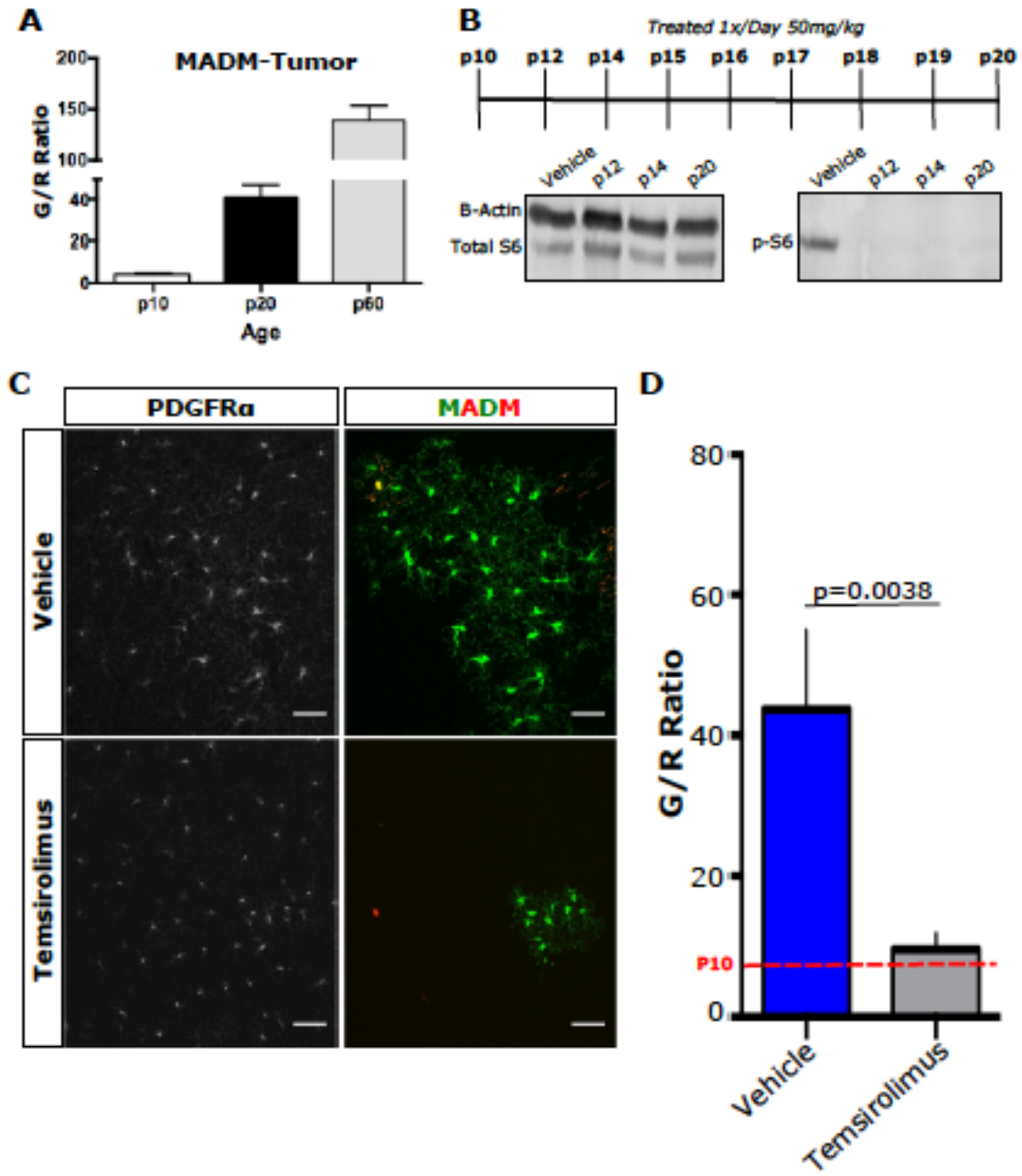
Figure 3.12 *mTOR* inhibition blocks PreT-OPC competition.

(A) G/R ratio of MADM-Tumor mice was measured at P10, P20, and P60 showing an 8-fold increase in G/R ratio between P10 and P60.

(B) Top, Temsirolimus treatment scheme to determine if *mTOR* inhibition blocks OPC competition. Bottom, verification of *mTOR* inhibition in treated mice at P12, P14, and P20.

(C) Following the treatment scheme in panel A, GFP+ clones were compared between treated and control animals. GFP+ clones in control mice are significantly larger than Temsirolimus treated mice. (Scale bar 25 µM)

(D) Quantification of the effect of *mTOR* inhibition shows a significant decrease in G/R ratio compared to control animals. Student *t* Test; Error Bar ± SEM; (n=5)

3.4 OPCs maintain homeostasis after radiation.

3.4.1 Experimental design to test the response of WT OPCs to radiation.

Previous work in both zebrafish and mice have shown that OPCs are highly dynamic cells that can maintain homeostatic cell density through a contact inhibition mechanism (Kirby et al., 2006; Hughes et al., 2013). To determine whether normal OPCs have an innate homeostatic mechanism, which can allow for complete recovery of OPC ablation following radiation, WT mice were treated with 15 Gγ irradiation (IR) at postnatal day 20 and brains were analyzed at a few time points over a 4-week time course. To determine the level of DNA damage, brains were stained with pH2a.X, a DNA damage marker, at 48hrs post-IR (Figure 3.13; first time point). Next, to determine whether OPCs died in response to IR, mice were analyzed at 1-week post-IR and the OPC density was quantified in addition to the percent of proliferating OPCs during a 4-day BrdU pulse (Figure 3.13; second time point). Next, to determine the dynamics of OPC recovery, mice were analyzed at 2 weeks and 4 weeks post-IR and the density of OPCs was quantified in addition to the percent of proliferating OPCs during a 4-day BrdU pulse (Figure 3.13; right 2 time points).

3.4.2 IR causes massive WT OPC death followed by gradual recovery of WT OPC density.

To determine the effect of IR on OPCs, we first treated P20 mice with 15 Gγ IR and then analyzed 48 hrs after radiation. Not surprisingly, more than 90% of all OPCs

were pH2a.X+, a known histone mark for DNA damage (Fig 3.14a). Knowing that a majority of OPCs had DNA damage following IR, we then waited 1 week and analyzed mice to determine the effect of the DNA damage on OPC numbers. Within 1 week, most NG2+, PDGFRa+ OPCs had been eliminated from the cortex compared to control animals (Figure 3.14b & 3.15a; left-most pictures and left bars). Additionally, there was no significant difference in the percent of proliferating OPCs at 1 week compared to controls (Figure 3.15b; left-most bars). Thus, the DNA damage sustained by OPCs initially caused massive cell death of OPCs. However, within 2 weeks, the density of OPCs had recovered to nearly 70% of the levels of control animals with a more than 5-fold increase in OPC proliferation (Figure 3.14b & 3.15a,b; middle pictures and bars). And by 4 weeks, OPCS numbers recovered to the same density as control animals including a restoration of normal OPC proliferation rates (Figure 3.14b & 3.15a,b; right-most pictures and bars).

3.4.3 Re-populating OPCs are derived from resident OPCs.

However, one possible explanation for the sharp decrease in OPC numbers is that both PDGFRα and NG2 expression are decreased following radiation. Additionally, the recovery of OPCs at 2 weeks could be from either surviving OPCs in the cortex or from neural stem cells (NSCs) residing in the SVZ. To address these issues we then used a tdTomato reporter under the control of NG2-CreER, an OPC-specific Cre that we have previously shown labels only OPCs but never NSCs (Galvao et al., 2014). At P10, mice were injected with Tamoxifen every other day for 8 days, followed by IR at P20,

and then analysis at 1 week and 2 weeks to determine if these cells are truly ablated

and if they come from tdTomato+ OPCs (Figure 3.16a). 1 week following IR, most of the

tdTomato+ cells are gone and the few remaining cells are PDGFRα+, thus showing that

OPCs are truly ablated after IR (Figure 3.16b). 2 weeks after IR, all of the PDGFRα+

cells in the ablated areas are also all tdTomato+ demonstrating that the recovering

PDGFRα+ cells in these areas come from tdTomato+ OPCs that survived the initial IR

(Figure 3.16c). Thus, the ability of OPCs to sense one another and recover from

grievous insults, such as IR, is an innate property of normal OPCs.

Figure 3.13 Experimental design to test the response of WT OPCs to Irradiation.

p20	48hrs	1 Week	2 Weeks	4 Weeks
Irradiation	DNA Damage	OPC Death	OPC Recovery	OPC Homeostasis
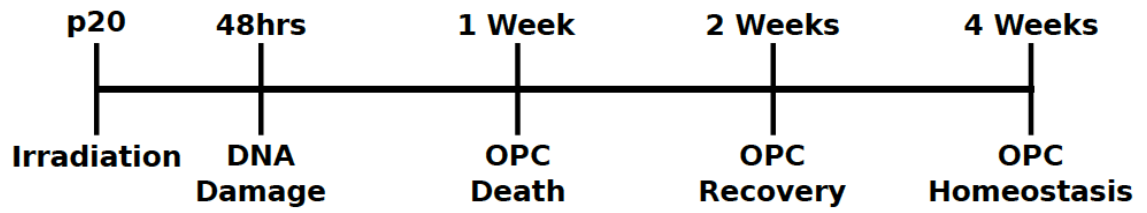
Figure 3.13 Experimental design to test the response of WT OPCs to Irradiation.

Mice were treated with 15 Gγ IR at P20 and then analyzed at various time points. At 48hrs mice were analyzed for DNA damage using pH2a.X, a DNA damage marker. 1 week following IR, the density of OPCs was analyzed. 2 weeks following IR, the density and proliferation of OPCs was analyzed. 4 weeks following IR, the full-recovery of OPC density and proliferation was analyzed.

Figure 3.14 Following IR, OPCs undergo cell death followed by gradual recovery.
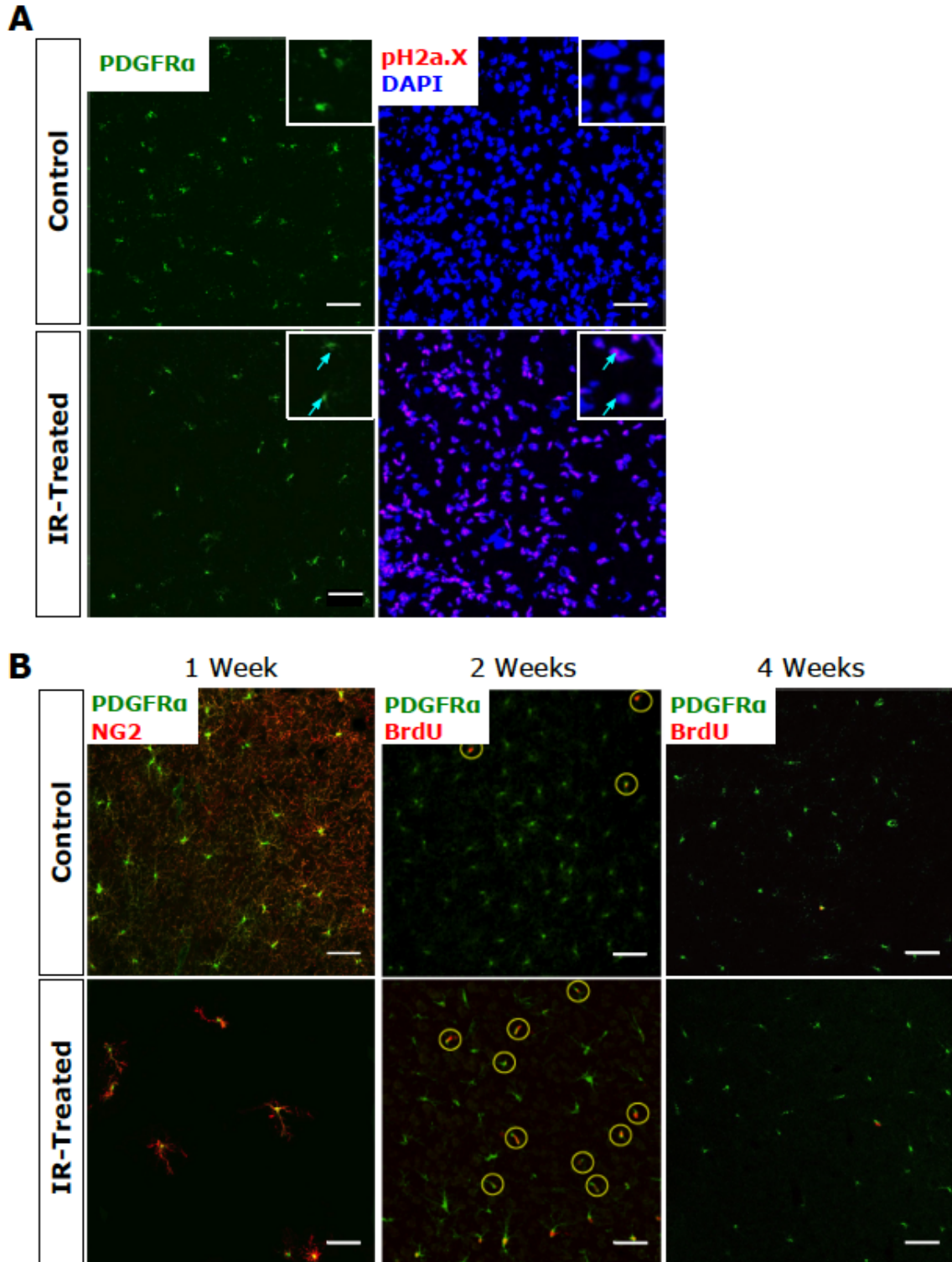
Figure 3.14 Following IR, OPCs undergo cell death followed by gradual recovery.

(A) 48hrs after IR, the level of DNA damage was compared between control and IR-treated animals. Compared to control animals, over 90% of OPCs in the IR-Treated were pH2a.X+, indicating DNA damage. Insets show zoomed in pictures with arrows indicating PDGFRa+, pH2a.X+ OPCs.

(B) 1 week following IR, OPC density in treated mice has significantly decreased in comparison to control animals. Within 2 weeks following IR, OPC density has increased significantly, to almost control animal levels. Additionally, a majority of OPCs in the brain are proliferating OPCs, as determined by BrdU labeling. 4 weeks following IR, OPC density had returned to control levels. Additionally, the percent of BrdU+ OPCs has slowed to control levels by this time. (n=5) (Scale bar 25 µM)

Figure 3.15 Quantification of OPC response to IR.
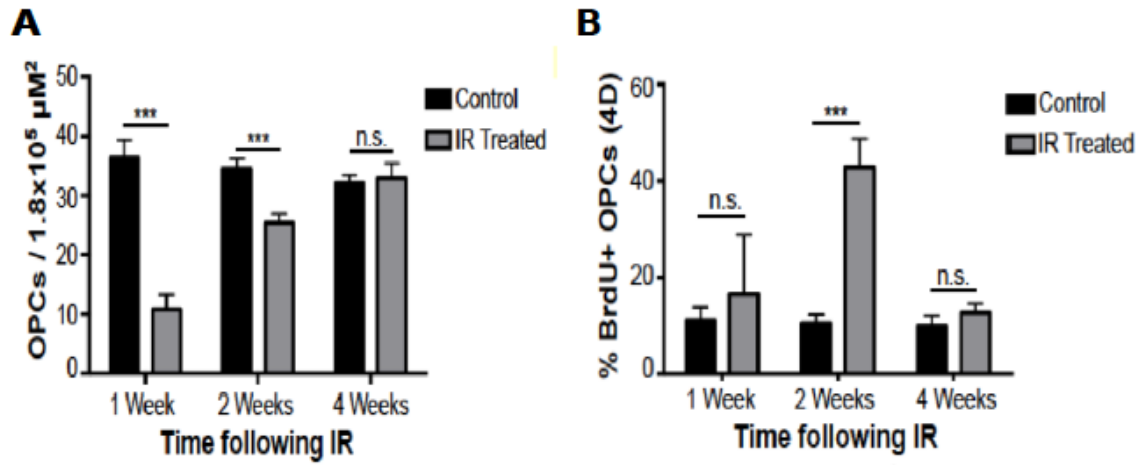
Figure 3.15 Quantification of OPC response to IR.

(A) OPC density at both 1 week and 2 weeks following IR was significantly (p<0.001) decreased compared to control animals. However, by 4 weeks, OPC density had returned to control levels.

(B) 1 week after IR, OPC proliferation was not significantly different compared to control animals. 2 weeks after IR, OPC proliferation was significantly (p<0.001) increased compared to control animals. By 4 weeks, OPC proliferation returned to normal levels, compared to control animals. (n=5) Student *t* Test; Error Bar ± SEM (*** *P* < 0.001)

Figure 3.16 Recovering OPCs are derived from resident OPCs.
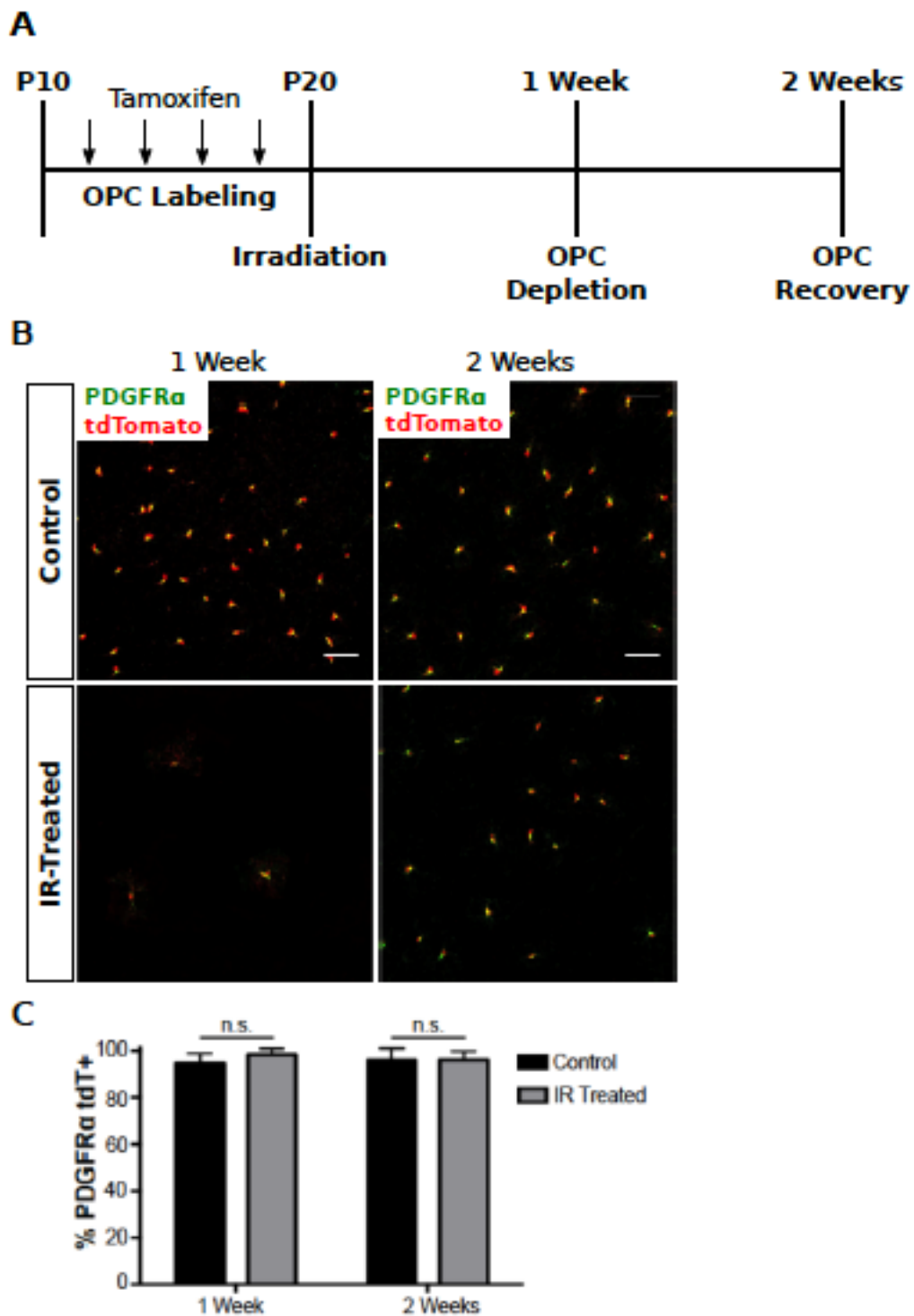
Figure 3.16 Recovering OPCs are derived from resident OPCs.

(A) Mice were treated with Tamoxifen every other day for 8 days starting at P10, to label all OPCs. At P20 mice were treated with 15 Gγ IR and then analyzed at various time points. 1 week following IR, mice were analyzed for the percent of tdT+ OPCs to determine if the elimination of PDGFRα+ cells was truly OPC elimination. 2 weeks following IR, the percent of tdT+ OPCs out of the total OPC population was quantified. (Scale bar 25 µM)

(B) 1 week following IR, tdT+ OPCs in IR-treated brains were ablated compared to control animals. By 2 weeks following IR, all OPCs in the brain are tdT+ OPCs, demonstrating that all OPCs are derived from native OPCs.

(C) Quantification of the percent of tdT+ OPCs within the total OPC population. At 1 week post-IR, nearly all OPCs are tdT+ in both control and IR-treated animals. At 2 weeks post-IR, nearly all OPCs in both control and IR-treated animals are tdT+. (n=5) Student *t* Test; Error Bar ± SEM

Discussion:

Glioma is particularly devastating for two reasons. First, A common problem in glioma treatments is the ability of tumor cells to relapse following treatment. However, the mechanisms by which the tumor cells are able to relapse remain unclear. One idea is that residual tumor cells are slow dividing cells, which allows them to escape the damaging effects of most chemotherapies and radiation due to their prolonged cell cycle time. However, there is no concrete evidence to support this hypothesis at this time. Second, low-grade glioma inevitably progress into high-grade tumors despite any kinds of intervention. Now the revelation of OPC competition could provide a novel interpretation of these problems, and also raise the possibility that the traditional cell-killing agents could fuel the cancer evolution process. Therefore, an anti-competition therapy would be needed for effective glioma prevention or even treatment.

D3.1 Expansion of p53,NF1-null OPCs creates precancerous field.

Previous studies have shown that during the progression from premalignant to malignant tumors, there is a progressive change in the make-up of the tissue (Braakhuis et al., 2003; Dakubo et al., 2007; Slaughter et al., 1953). The precancerous field, as it is referred to, allows for an accumulation of mutant cells in the host tissue. With this accumulation of cells, the probability of further mutations significantly increases as well. In our model, following the deletion of both *p53* and *NF1*, mutants OPCs quickly out-compete surrounding OPCs and completely overtake the brain parenchyma. This expansion creates a pool of mutant OPCs, one of which can gain further mutations that allow for transformation. However, by blocking the ability of *p53,NF1*-null OPCs to create

a precancerous field, we show that you can effectively block gliomagenesis, thus indicating that the precancerous OPC field is necessary for gliomagenesis.

D3.2 NF1 regulates OPC competition.

While other studies have shown that many of the regulators of cell competition are pathways heavily involved during development, we were able to demonstrate that *NF1* is a critical component of OPC competition. Although *NF1* is most commonly associated with Ras signaling, our NF1-GAP Dead data show that the ability of OPCs with loss of NF1-GAP activity do not compete as well as *NF1*-null OPCs. However, this lower level of competition could be due to several different reasons. Because the NF1-GAP Dead protein has not been studied extensively, we do not know whether this protein acts in a dominant negative fashion. If this is the case, the lack of complete competiveness of NF1-GAP Dead OPCs could be explained since all of the YFP+/Uncolored OPCs carry one copy of the NF1-GAP Dead allele and a WT NF1 allele. If the NF1-GAP Dead protein does interact in a dominant negative fashion, it could be creating YFP+/Uncolored OPCs with reduced GAP activity, thus making them more competitive, which blocks the competition of green OPCs (Figure 3.17a vs. 3.17b). A second explanation could be that the NF1-GAP Dead protein is not truly "Dead" and there may be residual GAP activity. However, the fact that GAP-Dead OPCs have increased competitive fitness and some can form tumors, suggests that OPC competitive fitness is regulated in part by the GAP domain of *NF1*. Thus, we have found a new gene that regulates cell competition.

Figure 3.17 Dominant negative schematic for NF1-GAP Dead allele
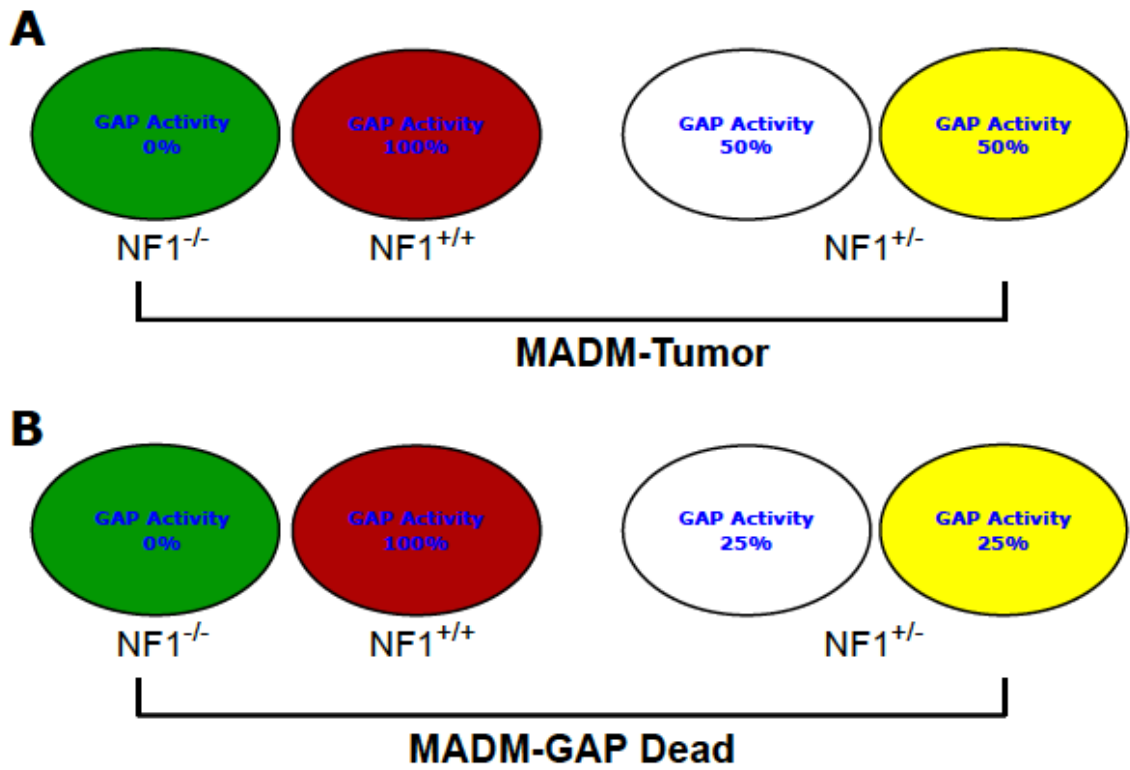
Figure 3.17 Dominant negative schematic for NF1-GAP Dead allele

(A) NF1-GAP activity for traditional MADM-Tumor model. GFP+ cells have 0% of NF1-GAP activity while RFP+ cells have 100%. YFP+/Uncolored cells have 50% NF1-GAP activity due to deletion of one *NF1* allele.

(B) NF1-GAP activity for MADM-NF1-GAP Dead model. If the NF1-GAP Dead allele is a dominant negative it could create YFP+/Uncolored cells that have reduced NF1-GAP activity despite have one *NF1* allele. This can be explained if the GAP-Dead allele interacts or interferes with the WT allele, thus reducing the level of NF1-GAP activity overall in the heterozygous population.

D3.3 OPC competition is necessary for transformation.

While competition has been shown to regulate mainly developmental processes or organs that continually self-renew, here we demonstrate that OPC competition is necessary for gliomagenesis. While many other studies show that competition occurs during development, we show that OPC competition is not developmentally regulated, as this process continues into adulthood (Bondar and Medzhitov, 2010; Clavería et al., 2013; Johnston et al., 1999). This continuation is a necessary process for OPC transformation and eventually manifests itself through tumor formation, a never yet seen phenomenon in cell competition. However, why this process is necessary for gliomagenesis remains unclear. The most plausible explanation is that through the elimination of non-mutant OPCs, the double-null OPCs are able to generate a large enough population that allows for further oncogenic changes necessary for transformation (Huszthy et al., 2012; Maher et al., 2001). Regardless, it is clear that cell competition is critical for transformation and this phenomenon should be exploited for future therapies. We demonstrated that by increasing the competitive fitness of non GFP+ OPCs, the ability of GFP+ cells to expand and transform was eliminated. Rather than trying to eliminate tumor cells that can always come back and eliminate more non-tumor cells, perhaps we should try to increase the ability of non-tumor cells to compete with tumor cells. However, how this can be harnessed for future therapies remains to be seen.

One promising area is to use cytostatic drugs such as mTOR inhibitor to block OPC competition as shown in Figure 3.10. There is an apparent paradox between this finding and our data showing the lack of mTOR activation at the population level (Figure 2.17). One explanation for this paradox is that rather then all PreT-OPCs having

elevated levels of *mTOR* signaling, there is random activation in individual OPCs that leads to GFP+ clones forming. If this is the case then only a few cells would give rise to the large clones seen by P60 and would explain why we never see elevated levels of *mTOR* signaling at P10 via protein analysis. However, the possibility remains that there may be higher levels of *mTOR* signaling in all PreT-OPCs at P10 but that the levels of all the other OPCs is lower due to the mixed population and cell competition. In this case, *mTOR* signaling would appear normal due to a select few GFP+ OPCs having high levels while the rest have lower levels than WT OPCs.

D3.4 Sensing between OPCs is an innate OPC mechanism.

Finally, we have found that while OPCs are susceptible to elimination through common tumor therapies (IR), permanent elimination of OPCs is not possible without the complete eradication of all OPCs. Previous work has shown that there are differences in OPC response to IR depending on the age of the animal, but no one has examined the repopulation of OPCs using lineage tracing (Foote and Blakemore, 2005; Fukuda et al., 2005; Irvine and Blakemore, 2007). Additionally, while we showed that OPCs within the cortex and olfactory bulb disappear within 1 week following IR, OPCs in the midbrain, thalamus, hypothalamus, and basal forebrain were not immediately responsive to IR-induced cell death. This suggests regional differences in OPC responsiveness, which is consistent with previous studies showing that there are different populations of OPCs within the brain with different functions (Dimou and Wegner, 2015; Dimou et al., 2008). Furthermore, the regenerative ability of WT OPCs suggests that understanding basic OPC properties may be beneficial for future glioma therapies, since their intrinsic ability to regenerate may be the reason for glioma relapse. While we tend to think that tumor

cells are resistant to IR because of the multitude of changes that they have undergone, it seems possible that Tu-OPCs are simply resistant to IR due to the nature of this population of cells. Thus, designing therapies that target OPC regeneration rather than tumor cell properties could prove effective against glioma relapse.

Chapter 4: Perspectives

In this thesis project, I have described the individual roles of *p53* and *NF1* during OPC transformation and the efficacy of gene restoration in tumor OPCs. Additionally, I have shown that there is competition between mutant and WT OPCs and this process is essential for gliomagenesis. However, despite the observations made, critical questions still need to be answered. During gliomagenesis, what is the critical change between pre-transforming OPCS and tumor OPCs? Does *Rb* contribute to PreT-OPC transformation? What role does *NF1* play in OPC competition during gliomagenesis? How do pre-malignant OPCs sense WT OPCs? The answers to these and other questions should help with new therapeutics and better outcomes for glioma patients.

4.1 What critical changes are needed for pre-malignant OPC transformation?

4.1.1 Are there changes at the DNA level that signal OPC transformation?

With our current data we can only analyze the properties of pre-transforming OPCs and tumor OPCs. However, the critical moment when OPC transformation initially occurs has not yet been analyzed. Understanding how these pre-transforming OPCs undergo transformation is critical for future therapies since these critical changes are most likely essential for gliomagenesis. Additionally, by studying these pre-malignant stages further, we can better understand the properties of OPCs that allow them to transform. This will help not only cancer biology but may also be important for other OPC-related diseases such as multiple sclerosis.

One possibility is that pre-transforming OPCs have decreased genomic stability due to the deletion of *p53* since *p53* is known to increase genomic stability. Thus, *p53* deletion could simply allow for an accumulation of genomic abnormalities that may result in OPC transformation. To test this, MADM-Tumor mice would be analyzed at various ages for genomic abnormalities. Starting at P90, mice would be analyzed every month until small lesions are present in the brain. Because the adult mouse brain cannot be efficiently dissociated, laser capture microscopy would be employed to capture pre-malignant OPCS. Genomic sequencing could be performed to determine the relative changes in the genome. Because, the amount of cells that would be captured during this process is low, a highly sensitive sequencing technique would need to employed due to the small starting material. *NG2*-eGFP mice would be used as a control and analyzed at the same time point in order to give a baseline to which pre-transforming OPCs would be compared. By comparing MADM-Tumor samples along the timeline, we could determine which genes are altered early during the pre-malignant stages and eventually which genes are commonly mutated in the early stages of OPC transformation. If there are commonly mutated genes, further experiments would need to be carried out to determine their importance to OPC transformation by either overexpressing or knocking down these genes of interest.

4.1.2 Are there changes at the RNA and/or protein level that signal OPC transformation?

A second possibility is that pre-transforming OPCs have changes at the transcriptomic level due to *NF1* deletion. It has been shown that *NF1* deletion in OPCs leads to an increase in *p53*-dependent cell-cycle arrest and senescence, owing to the aberrant oncogenic signaling present in these cells (Lloyd and Raff, 2001). Thus, *NF1*

deletion may lead to overall transcriptomic and ultimately proteomic changes in PreT-OPCs.

Similar to the previous experiment, MADM-Tumor mice would be analyzed at various ages for RNA and protein changes every month until small lesions form. Again, laser capture microscopy would be employed to capture cells from these small lesions and these cells would undergo both RNAseq and protein analysis with *NG2*-eGFP cells serving as a control.

If there are high levels of altered gene expression in small tumors, protein levels of these pathways and their downstream targets would be analyzed. One possibility is that while the RNA levels change, protein levels may stay the same as controls due to unaffected regulators. However, if both RNA and protein levels change, it could mean that these pathways are critical for PreT-OPC transformation. Interestingly, if the genomic sequence of these genes is unaffected, yet RNA and protein levels change, it could mean that activators/inhibitors of these pathways may be the critical components for transformation or that there are epigenetic changes that account for these changes. Furthermore, the microenvironment may play a role in RNA and protein levels and further experiments would need to be carried out to determine this possibility.

4.1.3 Is RB the critical change needed for transformation?

While *p53* and *NF1* deletion drive pre-transforming OPC proliferation and loss of differentiation, their remains to be seen if the third signaling pathway plays a role in OPC transformation. Because nearly 80% of all glioma patients harbor mutations in the *RB* signaling pathway, it may be that the change between pre-transforming and tumor OPCs is a change in *RB* signaling. This change could be a result of the decreased genomic

stability due to *p53* deletion. However whether this change is necessary or if the changes in these pathways follow a sequential order is not known.

To address this, tumor OPCs would first be analyzed for changes in the canonical *RB* signaling pathway genes, specifically *CDK4*, *CDKN2A*, and *CDKN2B*. If this signaling pathway is mutated in a majority of tumors derived from MADM-Tumor mice, then that would suggest that this pathway may be necessary for OPC transformation. However, if this signaling pathway is not critical, then we would expect to see some degree of mutation within the pathway but this would not be consistent or significant compared to other changes. It would be surprising if this pathway were not mutated given the high propensity for *RB* signaling pathway mutations in human samples. Furthermore, if this signaling pathway was altered, functionally restoring *Rb* in tumor cells and determining if they stop Tu-OPC progression or deleting *Rb* in PreT-OPCs to determine if transformation occurs faster, could be carried out to further investigate *Rb*'s role in OPC transformation.

4.2 Role of *NF1* in OPC competition?

Data presented in Chapter 3 show that the deletion of *NF1* mediates OPC competition and that this process is at least partially regulated by the GAP domain of *NF1*. However, whether this domain is the only functional domain in *NF1*'s role during competition is unclear. While *NF1*-GAP-dead OPCs do display increased competitive fitness, there are clear differences in their ability to expand compared to *NF1*-null OPCs. First, the *NF1*-GAP-dead OPCs show significant decreases in proliferation (11.83 ± 2.89 vs. 25.85 ± 2.14) and expansion within the OPC population (49.15 ± 4.54 vs. 73.34 ± 2.74), which suggests that these OPCs may have decreased competitive fitness.

Additionally, while MADM-Tumor mice form tumors with 100% penetrance, MADM-GAP-dead mice had less then a 50% penetrance rate. These data suggest that while *NF1* deletion does promote OPC competition, the exact mechanism of *NF1* mediating competition may be outside *NF1*'s GAP function. Thus, understanding how NF1 mediates OPC competition during gliomagenesis should provide new insights for use in future therapeutics.

4.2.1 Functionality of NF1-GAP-dead allele.

Our data show that while the role of *NF1* in OPC competition is critical, whether or not *NF1*'s GAP activity is the only component in *NF1*'s control of competition is unclear. While MADM-GAP-dead mice showed expansion of pre-transforming OPCs and eventual transformation in some mice, the penetrance and expansion rates were significantly reduced. This suggests that the *NF1*-GAP-dead allele may not completely abolish GAP function and/or that this allele may act in a dominant negative fashion. Regardless of which holds true, the functionality of the *NF1*-GAP-dead allele is critical since this will provide insights into whether *NF1* mediates OPC competition in a *Ras* dependent fashion.

To test whether this allele is truly GAP-dead, mutant OPCs homozygous for this allele and mutant OPCs homozygous for the *NF1*-null allele could be compared to determine the relative percent of activated Ras. Mutant OPCs would be purified and a Ras pull-down would be performed to determine the relative levels of GTP vs GDP-bound Ras. If the *NF1*-GAP-dead allele does not completely abolish NF1's GAP activity, the amount of GTP-bound Ras would be lower than the amount of GTP-bound Ras in

NF1-null OPCs. If the NF1-GAP-dead allele does in fact abolish *NF1* GAP activity, then the amount of GTP-bound Ras should be the same between both populations of OPCs.

By understanding the function of the NF1-GAP-dead protein, we can determine whether the decrease in expansion is due to if *NF1* has functions outside its GAP activity that play a role in OPC competition or if the NF1-GAP-Dead protein acts in a dominant negative function (see 4.2.2). If there are domains outside it's GAP domain that are vital for competition, then understanding these would be vital for understanding *NF1*'s role as a TSG. This could be a major change in *NF1* biology since most studies look at *NF1*'s role as a RasGAP.

4.2.2 Why do mutant OPCs in MADM-NF1-GAP-dead model compete less effectively than those in MADM-NF1-null model do?

There are two possible explanations for why MADM-p53,NF1-GAP-dead mice had reduced competition of mutant OPCs and exhibited reduced malignancy in comparison to MADM-p53,NF1-null mice. On one hand, it is possible that NF1-GAP-dead/NF1-GAP-dead OPCs are less competitive than NF1-null OPCs, i.e. weaker aggressors. On the other hand, it is equally possible that NF1-GAP-dead/+ OPCs are more resistance to competition than NF1-/+ heterozygous OPCs.

Regardless of the GAP activity of the *NF1*-GAP-dead allele, there may be a difference in the competitive fitness of these OPCs compared to *NF1*-null OPCs. There is the possibility that there are inherent differences in these two populations of OPCs similar to the differences between different populations of tumor cells. Maybe a region outside of the GAP domain is critical for OPC competition and thus, *NF1*-null OPCs are

more competitive then *NF1*-GAP-dead OPCs. Or perhaps these two populations are as competitive as one another and the differences are simply the microenvironment in which they reside.

To understand whether these two populations of OPCs have differences in their competitive fitness, both *NF1*-null and *NF1*-GAP-dead OPCs can be purified and grown in vitro in a co-culture assay. Starting with a 1:1 ratio, these cells can be mixed at various ratios and the percent of proliferating and dying OPCs can be assessed using an EdU pulse and staining for TUNEL. Because we can purify OPCs with different colors using our transgenic models, one population can be colored while the other population can be purified from a non-colored background. If one population is more competitive then the other, then there should be decreased proliferation and increased cell death in the less competitive OPC population. However, if they have the same level of competitive fitness, then the percent of dying and proliferating OPCs should be similar. Additional studies would be needed to determine whether rescue of the *NF1*-GAP domain could block competitive fitness or whether full length NF1 is needed for an anti-competition phenotype.

The second possibility involves the colorless, "defender" heterozygous OPCs being more competitive in the MADM-GAP-dead mice then in the MADM-Tumor mice. If this is the case, it could be explained by the GAP-Dead protein acting in a dominant negative fashion. Because all OPCs in MADM mice are heterozygous for the mutant alleles to begin with, all OPCs in the MADM-GAP-dead mice carry one copy of the *NF1*-GAP-dead allele. If the allele does act in a dominant negative fashion, then while *NF1*-GAP-dead homozygous OPCs have no GAP activity, all of the uncolored and YFP+ OPCs may only have 20% GAP activity compared to the 50% present in the normal MADM-Tumor model. Because heterozygous OPCs in the normal MADM-Tumor model

have complete excision of the *NF1* coding sequence, there is no way for the mutant allele to interfere with the WT allele. However, because the *NF1*-GAP-dead allele is a knock-in and is not dependent on Cre-mediated excision, the NF1 protein is translated and present in these cells along with the WT copy and could in fact interfere with the WT copies ability to inactivate Ras.

To test whether the *NF1*-GAP-dead allele is a dominant negative, OPCS from the mice that *NF1+/-* and mice heterozygous for the *NF1*-GAP-dead allele would be purified. A Ras pull-down would then be performed on these two populations of OPCs and the amount of GTP-bound Ras would be compared. If the *NF1*-GAP-dead allele does act in a dominant negative fashion, the amount of GTP-bound Ras should be higher then the amount of GTP-bound Ras in the *NF1+/-* OPCs. If the *NF1*-GAP-dead allele is not a dominant negative then the amount of GTP-bound Ras should be the same between both OPC populations.

4.3 How do pre-malignant OPCs sense WT OPCs?

4.3.1 Is OPC sensing mediated through cell contact or secreted factors?

Although we have shown that pre-transforming OPCs eliminate all other OPCs during the premalignant stages of gliomagenesis, we do not know how this is mediated. Other studies have shown that cells sense one another through cell contact based mechanisms while others have shown that this sensing is mediated through secretion of factors (Gondek et al., 2005; Murphy et al., 2014; Raff et al., 1993). These studies have used systems in which the microenvironment (Gondek), or different populations of cells (Murphy and Raff) regulate cell death, replacement of cells, or immune response. While

Hughes et *al*. showed the OPCs sense one another through contact mediated repulsion; this does not eliminate the possibility that during the expansion and takeover of the OPC population, pre-transforming OPCs release factors, which eliminate WT OPCs (Hughes et al., 2013a). Understanding this mechanism would allow future studies designed to test the ability of novel inhibitors targeting either cell contact or secreted factors that mediate the killing of non-mutant cells.

Because pre-transforming and WT OPCs can be grown *in vitro*, we would start by analyzing which of the above two mechanisms mediates this killing of WT OPCs. Both pre-transforming and WT OPCs would be grown separately and also in a co-culture, which a small percentage of pre-transforming OPCs compared to WT OPCs, since this recapitulates the *in vivo* setting. Pre-transforming OPCs would be labeled using a membrane bound GFP while WT OPCs would be labeled with a membrane bound RFP to allow for precise visualization of filopodia. OPCs would then be grown for a predetermined time, depending on the speed at which WT OPCs are eliminated and cell death would be determined using TUNEL. After determining the optimal time frame, these populations would then be subjugated to live imaging, to allow for real-time analysis of OPC touching in the co-culture system. If cell-contact mediated WT OPC death, we would observe that pre-transforming OPCs, labeled with GFP, would be touching WT OPCs, labeled with RFP, and following contact, WT OPCs would then undergo cell death.

While the observation of WT OPCs dying following sensing by pre-transforming OPCs implies that this mechanism is sufficient for WT OPC death, secreted factors may still play a role in this competition. To address this possibility, WT and pre-transforming OPCs will be purified and plated into a trans well dish. One dish will have WT OPCs and pre-transforming OPCs separated while a second dish will have WT OPCs alone with a

mix of WT and pre-transforming OPCs, in case pre-transforming OPCs only release factors in the presence of another OPC population. Cells will be analyzed at the same time point as above using both TUNEL and EdU. If pre-transforming OPCs do secrete factors that allow for the elimination of WT OPCs, then either one or both of the dishes will show decreases in WT OPC proliferation and/or increases in WT OPC cell death. However, if secreted factors do not play a role, we would expect to see no difference in WT OPC cell death or proliferation.

If pre-transforming OPCs do secrete factors, the next step would involve determining which factors are secreted. To determine this, media from the co-culture system would need to be analyzed using an ELISA to look for cytokines/chemokines and determining which is abundantly up regulated compared to control media. If some factor continually shows up in the panel, then future experiments to determine the efficacy of this factor in driving WT OPC cell death would be needed to uncover the mechanism by which this occurs.

However, if the sensing were contact-based, then co-culture experiments would need to be carried out. PreT-OPCs could be plated on dishes with WT OPCs either dispersed evenly throughout the dish or an edge could be made to distinguish between the two populations. By using different fluorescently labeled populations, we could stain for signs of cell death and proliferation and analyze whether cell death of WT OPCs was higher at the edge between the two populations and/or if proliferation of PreT-OPCs increased at this edge. If it were contact-mediated sensing, we would expect WT OPC death to be higher while PreT-OPC proliferation may be higher or the same.

4.3.2 Is OPC competition dose dependent?

Many other studies have shown that there is a dose dependent response during cell competition. However, whether this applies to OPC competition mediated by *NF1* deletion is not known. This would be important considering that most patients with *NF1* mutations carry germ line mutations and thus are heterozygous for *NF1*. If loss of just one allele were sufficient for *NF1*-null OPC competition, this would be a less favorable outcome for patients since these OPCs would be able to take over the entire OPC population and theoretically increase the chance of OPC transformation. Therefore, determining the dose dependent effects of *NF1* deletion on OPC competition could be vital for patient susceptibility to gliomagenesis.

To test this, both *in vivo* and *in vitro* systems would be employed to better ascertain the effects of gene dose on OPC competition. First, using our glioma CKO model, heterozygous mice would be generated that would be both *p53* and *NF1* heterozygous. To visualize WT and *NF1*-het OPCs, the Rosa-tdT reporter and the OPC specific Cre, *NG2*-CreER, would be incorporated to allow for the temporal excision of both *p53* and *NF1* in addition to the permanent labeling of these cells with tdT. Mice would be given low doses of tamoxifen to label less then 20% of the total OPC population. Following tamoxifen administration, mice would first be analyzed at 7dpi to determine the number of OPCs and the relative clone size of labeled OPCs. Following this, mice would then be analyzed at 60dpi as well as 120dpi to determine if the tdT+ OPCs had expanded in both cell number, proliferation, and clone size compared to initial labeling. Furthermore, the non-colored OPC population and relative clone size would be analyzed to determine the effects on this population. If NF1-het OPCs are able to out-compete WT OPCs, then the total number of WT OPCs would go down as would clone size while tdT+ OPCs would increase in cell number and clone size.

This does not address whether *NF1*-null OPCs outcompete *NF1*-het OPCs however. To test this, *NF1*-null OPCs and *NF1*-het OPCs would be purified and grown *in vitro*. *NF1*-null OPCs would then be labeled using a GFP reporter and then co-cultured with *NF1*-het OPCs at varying ratios. If *NF1*-null OPCs are able to outcompete *NF1*-het OPCs, then the percent of TUNEL+ colorless OPCs should increase while the percent of EdU+ colorless OPCs should decrease. Additionally, *NF1*-het OPCs would be co-cultured with GFP labeled WT OPCs to determine the efficacy of *NF1*-het OPCs to outcompete WT OPCs *in vitro* as well. This data should match up well with the *in vivo* data if the *in vitro* system does not have strong anti-survival effects on *NF1*-het OPCs.

4.4 Clinical Implications

While current glioma treatments include surgical resection, localized radiotherapy, and chemotherapy, the efficacy of this regiment remains minimal (De Bonis et al., 2013). The data presented here raises several important points, which could have a large impact on future treatment designs. First and foremost, the data presented in Chapter 2 suggest that while drugs targeting individual aberrant pathways has profound efficacy, each major pathway plays distinct roles in OPC transformation. While targeting *NF1* would provide decreased tumor OPC proliferation and increased differentiation, the long-term effect is unknown since the affect of increased oligodendrocyte numbers in the brain is unclear. However, given that the restoration of p*53* function led to massive tumor OPC death and cell cycle arrest, it seems plausible that combinatorial drug treatment would have the most profound effect on tumor OPCs. Future treatment schemes could incorporate both Ras/RTK inhibitors along with p53

activators which would not only slow cell growth but lead to massive Tu-OPC death as evidenced in Chapter 2.

Additionally, while most treatment schemes look to eliminate tumor cells, data in Chapter 3 suggests that simply killing Tu-OPCs might not be advantageous as once thought. Because both PreT and Tu-OPCs eliminate all the WT OPCs in the brain, there is not competition from other OPCs to halt their growth. Thus, finding drugs that either decrease the ability of PreT and Tu-OPCs to out-compete WT OPCs or increase the competitive fitness of WT OPCs, as shown in Chapter 3.3, may be the next step in glioma treatment. Although our model incorporates two TSGs, our data strongly suggest that not only is *NF1* the gene that increases the competitive fitness of OPCs but that the GAP domain of *NF1* is critical for OPC competition. This makes it clear that in order to start the design of anti-competition drugs, we should start at this place.

In this thesis, I have presented data that reveals distinct biological roles of p53 and NF1 in the progression of gliomagenesis in OPCs, the cell of origin. Future studies should investigate the in vivo functional impacts of TSG restoration in OPCs as potential therapeutic interventions. Additionally, I have also shown that during the progression towards malignancy, mutant OPCs progressively out-compete WT OPCs to create a precancerous field, which most likely contributes to gliomagenesis. By blocking this competition process, I showed that we could successfully block gliomagenesis despite having the same mutant cells that always usually form tumors. Future studies are needed to investigate how this competition takes place, either through cell-cell mediated contact, release of signals, or both. Insight into both of these functional contributions in Tu-OPCs will undoubtedly generate novel platforms to develop therapies with greater anti-tumor efficacy for glioma patients.

4.5 Broad Implications on the Glioma Field

In this thesis, I have presented work that demonstrates the distinct roles of individual tumor suppressor genes in suppressing gliomagenesis and the role of cell competition in gliomagenesis. First, we showed that the loss of *p53* had no detectable effect on OPC biology *in vivo* while the loss of *NF1* led to deficiencies in OPC differentiation properties. However, upon further analysis, loss of p*53* led to increases in OPC senescence *in vitro*. This unique analysis of OPC biology *in vivo* led us to ask whether restoration of tumor suppressor genes *in vitro* could restore OPC differentiation functions. However, the effect of individual tumor suppressor gene restoration has never been shown in the cell of origin in glioma. Here we have looked at the restoration of tumor suppressor genes in a unique fashion by looking at the effects on OPC biology rather than simply cell death or proliferation.

The restoration of NF1-GAP activity had the expected effect of inhibiting proliferation in Tu-OPCs but also led to a substantial increase in OPC differentiation, a phenotype that has not been reported in previous glioma studies. This suggests that future glioma therapies may be efficacious in promoting Tu-OPC differentiation, which would be a completely novel readout for glioma treatment paradigms. However, the effect of increased oligodendrocytes in the brain has not been extensively studied and may result in unforeseen side effects. However, the fact that Tu-OPCs still have the capability to differentiate suggests that studying OPC differentiation pathways and how these are altered following NF1 deletion seems advantageous for future clinical research. This suggests that understanding the basic biology of OPCs could have an immediate affect on glioma therapies and possibly that the transformative properties of glioma cells may simply come from being an OPC.

Additionally, while *mTOR* has long been studied in cancer biology, no previous studies have addressed the necessity of *mTOR* in OPC transformation. Here we showed that while *mTOR* is dispensable for the reactivation of PreT-OPCS, it is absolutely necessary for OPC transformation. This reaffirms the idea that *mTOR* inhibitors should be pursued for glioma treatments. Recent work has shown that while previous *mTOR* inhibitors have failed in the clinic, the ability of inhibitors to reach target tumor cells is the key to therapeutic efficacy (Fan et al., 2017). This recent work demonstrates that *mTOR* inhibitors are efficacious and that the lack of inhibitor penetration is what limits efficacy.

The restoration of *p53* in Tu-OPCs led to increases in both cell-cycle arrest and cell death. This data suggests that Tu-OPCs do in fact have a strong response to both TSGs and that both could be therapeutically beneficial for patients. Because drugs similar to Prima-1, which restores normal function to mutant p53, are growing in number, the efficacy of newer generation drugs should be tested glioma patients. A large reason for the lack of studies is most likely due to blood-brain barrier penetration, but with the advent of novel delivery methods, such as nanoparticles, it seems perfectly plausible to have these inhibitors show efficacy *in vivo*.

Furthermore, the ability to analyze pre-malignant phenotypes of OPCs in vivo allowed us to ascertain how the process of gliomagenesis unfolds. First, there is alteration of mutant OPC proliferation, differentiation, and cell numbers, which would have been missed had conventional mouse models been used. By using MADM, we were able to readily mimic the human disease more closely since cancer is a clonal disease, as is MADM labeling. Additionally, without the ability to distinguish between WT and mutant OPCs throughout the pre-malignant phase, we would have completely missed the progressive change in the OPC population that eventually ends in GFP+

OPCs taking over the total OPC population. Conventional tumor models either label all cells or they inject tumor cells into at later stages, which limits the ability to study the entire process. More models should be developed that allow for early stage studies during tumor progression, since vital aspects of this process may have yet to be revealed. Also, it may be beneficial to patients if more early prognostic tests or exams could be developed in patients who are at a higher risk for glioma, such as patients with Li-Fraumeni disease. Being able to identify PreT-OPCs in patients would be advantageous so that clinicians could better determine whether early treatments could block the inevitability of mutant cells undergoing transformation. This may prove an invaluable tool for doctors and patients alike, since if we find drugs that can slow or inhibit early growth or differentiation defects, they may be dispensed to patients who are diagnosed before a full-blown tumor is found.

The second part of the thesis presented data that revealed a novel process during gliomagenesis that is critical for tumor formation. While developmental biologists have long studied cell competition, we presented the first evidence that not only do various populations of OPCs compete with one another, but that this process may be the cornerstone of OPC transformation during gliomagenesis. Glioma researchers have long thought that the ability of cells to transform is due to the overgrowth of one cell in the brain that leads to an overall increase in cell density. However, we show that the key to this process is the hostile take-over of the OPC population by a tiny fraction of OPCs with increased competitive fitness. This may explain why glioma formation occurs later in life, as this process may take years to occur from a single cell in a human.

Furthermore, our data showing that by increasing the competitive fitness of non-GFP+ OPCs, malignant transformation is completely blocked, a result that is almost unheard of in glioma biology. Since cell competition sets up an evolutionary paradigm in

glioma, the killing of less fit glioma cells would lead to increased availability of resources/space for more fit/resistant glioma cells, in effect this would promote the overall fitness/malignancy of the tumor as a whole. Therefore, we would have to reconsider treatment paradigms. Our data suggest that unique therapies tailored to addressing the competitive fitness differences in different populations may be advantageous. In addition, another paradigm shift would be the idea that by mutant OPCs that cannot transform but have increased competitive fitness, one would be able to effectively block Tu-OPC growth. This would completely shift the notion that mutant cells are the problem, to the notion that mutant cells may be the answer to effective glioma treatment. This would require more studies into the effect of single NF1 deletion in OPCs in humans but one piece of data gives a glimmer of hope. While NF patients are known to form various tumors, very few actually develop malignant gliomas, which may be a consequence of the global increased competitive fitness that we saw in the MADM-AC mice. It also makes sense that patients with germ line mutations in *p53* almost always form malignant tumors, since we saw no change in competitive fitness in these mice.

Furthermore, because we observed such a low level of *mTOR* in PreT-OPCs compared to Tu-OPCs, it seems paradoxical that *mTOR* inhibition could block the early expansion of PreT-OPCs in vivo. One explanation is that the inhibition of *mTOR* has a non-cell autonomous effect and that the observed phenotype is due to inhibition in neurons or astrocytes, with previous work demonstrating that neurons are heavily regulated by *mTOR*. If this is the case, then neuronal signaling to OPCs could be one avenue by which we target OPC competitive fitness. A second explanation is that the level of *mTOR* observed in PreT-OPCs compared to Tu-OPCs may be enough to increase the competitive fitness of these cells, just not to the point of Tu-OPCs. This

would make sense since *mTOR* is known to regulate and be invaluable for OPC development. A third explanation is that *mTOR* inhibition may be having a dual effect on WT and PreT-OPCs. Perhaps *mTOR* inhibition not only decreases PreT-OPC competitive fitness but at the same time it increases WT OPC competitive fitness. Perhaps in a WT OPC, *mTOR* at this age plays a more suppressive role in OPC activation and that by blocking it, WT OPCs become more like PreT-OPCs in their activity levels. This would suggest that clinically, it may be beneficial to look at both the effect of *mTOR* inhibitors on tumor cells and also the surrounding WT environment.

The last part of my thesis gave evidence that OPCs are naturally more resistant to conventional ablation than previously thought. Because WT OPCs were able to bounce back from a relatively high level of population ablation and repopulate the brain to normal levels by 4 weeks, it seems like OPC properties and not tumor properties may be the underlying root of the problems with tumor therapies. While the loss of different tumor suppressor genes like *NF1* and *p53* may increase specific properties of the OPCs, OPCs have an innate mechanism of density sensing that allows for rapid growth in a short period of time. One thing that needs to be addressed is if *NF1*-null OPCs have an increased rate of repopulation compared to WT OPCs. Perhaps using focused injury either through the use of ultrasound, irradiation, or a genetic tool such as DTA, would allow for analysis of the recovery rate of *NF1*-null vs. WT OPCs. If *NF1*-null OPCs do in fact recover at a faster rate, this suggests that *NF1* deletion gives an even larger competitive advantage over WT cells since following resection or ablation of Tu-OPCs would allow for *NF1*-null OPCs to take over the empty space. However, if *NF1*-null and WT OPCs have similar rates of recovery, then this suggests that more emphasis should be put on OPC biology then tumor biology to understand the mechanisms in place for this process. While this latter result may seem grim, it may be the data needed to shift

the glioma paradigm to more of an OPC biology focus, which may be needed to truly

understand the basis of the disease.

Chapter 5: Methods and Materials:

5.1 Mouse lines and genotyping

All animal procedures were based on animal care guidelines approved by the Institutional Animal Care and Use Committee at the University of Virginia. The following mouse strains were used to obtain experimental and control mice: TGML/GTML (generated by H.Z.), hGFAP-Cre (stock no. 004600, JAX), NG2-Cre (stock no. 008533; JAX), NG2-CreER (stock no. 008538, JAX), p53^{KO} (stock no. 002101; JAX), Rosa-tdTomato (stock no. 007908; JAX), *neurofibromin 1 (NF1)*^{Flox} (strain no. 01XM4; NCI) and p53^{flox} (strain no. 01XC2; NCI), mTOR^{Flox} (stock no. 011009, JAX). Mice used for single TSG studies were MADM (TGML11/GTML11), NF1 Flox or p53KO. Mice used for glioma generation and purification of OPC-like tumor cells were MADM mice (TG11/GT11), hGFAP-Cre, p53KO, NF1 flox. Mice used for purification of p53 null, NF1 null OPCs were p53^{KO}, NF1^{flox}/p53^{flox}, NF1^{flox}; hGFAP-Cre; Rosa-tdT. Wild type OPCs were generated from mice carrying no p53 or NF1 allele and no Cre. Mice used for mTOR studies were p53^{flox},NF1^{flox}/p53^{flox}, NF1^{flox}; Rosa-tdT; mTOR^{flox} (either single or double); NG2-CreER. All genotyping was performed as previously described (Galvao et al., 2014; Liu et al., 2011a).

5.2 Tamoxifen administration

For all adult mice, tamoxifen citrate tablets (20mg/tablet; Mylan) were ground and dissolved at 20mg/mL and delivered via oral gavage (150mg/kg; final concentration). For perinatal mice, tamoxifen (Sigma (T5648) was dissolved in 100% ethanol at 200mg/mL in 37° water bath and then further diluted in oil to 20mg/mL. Solution was injected subcutaneously at the nape.

5.3 5-Bromo-2'-deoxyuridine administration

5-Bromo-2'-deoxyuridine (BrdU) was given by i.p. injection at 50mg/kg. Mice were given one injection per day for 3hrs (MADM p10), 4 days (MADM p60 and p240), or 7 days (CKO) and killed 24hrs after the last injection for adult mice.

5.4 Tissue Collection

To dissect brains, mice were transcardially perfused with PBS supplemented with procaine and heparin (Sigma), followed by 4% (wt/vol) paraformaldehyde. Brains were then dissected and postfixed in 4% (wt/vol) paraformaldehyde O/N at 4°C. Brains were then washed in PBS 3x at RT and cryoprotected in 30% (wt/vol) sucrose O/N at 4°C. Brains were then embedded in OCT and stored at -80°C until sectioned.

5.5 Immuno-staining

Brains were cut as 25μm-thick sections on glass slides. Brain slices were allowed to dry at RT for 1hr prior to staining. Brains were washed 3 times with PBS for 10 minutes each. Brains were then incubated in blocking/permeabilization buffer (5%NDS in PBS with 0.3% triton X-100) for 20 minutes at RT. Primary antibody incubation was performed at 4° C overnight in the same blocking/permeabilization buffer. Secondary antibody incubation was performed for 2 to 4 hours at RT in blocking/permeabilization buffer. DAPI solution was added for 20 minutes for tissue as the last step before mounting. Secondary antibodies were from the Alexa Fluor® family, purchased from Invitrogen.

Antigen	Species	Dilution	Source	Catalog no.
APC-CC1	Mouse	1:100	Millipore	OP80
BrdU	Rat	1:250	AbD Serotec	OBT0030G
GFP	Chicken	1:500	Aves Lab	GFP-1020
c-myc	Goat	1:200	Novus	NB600-338
MBP	Mouse	1:500 (TC)	Covance	SMI-99P
NG2	Rabbit	1:250	Millipore	AB5320
PDGFRα	Goat	1:200 (1:400 TC)	R&D Systems	AF1062
tdTomato	Rabbit	1:100	Clontech	632496

For BrdU immunostaining, brain slices were washed 3 times with PBS and then post-fixed at RT with 4% PFA for 20 minutes. Slices were then treated with freshly prepared 2 N HCl prepared in PBS at 37° C for 30 minutes. Sections were then washed 4 times with PBS for 7 minutes each and then normal immunostaining steps were followed

When Edu (5-ethynyl-2'-deoxyuridine, Invitrogen, cat. #10044) reaction was performed, it was added to media and cells were incubated for 3 hours. Cells were fixed with 4% PFA, permeabilized with 0.1% PBT and Alexa Fluor® 647 azide (Invitrogen, cat. #A10277) was used for the detection reaction using a Click-iT reaction.

For *in vitro* work, cells were grown on 12 mm glass coverslips coated with poly-D-lysine (Sigma). Cultured cells were fixed by the addition of 0.5 mL 4% paraformaldehyde (PFA) for 30 minutes at room temperature, followed by 3 washes with PBS. Slides were allowed to air dry for at least 30 minutes to allow cells to tightly attach onto the coverslips. Cells were incubated in blocking/permeabilization buffer (10%

normal donkey serum – NDS – in PBS with 0.1% triton X-100) for 30 minutes at RR

prior to primary antibody incubation for 1hr at RT. All primary antibodies were diluted in

the blocking/permeabilization buffer. Incubation with appropriate secondary antibodies

diluted in 10% NDS in PBS was performed for 30 minutes at RT. When DAPI was

performed, cells were incubated in DAPI solution (Sigma, cat. # 32670-25MG-F) 0.001

ug/uL for 5 minutes, and then coverslips were mounted on slides with anti-fade gel

mounting media (EMS, cat. # 17985-10).

5.6 Cell culture conditions

Wild type OPCs and *p53*-null, *NF1*-null mouse OPCs were purified from P8 mice,

and OPC-like tumor cells were purified from fresh glioma tissues through PDGFRA-

immunopanning as previously described (Liu et al., 2011a). Cells were maintained in

Neurobasal (NB) media (Gibco 21103-049) supplemented with B27 (50X, Gibco 17504-

044), GlutaMAX (100X, Gibco 35050-061), Penicilin/Streptomycin (100X, Gibco

15140122), plus 10 ng/mL PDGF-AA (Peprotech 100-13A) for tumor OPC experiments.

For all experiments in this paper, Tu-OPC cell lines used were between passages 2 to

10. The viral packaging line HEK 293T was maintained in DMEM media with High

Glucose (Gibco, 11995-065) supplemented with 10% fetal bovine serum (FBS - GIBCO,

16000-044), and switched to NB media supplemented with B27, GlutaMAX and

Penicilin/Streptomycin (without growth factors) after lentiviral vector transfection (see

Viral production and infection). All cells were kept in a 5% CO_2 incubator at 37°C.

5.7 Lenti virus production and cell infection

Lenti virus production was performed through calcium phosphate transfection of

HEK 293T cell line with a 3rd generation packaging system (3 packaging plasmids +

vector plasmid). 6-12 hours after transfection, HEK 293T cells were switched to NB

media supplemented with B27 and Glutamax as described above. Media was collected

daily for 3-4 days, and filtered through a 0.22 um pore syringe filter membrane before it

was added to the target cells. The media added to the target cells was then

supplemented with the respective growth factors. Two rounds of infection were

performed, with 24 hours for each round of infection.

5.8 Quantitative real time PCR

Total RNA was extracted by TRI Reagent® (Sigma, cat. # T9494-200ML). RNA

samples were then treated with DNAse I (New England Biolabs Inc., cat. # M0303) and

cDNA was synthesized using iScript Reverse Transcription Supermix (Bio-Rad, 170-

8841). qPCR was performed in an Applied Biosystems StepOnePlus^{TM} Real-Time PCR

System for 40 cycles (denaturation: 95°C C, 3 seconds; annealing: 60°C, 30 seconds),

followed by a default Melting Curve program. PCR amplification was performed in KAPA

SYBR FAST ABI Prism qPCR Kit (KAPA Biosystems, KK4605). For normalization of

gene expression, beta-actin control primers were used. Ct values were averaged for

triplicate reactions and measured within the geometric amplification phase.

5.9 Western blotting

Cells were lysed in cold lysis buffer 17 (R&D, 895943), supplemented with

protease inhibitor cocktail tablets (Roche, 11836153001 – 1 tablet for 10 mL of Lysis

buffer) and Halt Phosphatase Inhibitor (100X, Thermo Scientific, 1862495). Total protein

was adjusted according to concentration measured by Pierce® BCA Protein Assay Kit

(Thermo Scientific, cat. # 23227), and Beta-Actin antibody (Sigma, cat. # A5441) was

used for normalization as internal control. Samples were run in Mini-PROTEAN® TGX^{TM}

Gels (Bio-Rad, cat. # 456-9033). Transfer was performed with Nitrocellulose membranes (Amersham, cat. # RPN 2020 D), and membranes were blocked in 5% BSA solution for 1 hour at RT. Primary antibody incubation was performed O/N at 4°C. Primary antibodies used are below. Membranes were washed with TBST and then secondary incubation was performed at RT for 1 hr. Secondary antibodies used were all purchased from Li-Cor® or Jackson and detection was performed in an Odyssey Infrared Imaging System or Gel Doc.

Antigen	Species	Dilution	Source	Catalog no.
Total 4EBP1	Rabbit	1:1000	Cell Signaling	9452
p-4EBP1	Rabbit	1:500	Cell Signaling	2855
Total AKT	Mouse	1:1000	Cell Signaling	2920
p-AKT	Rabbit	1:500	Cell Signaling	9275
Total ERK	Mouse	1:1000	Cell Signaling	9107
p-ERK	Rabbit	1:500	Cell Signaling	4370
Total 70S6K	Rabbit	1:1000	PMID # 17967879	-
p-70S6K	Mouse	1:500	Cell Signaling	9206

5.10 MTT assay

MTT solution (Invitrogen, M-6494) 5 mg/mL was added to cell media in a 1:10 dilution, and incubated in the dark at 37°C, 5% CO_2 for 3 hours. Media was then

aspirated and formazan crystals were dissolved in DMSO. Absorbance was read on

a plate reader at 570 nm wavelength.

5.11 Drug assays

PreT-OPC and Tu-OPC cells were plated in 96-well plates at the same density,

and then treated with different concentrations of Temsirolimus (Selleckchem, cat. #

S1044), BEZ235 (Selleckchem, cat. # S1105), or PD0325901 (Selleckchem cat. #

S1036) 72 hours after treatment, cell viability was accessed by MTT assay.

5.12 Radiation

After anesthesia, mice were submitted to 15Gγ irradiation at a rate of 3 Gγ per

minute using an Xstrahl RS320 X-ray irradiator, courtesy of the department of Radiation

Oncology.

5.13 Imaging

Fluorescent images were acquired on a Zeiss LSM 710 at the Advanced

Microscope Facility at the University of Virginia. All images were processed with ImageJ.

5.14 Quantifications and Statistics

For all *in vivo* quantifications, images were systematically taken throughout the

entire brain including a dorsal to ventral analysis and medial to lateral. All quantifications

are representative of >200 cells positive for each marker/mouse analyzed. For $p53^{-/-}$ and

WT brains, quantifications are representative of at least 50 cells/marker/mouse since

labeling efficiency using MADM is significantly lower. For *in vitro* quantifications, >300

cells/marker were counted per experiment to obtain quantifications. Data are shown as

an average of 3 (*in vitro*) or >5 (*in vivo*) independent experiments ± standard deviation (SD) or standard error of the mean (SEM). Significance was determined by P value from the Student *t* Test.

Literature Cited

Agnihotri, S., Burrell, K.E., Wolf, A., Jalali, S., Hawkins, C., Rutka, J.T., and Zadeh, G. (2013). Glioblastoma, a Brief Review of History, Molecular Genetics, Animal Models and Novel Therapeutic Strategies. Arch. Immunol. Ther. Exp. (Warsz). *61*, 25–41.

Ajami, B., Bennett, J.L., Krieger, C., Tetzlaff, W., and Rossi, F.M. V (2007). Local self-renewal can sustain CNS microglia maintenance and function throughout adult life. Nat. Neurosci. *10*, 1538–1543.

Ali, C., and Trafalis, D.T. (2015). Pharmacology & Therapeutics Glioblastoma multiforme : Pathogenesis and treatment. Pharmacol. Ther. *152*, 63–82.

Amoyel, M., and Bach, E.A. (2014). Cell competition: how to eliminate your neighbours. Development *141*, 988–1000.

Assanah, M., Lochhead, R., Ogden, A., Bruce, J., Goldman, J., and Canoll, P. (2006). Glial progenitors in adult white matter are driven to form malignant gliomas by platelet-derived growth factor-expressing retroviruses. J. Neurosci. *26*, 6781–6790.

Baker, N.E., and Li, W. (2008). Cell competition and its possible relation to cancer. Cancer Res. *68*, 5505–5507.

Belachew, S., Aguirre, A.A., Wang, H., Yuan, X., Anderson, S., Kirby, M., and Gallo, V. (2002). Cyclin-Dependent Kinase-2 Controls Oligodendrocyte Progenitor Cell Cycle Progression and Is Downregulated in Adult Oligodendrocyte Progenitors. J. Neurosci. *22*, 8553–8562.

Bennett, M.R., Rizvi, T. a, Karyala, S., McKinnon, R.D., and Ratner, N. (2003). Aberrant growth and differentiation of oligodendrocyte progenitors in neurofibromatosis type 1 mutants. J. Neurosci. *23*, 7207–7217.

Bilder, D., Li, M., and Perrimon, N. (2000). Cooperative regulation of cell polarity and growth by Drosophila tumor suppressors. Science *289*, 113–116.

Billon, N., Jolicoeur, C., Ying, Q.L., Smith, A., and Raff, M. (2002). Normal timing of oligodendrocyte development from genetically engineered , lineage-selectable mouse ES cells. J. Cell Sci. *115*, 3657–3665.

Biteau, B., Hochmuth, C.E., and Jasper, H. (2011). Review Maintaining Tissue Homeostasis : Dynamic Control of Somatic Stem Cell Activity. Stem Cell *9*, 402–411.

Bondar, T., and Medzhitov, R. (2010). p53-Mediated Hematopoietic Stem and Progenitor Cell Competition. Cell Stem Cell *6*, 309–322.

De Bonis, P., Fiorentino, A., Anile, C., Balducci, M., Pompucci, A., Chiesa, S., Sica, G., Lama, G., Maira, G., and Mangiola, A. (2013). The impact of repeated surgery and adjuvant therapy on survival for patients with recurrent glioblastoma. Clin. Neurol. Neurosurg. *115*, 883–886.

Bonnet, D., and Dick, J.E. (1997). Human acute myeloid leukemia is organized as a hierarchy that originates from a primitive hematopoietic cell. Nat. Med. *3*, 730–737.

Braakhuis, B.J.M., Tabor, M.P., Kummer, J.A., and Brakenhoff, R.H. (2003). A Genetic Explanation of Slaughter ' s Concept of Field Cancerization : Evidence and Clinical Implications A Genetic Explanation of Slaughter ' s Concept of Field Cancerization : Evidence and. Cancer Res *63*, 1727–1730.

Bremner, R., Chen, D., Pacal, M., and Mahima, I.L. (2004). The RB Protein Family in Retinal Development and Retinoblastoma : New Insights from New Mouse Models. Dev. Neurosci. *8*, 417–434.

Brennan, C., Momota, H., Hambardzumyan, D., Ozawa, T., Tandon, A., Pedraza, A., and Holland, E. (2009). Glioblastoma subclasses can be defined by activity among signal transduction pathways and associated genomic alterations. PLoS One *4*.

Brennan, C.W., Verhaak, R.G.W., McKenna, A., Campos, B., Noushmehr, H., Salama,

S.R., Zheng, S., Chakravarty, D., Sanborn, J.Z., Berman, S.H., et al. (2013). The Somatic Genomic Landscape of Glioblastoma. Cell *155*, 462–477.

Brumby, A.M., and Richardson, H.E. (2003). scribble mutants cooperate with oncogenic Ras or Notch to cause neoplastic overgrowth in Drosophila. EMBO J. *22*, 5769–5779.

Cadinu, D., Hooda, J., Alam, M.M., Balamurugan, P., Henke, R.M., and Zhang, L. (2014). Comparative proteomic analysis reveals characteristic molecular changes accompanying the transformation of nonmalignant to cancer lung cells. EuPA Open Proteomics *3*, 1–12.

Canoll, P., and Goldman, J.E. (2008). The interface between glial progenitors and gliomas. Acta Neuropathol. *116*, 465–477.

De Castro, F., and Bribián, A. (2005). The molecular orchestra of the migration of oligodendrocyte precursors during development. Brain Res. Rev. *49*, 227–241.

Cavaliere, F., Urra, O., Alberdi, E., and Matute, C. (2012). Oligodendrocyte differentiation from adult multipotent stem cells is modulated by glutamate. Cell Death Dis. *3*, 268–275.

Chen, A.H., and Silver, P.A. (2012). Designing biological compartmentalization. Trends Cell Biol. *22*, 662–670.

Chen, J., McKay, R.M., and Parada, L.F. (2012). Malignant Glioma: Lessons from Genomics, Mouse Models, and Stem Cells. Cell *149*, 36–47.

Chipuk, J.E. (2015). Targeting aggressive cancer stem cells in glioblastoma. Front. Oncol. *5*, 1–9.

Chlenski, A., and Cohn, S.L. (2010). Modulation of matrix remodeling by SPARC in neoplastic progression. Semin. Cell Dev. Biol. *21*, 55–65.

Chow, L.M.L., Endersby, R., Zhu, X., Rankin, S., Qu, C., Zhang, J., Broniscer, A., Ellison, D.W., and Baker, S.J. (2011). Cooperativity within and among Pten , p53 , and Rb Pathways Induces High-Grade Astrocytoma in Adult Brain. Cancer Cell *19*, 305–316.

Clavería, C., Giovinazzo, G., Sierra, R., and Torres, M. (2013). Myc-driven endogenous cell competition in the early mammalian embryo. Nature *500*, 39–44.

Cloughesy, T.F., Yoshimoto, K., Nghiemphu, P., Brown, K., Dang, J., Zhu, S., Hsueh, T., Chen, Y., Wang, W., Youngkin, D., et al. (2008). Antitumor activity of rapamycin in a phase I trial for patients with recurrent PTEN-deficient glioblastoma. PLoS Med. *5*, 0139–0151.

Cloughesy, T.F., Cavenee, W.K., and Mischel, P.S. (2014). Glioblastoma: From Molecular Pathology to Targeted Treatment. Annu. Rev. Pathol. Mech. Dis. *9*, 1–25.

Corral, T., Jiménez, M., Hernández-Muñoz, I., De Castro, I.P., and Pellicer, A. (2003). NF1 Modulates the Effects of Ras Oncogenes: Evidence of Other NF1 Function Besides Its GAP Activity. J. Cell. Physiol. *197*, 214–224.

Crawford, A.H., Stockley, J.H., Tripathi, R.B., Richardson, W.D., and Franklin, R.J.M. (2014). Oligodendrocyte progenitors : Adult stem cells of the central nervous system? Exp. Neurol. *260*, 50–55.

Dakubo, G.D., Jakupciak, J.P., Birch-Machin, M.A., and Parr, R.L. (2007). Clinical implications and utility of field cancerization. Cancer Cell Int. *7*, 2.

Dasgupta, B., and Gutmann, D.H. (2003). Neurofibromatosis 1: closing the GAP between mice and men. Curr. Opin. Genet. Dev. *13*, 20–27.

Dawson, M. (2003). NG2-expressing glial progenitor cells: an abundant and widespread population of cycling cells in the adult rat CNS. Mol. Cell. Neurosci. *24*, 476–488.

Diaz-Benjumea, F.J., and Hafen, E. (1994). The sevenless signalling cassette mediates Drosophila EGF receptor function during epidermal development. Development *120*, 569–578.

Dimou, L., and Wegner, M. (2015). Oligodendroglial heterogeneity in time and space (

NG2 glia in the CNS). E-Neuroforum *3*, 69–72.

Dimou, L., Simon, C., Kirchhoff, F., Takebayashi, H., and Götz, M. (2008). Progeny of Olig2-expressing progenitors in the gray and white matter of the adult mouse cerebral cortex. J. Neurosci. *28*, 10434–10442.

Dunn, G.P., Rinne, M.L., Wykosky, J., Genovese, G., Quayle, S.N., Dunn, I.F., Agarwalla, P.K., Chheda, M.G., Campos, B., Wang, A., et al. (2012). Emerging insights into the molecular and cellular basis of glioblastoma. Genes Dev. 756–784.

Eichenlaub, T., and Cohen, S.M. (2016). Cell Competition Drives the Formation of Metastatic Tumors in a Drosophila Model of Epithelial Tumor Article Cell Competition Drives the Formation of Metastatic Tumors in a Drosophila Model of Epithelial Tumor Formation. Curr. Biol. *26*, 419–427.

Ellenbroek, S.I.J., Iden, S., and Collard, J.G. (2012). Cell polarity proteins and cancer. Semin. Cancer Biol. *22*, 208–215.

Engel, U., and Wolswijk, G. (1996). Oligodendrocyte-type-2 astrocyte (O-2A) progenitor cells derived from adult rat spinal cord: In vitro characteristics and response to PDGF, bFGF and NT-3. Glia *16*, 16–26.

Enomoto, M., and Igaki, T. (2011). Deciphering tumor-suppressor signaling in flies: Genetic link between Scribble/Dlg/Lgl and the Hippo pathways. J. Genet. Genomics *38*, 461–470.

Fabian, A., Vereb, G., and Szollosi, J. (2013). The Hitchhikers Guide to Cancer Stem Cell Theory : Markers , Pathways and Therapy. Cytom. Part A *83*, 62–71.

Fan, Q., Aksoy, O., Wong, R.A., Ilkhanizadeh, S., Novotny, C.J., Gustafson, W.C., Truong, A.Y.-Q., Cayanan, G., Simonds, E.F., Haas-Kogan, D., et al. (2017). A Kinase Inhibitor Targeted to mTORC1 Drives Regression in Glioblastoma. Cancer Cell *31*, 424–435.

Fearon, E.F., and Vogelstein, B. (1990). for Colorectal Tumorigenesis. *61*, 759–767.

Ffrench-Constant, C., and Raff, M.C. (1986). Proliferating bipotential glial progenitor cells in adult rat optic nerve. Nature *319*, 499–502.

Foote, a. K., and Blakemore, W.F. (2005). Repopulation of oligodendrocyte progenitor cell depleted tissue in a model of chronic demyelination. Neuropathol. Appl. Neurobiol. *31*, 105–114.

Franklin, R.J.M., and Barnett, S.C. (1997). Review Do Olfactory Glia Have Advantages Over Schwann Cells for CNS Repair ? J. Neurosci. Res. *672*, 665–672.

Franklin, R.J.M., and Ffrench-Constant, C. (2008). Remyelination in the CNS : from biology to therapy. Nat. Rev. Neurosci. *9*, 839–855.

Freed-pastor, W.A., and Prives, C. (2012). Mutant p53 : one name , many proteins. Genes Dev. *26*, 1268–1286.

Friedmann-Morvinski, D., Bushong, E., Ke, E., Soda, Y., Marumoto, T., Singer, O., Ellisman, M.H., and Verma, I.M. (2012). Dedifferentiation of Neurons and Astrocytes by Oncogenes Can Induce Gliomas in Mice. Science (80-.). *338*, 1080–1085.

Froldi, F., Ziosi, M., Garoia, F., Pession, A., Grzeschik, N. a, Bellosta, P., Strand, D., Richardson, H.E., Pession, A., and Grifoni, D. (2010). The lethal giant larvae tumour suppressor mutation requires dMyc oncoprotein to promote clonal malignancy. BMC Biol. *8*, 33.

Fruttiger, M., Karlsson, L., Hall, a C., Abramsson, a, Calver, a R., Boström, H., Willetts, K., Bertold, C.H., Heath, J.K., Betsholtz, C., et al. (1999). Defective oligodendrocyte development and severe hypomyelination in PDGF-A knockout mice. Development *126*, 457–467.

Fukuda, A., Fukuda, H., Swanpalmer, J., Hertzman, S., Lannering, B., Marky, I., Björk-Eriksson, T., and Blomgren, K. (2005). Age-dependent sensitivity of the developing brain

to irradiation is correlated with the number and vulnerability of progenitor cells. J. Neurochem. *92*, 569–584.

Galvao, R.P., Kasina, A., McNeill, R.S., Harbin, J.E., Foreman, O., Verhaak, R.G.W., Nishiyama, A., Miller, C.R., and Zong, H. (2014). Transformation of quiescent adult oligodendrocyte precursor cells into malignant glioma through a multistep reactivation process. Proc. Natl. Acad. Sci. *111*, E4214–E4223.

Giacinti, C., and Giordano, A. (2006). RB and cell cycle progression. Oncogene *25*, 5220–5227.

Gibson, E.M., Purger, D., Mount, C.W., Goldstein, A.K., Lin, G.L., Wood, L.S., Inema, I., Miller, S.E., Bieri, G., Zuchero, J.B., et al. (2014). Oligodendrogenesis and Adaptive Myelination in the Mammalian Brain. Science (80-.). *344*, 487–499.

Gondek, D.C., Lu, L., Quezada, S.A., and Noelle, R.J. (2005). Cutting Edge: Contact-Mediated Suppression by CD4 + CD25 + Regulatory Cells Involves a Granzyme B-Dependent, Perforin-Independent Mechanism. J. Immunol. *11*, 1783–1786.

Gorgoulis, V., LV, V., P, K., P, Z., A, K., T, L., M, V., Jr, D.R., NG, K., Levy B, K.D., et al. (2005). Activation of the DNA damage checkpoint and genomic instability in human precancerous lesions. Nature 907–913.

Greaves, M., and Maley, C.C. (2012). Clonal evolution in cancer. Nature *481*, 306–313.

Gutmann, D.H., Parada, L.F., Silva, a. J., and Ratner, N. (2012). Neurofibromatosis Type 1: Modeling CNS Dysfunction. J. Neurosci. *32*, 14087–14093.

Haar, C.P., Hebbar, P., Wallace, G.C., Das, A., Vandergrift, W.A., Joshua, I.I.I., Giglio, P., Patel, S.J., Ray, S.K., and Banik, N.L. (2012). Drug Resistance in Glioblastoma : A Mini Review. Neurochem Researc *37*, 1192–1200.

Halder, G., and Johnson, R.L. (2011). Hippo signaling: growth control and beyond. Development *138*, 9–22.

Harajly, M., Zalzali, H., Nawaz, Z., Ghayad, S.E., Ghamloush, F., Basma, H., Zainedin, S., Rabeh, W., Jabbour, M., Tawil, A., et al. (2016). p53 Restoration in Induction and Maintenance of Senescence : Differential Effects in Premalignant and Malignant Tumor Cells. Mol. Cell. Biol. *36*, 438–451.

Henner, A., Ventura, P.B., Jiang, Y., and Zong, H. (2013). MADM-ML, a Mouse Genetic Mosaic System with Increased Clonal Efficiency. PLoS One *8*, e77672.

Hill, R.A., Patel, K.D., Medved, J., Reiss, A.M., and Nishiyama, A. (2013). NG2 Cells in White Matter But Not Gray Matter Proliferate in Response to PDGF. J. Neurosci. *33*, 14558–14566.

Hogan, C., Dupré-Crochet, S., Norman, M., Kajita, M., Zimmermann, C., Pelling, A.E., Piddini, E., Baena-López, L.A., Vincent, J.-P., Itoh, Y., et al. (2009). Characterization of the interface between normal and transformed epithelial cells. Nat. Cell Biol. *11*, 460–467.

Hogan, C., Kajita, M., Lawrenson, K., and Fujita, Y. (2011). Interactions between normal and transformed epithelial cells: Their contributions to tumourigenesis. Int. J. Biochem. Cell Biol. *43*, 496–503.

Hong, H., Takahashi, K., Ichisaka, T., Aoi, T., Kanagawa, O., Nakagawa, M., Okita, K., and Yamanaka, S. (2009). Suppression of induced pluripotent stem cell generation by the p53-p21 pathway. Nature *460*, 1132–1135.

Hruban, R.H., Wilentz, R.E., and Kern, S.E. (2000). Genetic progression in the pancreatic ducts. Am. J. Pathol. *156*, 1821–1825.

Hughes, E.G., Kang, S.H., Fukaya, M., and Bergles, D.E. (2013a). Oligodendrocyte progenitors balance growth with self-repulsion to achieve homeostasis in the adult brain. Nat. Neurosci. *16*, 668–676.

Hughes, E.G., Kang, S.H., Fukaya, M., and Bergles, D.E. (2013b). Oligodendrocyte

progenitors balance growth with self-repulsion to achieve homeostasis in the adult brain. Nat. Neurosci. *16*, 668–676.

Huse, J.T., and Holland, E.C. (2010). Targeting brain cancer: advances in the molecular pathology of malignant glioma and medulloblastoma. Nat. Rev. Cancer *10*, 319–331.

Huszthy, P.C., Daphu, I., Niclou, S.P., Stieber, D., Nigro, J.M., Sakariassen, P.O., Miletic, H., Thorsen, F., and Bjerkvig, R. (2012). In vivo models of primary brain tumors: Pitfalls and perspectives. Neuro. Oncol. *14*, 979–993.

Igaki, T., Pastor-Pareja, J.C., Aonuma, H., Miura, M., and Xu, T. (2009). Intrinsic Tumor Suppression and Epithelial Maintenance by Endocytic Activation of Eiger/TNF Signaling in Drosophila. Dev. Cell *16*, 458–465.

Irvine, K.A., and Blakemore, W.F. (2007). A different regional response by mouse oligodendrocyte progenitor cells (OPCs) to high-dose X-irradiation has consequences for repopulating OPC-depleted normal tissue. Eur. J. Neurosci. *25*, 417–424.

Ismat, F. a., Xu, J., Min, M.L., and Epstein, J. a. (2006). The neurofibromin GAP-related domain rescues endothelial but not neural crest development in Nf1-/- mice. J. Clin. Invest. *116*, 2378–2384.

Johnston, L.A. (2009). Competitive interactions between cells: death, growth, and geography. Science *324*, 1679–1682.

Johnston, L.A., Prober, D.A., Edgar, B.A., Eisenman, R.N., and Gallant, P. (1999). Drosophila myc regulates cellular growth during development. Cell *98*, 779–790.

Kajita, M., Hogan, C., Harris, A.R., Dupre-Crochet, S., Itasaki, N., Kawakami, K., Charras, G., Tada, M., and Fujita, Y. (2010). Interaction with surrounding normal epithelial cells influences signalling pathways and behaviour of Src-transformed cells. J. Cell Sci. *123*, 171–180.

Karnoub, A.E., and Weinberg, R.A. (2008). Ras oncogenes : split personalities. Mol. Cell Biol. *9*, 517–531.

Kaul, A., Toonen, J.A., Cimino, P.J., Gianino, S.M., and Gutmann, D.H. (2015). Akt- or MEK-mediated mTOR inhibition suppresses Nf1 optic glioma growth. Neuro. Oncol. *17*, 843–853.

Kessaris, N., Fogarty, M., Iannarelli, P., Grist, M., Wegner, M., and Richardson, W.D. (2006). Competing waves of oligodendrocytes in the forebrain and postnatal elimination of an embryonic lineage. Nat. Neurosci. *9*, 173–179.

Khleif, S.N., Degregorit, J., Yee, C.L., Otterson, G.A., Kaye, F.J., Nevinst, J.R., and Howley, P.M. (1996). Inhibition of cyclin D-CDK4 / CDK6 activity is associated with an E2F-mediated induction of cyclin kinase inhibitor activity. Proc. Natl. Acad. Sci. *93*, 4350–4354.

Khoo, K.H., Hoe, K.K., Verma, C.S., and Lane, D.P. (2014). Drugging the p53 pathway: understanding the route to clinical efficacy. Nat. Rev. Drug Discov. *13*, 217–236.

Kirby, B.B., Takada, N., Latimer, A.J., Shin, J., Carney, T.J., Kelsh, R.N., and Appel, B. (2006). In vivo time-lapse imaging shows dynamic oligodendrocyte progenitor behavior during zebrafish development. *9*, 1506–1511.

Kleihues, P., and Ohgaki, H. (1999). Primary and secondary glioblastomas: From concept to clinicaldiagnosis. Neuro. Oncol. *1*, 44–51.

Klose, A., Ahmadian, M.R., Schuelke, M., Scheffzek, K., Hoffmeyer, S., Gewies, A., Schmitz, F., Kaufmann, D., Peters, H., Wittinghofer, A., et al. (1998). Selective disactivation of neurofibromin GAP activity in neurofibromatosis type 1. Hum. Mol. Genet. *7*, 1261–1268.

Kosaka, N., Iguchi, H., Yoshioka, Y., Hagiwara, K., Takeshita, F., and Ochiya, T. (2012). Competitive interactions of cancer cells and normal cells via secretory microRNAs. J. Biol. Chem. *287*, 1397–1405.

Kruse, J.P., and Gu, W. (2009). Modes of p53 Regulation. Cell *137*, 609–622.

Kucinski, I., Suijkerbuijk, S.J.E., Kolahgar, G., Kucinski, I., and Piddini, E. (2016). Cell Competition Drives the Growth of Intestinal Adenomas in Drosophila Article Cell Competition Drives the Growth of Intestinal Adenomas in Drosophila. Curr. Biol. *26*, 428–438.

De La Cova, C., Abril, M., Bellosta, P., Gallant, P., and Johnston, L.A. (2004). Drosophila myc regulates organ size by inducing cell competition. Cell *117*, 107–116.

Lambert, J.M.R., Gorzov, P., Veprintsev, D.B., Söderqvist, M., Segerbäck, D., Bergman, J., Fersht, A.R., Hainaut, P., Wiman, K.G., and Bykov, V.J.N. (2009). PRIMA-1 Reactivates Mutant p53 by Covalent Binding to the Core Domain. Cancer Cell *15*, 376–388.

Lassman, A.B., Rossi, M.R., Razier, J.R., Abrey, L.E., Lieberman, F.S., Grefe, C.N., Lamborn, K., Pao, W., Shih, A.H., Kuhn, J.G., et al. (2005). Cancer Therapy : Clinical Molecular Study of Malignant Gliomas Treated with Epidermal Growth Factor Receptor Inhibitors : Tissue Analysis from North American Brain Tumor Consortium Trials 01-03 and 00-01. Clin. Cancer Res. *11*, 7841–7851.

Lawrence, Y.R., Mishra, M. V, Werner-wasik, M., and Andrews, D.W. (2012). Improving Prognosis of Glioblastoma in the 21st Century : Who Has Benefited Most ? Cancer 4228–4234.

Lee, D.Y., Yeh, T.H., Emnett, R.J., White, C.R., and Gutmann, D.H. (2010). Neurofibromatosis-1 regulates neuroglial progenitor proliferation and glial differentiation in a brain region-specific manner. Genes Dev. *24*, 2317–2329.

Lehmann, B.D., and Pietenpol, J. a. (2012). Targeting mutant p53 in human tumors. J. Clin. Oncol. *30*, 3648–3650.

Lemmon, M.A., and Schlessinger, J. (2010). Cell signaling by receptor tyrosine kinases. Cell *141*, 1117–1134.

Levine, A.J. (1997). p53 , the Cellular Gatekeeper for Growth and Division. Cell *88*, 323–331.

Levine, A.J., and Oren, M. (2009). The first 30 years of p53: growing ever more complex. Nat. Rev. Cancer *9*, 749–758.

Li, T., Kon, N., Jiang, L., Tan, M., Ludwig, T., Zhao, Y., Baer, R., and Gu, W. (2012). Tumor suppression in the absence of p53-mediated cell-cycle arrest, apoptosis, and senescence. Cell *149*, 1269–1283.

Li, W., You, L., Cooper, J., Schiavon, G., Pepe-Caprio, A., Zhou, L., Ishii, R., Giovannini, M., Hanemann, C.O., Long, S.B., et al. (2010). Merlin/NF2 Suppresses Tumorigenesis by Inhibiting the E3 Ubiquitin Ligase CRL4DCAF1 in the Nucleus. Cell *140*, 477–490.

Lim, S., and Kaldis, P. (2013). Cdks , cyclins and CKIs : roles beyond cell cycle regulation. Development *3093*, 3079–3093.

Lin, G., Mela, A., Guilfoyle, E.M., and Goldman, J.E. (2009). Neonatal and adult O4+ oligodendrocyte lineage cells display different growth factor responses and different gene expression patterns. J. Neurosci. Res. *87*, 3390–3402.

Lindberg, N., Kastemar, M., Olofsson, T., Smits, a, and Uhrbom, L. (2009). Oligodendrocyte progenitor cells can act as cell of origin for experimental glioma. Oncogene *28*, 2266–2275.

Lindberg, N., Jiang, Y., Xie, Y., Bolouri, H., Kastemar, M., Olofsson, T., Holland, E.C., and Uhrbom, L. (2014). Oncogenic signaling is dominant to cell of origin and dictates astrocytic or oligodendroglial tumor development from oligodendrocyte precursor cells. J. Neurosci. *34*, 14644–14651.

Liu, C., Sage, J.C., Miller, M.R., Verhaak, R.G.W., Hippenmeyer, S., Vogel, H., Foreman, O., Bronson, R.T., Nishiyama, A., Luo, L., et al. (2011a). Mosaic analysis with

double markers reveals tumor cell of origin in glioma. Cell *146*, 209–221.

Liu, C., Sage, J.C., Miller, M.R., Verhaak, R.G.W., Hippenmeyer, S., Vogel, H., Foreman, O., Bronson, R.T., Nishiyama, A., Luo, L., et al. (2011b). Mosaic Analysis with Double Markers Reveals Tumor Cell of Origin in Glioma. Cell *146*, 209–221.

Llaguno, S.R.A., Wang, Z., Sun, D., Burns, D.K., Johnson, J.E., Parada, L.F., Llaguno, S.R.A., Wang, Z., Sun, D., Chen, J., et al. (2015). Adult Lineage-Restricted CNS Progenitors Specify Article Adult Lineage-Restricted CNS Progenitors Specify Distinct Glioblastoma Subtypes. Cancer Cell *28*, 429–440.

Lloyd, A.C., and Raff, M.C. (2001). Lack of Replicative Senescence in Cultured Rat Oligodendrocyte Precursor Cells. Science (80-.). *291*, 868–872.

Lote, B.K., Egeland, T., Hager, B., Stenwig, B., Skullerud, K., Berg-johnsen, J., Storm-mathisen, I., and Hirschberg, H. (1997). Survival , Prognostic Factors , and Therapeutic Efficacy in Low-Grade Glioma : A Retrospective Study in 379 Patients. J. Clin. Oncol. *15*, 3129–3140.

Lujambio, A., Akkari, L., Simon, J., Grace, D., Tschaharganeh, D.F., Bolden, J.E., Zhao, Z., Thapar, V., Joyce, J. a., Krizhanovsky, V., et al. (2013). Non-cell-autonomous tumor suppression by p53. Cell *153*, 449–460.

Maglietta, R., Liuzzi, V.C., Cattaneo, E., Laczko, E., Piepoli, A., Panza, A., Carella, M., Palumbo, O., Staiano, T., Buffoli, F., et al. (2012). Molecular pathways undergoing dramatic transcriptomic changes during tumor development in the human colon. BM *12*, 1–16.

Maher, E. a., Furnari, F.B., Bachoo, R.M., Rowitch, D.H., Louis, D.N., Cavenee, W.K., and DePinho, R. a. (2001). Malignant glioma: Genetics and biology of a grave matter. Genes Dev. *15*, 1311–1333.

McClatchey, A.I. (2007). Neurofibromatosis. Annu. Rev. Pathol. *2*, 191–216.

McLendon, R., Friedman, A., Bigner, D., Van Meir, E.G., Brat, D.J., M. Mastrogianakis, G., Olson, J.J., Mikkelsen, T., Lehman, N., Aldape, K., et al. (2008). Comprehensive genomic characterization defines human glioblastoma genes and core pathways. Nature *455*, 1061–1068.

McTigue, D.M., and Tripathi, R.B. (2008). Normal oligodendrocyte development Myelin : more than just a pretty wrapping. J. Neurochem. *107*, 1–19.

Menendez, D., Inga, A., and Resnick, M. a (2009). The expanding universe of p53 targets. Nat. Rev. Cancer *9*, 724–737.

Menéndez, J., Pérez-Garijo, A., Calleja, M., and Morata, G. (2010). A tumor-suppressing mechanism in Drosophila involving cell competition and the Hippo pathway. Proc. Natl. Acad. Sci. U. S. A. *107*, 14651–14656.

Montero, J., Dutta, C., Bodegom, D. Van, Weinstock, D., and Letai, A. (2013). p53 regulates a non-apoptotic death induced by ROS. Cell Death Differ. *20*, 1465–1474.

Morata, G., and Ripoll, P. (1975). Minutes: Mutants of Drosophila autonomously affecting cell division rate. Dev. Biol. *42*, 211–221.

Morcos, P., Thapar, N., Tusneem, N., Stacey, D., and Tamanoi, F. (1996). Identification of neurofibromin mutants that exhibit allele specificity or increased Ras affinity resulting in suppression of activated ras alleles. Mol. Cell. Biol. *16*, 2496–2503.

Moreno, E. (2008). Is cell competition relevant to cancer? Nat. Rev. Cancer *8*, 141–147.

Moreno, E., and Basler, K. (2004). dMyc transforms cells into super-competitors. Cell *117*, 117–129.

Moser, R.P. (1988). Surgery for Glioma Relapse: Factors That Influence a Favorable Outcome. Cancer *17*, 381–390.

Murphy, K., Logsdon, N.J., and Sessions, S.K. (2014). Secreted factor(s) from young cells restores susceptibility to cell death in senescent myofibroblasts. BioOne *85*, 218–

223.

Muzumdar, M.D., Luo, L., and Zong, H. (2007). Modeling sporadic loss of heterozygosity in mice by using mosaic analysis with double markers (MADM). Proc. Natl. Acad. Sci. U. S. A. *104*, 4495–4500.

Neto-Silva, R.M., de Beco, S., and Johnston, L.A. (2010). Evidence for a growth-stabilizing regulatory feedback mechanism between Myc and Yorkie, the drosophila homolog of Yap. Dev. Cell *19*, 507–520.

Nishiyama, A., Komitova, M., Suzuki, R., and Zhu, X. (2009). Polydendrocytes (NG2 cells): multifunctional cells with lineage plasticity. Neuroscience *10*, 9–22.

Nowell, P.C. (1976). Linked references are available on JSTOR for this article : The Clonal Evolution of Tumor Cell Populations. Science (80-.). *194*, 23–28.

Ohgaki, H., and Kleihues, P. (2007). Genetic Pathways to Primary and Secondary Glioblastoma. Am. J. Pathol. *170*, 1445–1453.

Ohgaki, H., and Kleihues, P. (2013). The Definition of Primary and Secondary Glioblastoma. Clin. Cancer Res. *19*, 764–772.

Ostrom, Q.T., Bauchet, L., Davis, F.G., Deltour, I., Fisher, J.L., Langer, C.E., Pekmezci, M., Schwartzbaum, J.A., Turner, M.C., Walsh, K.M., et al. (2014). The epidemiology of glioma in adults: a "state of the science" review. Neuro. Oncol. 1–18.

Pan, D. (2010). The hippo signaling pathway in development and cancer. Dev. Cell *19*, 491–505.

Park, V.M., Kenwright, K. a., Sturtevant, D.B., and Pivnick, E.K. (1998). Alternative splicing of exons 29 and 30 in the neurofibromatosis type 1 gene. Hum. Genet. *103*, 382–385.

Persson, A.I., Petritsch, C., Swartling, F.J., Itsara, M., Sim, F.J., Auvergne, R., Goldenberg, D.D., Vandenberg, S.R., Nguyen, K.N., Yakovenko, S., et al. (2010). Article Non-Stem Cell Origin for Oligodendroglioma. Cancer Cell *18*, 669–682.

Petrova, E., Soldini, D., and Moreno, E. (2011). The expression of SPARC in human tumors is consistent with its role during cell competition. Commun. Integr. Biol. *4*, 171–174.

Petrova, E., López-Gay, J.M., Rhiner, C., and Moreno, E. (2012). Flower-deficient mice have reduced susceptibility to skin papilloma formation. Dis. Model. Mech. *5*, 553–561.

Pierce, S.B., Yost, C., Anderson, S.A.R., Flynn, E.M., Delrow, J., and Eisenman, R.N. (2008). Drosophila growth and development in the absence of dMyc and dMnt. Dev. Biol. *315*, 303–316.

Portela, M., Casas-Tinto, S., Rhiner, C., López-Gay, J.M., Domínguez, O., Soldini, D., and Moreno, E. (2010). Drosophila SPARC is a self-protective signal expressed by loser cells during cell competition. Dev. Cell *19*, 562–573.

Pouratian, N., and Schiff, D. (2010). Management of Low-Grade Glioma. Curr. Neurol. Neurosci. Reports 224–231.

Prives, C., and Hall, P. (1999). The p53 pathway. J. Pathol. *187*, 112–126.

Prober, D. a, and Edgar, B. a (2000). Ras1 promotes cellular growth in the Drosophila wing. Cell *100*, 435–446.

Psachoulia, K., Jamen, F., Young, K.M., and Richardson, W.D. (2009). Glia Biology : Cell cycle dynamics of NG2 cells in the postnatal and ageing brain. Neuron Glia Biol. *5*, 57–67.

Raff, M.C., Miller, R.H., and Noble, M. (1983). A glial progenitor cell that develops in vitro into an astrocyte or an oligodendrocyte depending on culture medium. Nature *303*, 390–396.

Raff, M.C., Barres, B.A., Burne, J.F., Coles, H.S., Ishizaki, Y., and Jacobson, M.D. (1993). Programmed cell death and the control of cell survival : Lessons from the

Nervous System. Science (80-.). *262*, 695–700.

Ramirez, Y.P., Weatherbee, J.L., Wheelhouse, R.T., and Ross, A.H. (2013). Glioblastoma Multiforme Therapy and Mechanisms of Resistance. Pharmaceuticals *6*, 1475–1506.

Ren, S., and Rollins, B.J. (2004). Cyclin C / Cdk3 Promotes Rb-Dependent G0 Exit. Cell *117*, 239–251.

Rhiner, C., and Moreno, E. (2009). Super competition as a possible mechanism to pioneer precancerous fields. Carcinogenesis *30*, 723–728.

Rhiner, C., L??pez-Gay, J.M., Soldini, D., Casas-Tinto, S., Mart??n, F.A., Lombard??a, L., and Moreno, E. (2010). Flower forms an extracellular code that reveals the fitness of a cell to its neighbors in Drosophila. Dev. Cell *18*, 985–998.

Richardson, W.D., Kessaris, N., and Pringle, N. (2006). Oligodendrocyte wars. Nat. Rev. Neurosci. *7*, 11–18.

Rivers, L.E., Young, K.M., Rizzi, M., Jamen, F., Psachoulia, K., Wade, A., Kessaris, N., and Richardson, W.D. (2008). PDGFRA/NG2 glia generate myelinating oligodendrocytes and piriform projection neurons in adult mice. Nat. Neurosci. *11*, 1392–1401.

Rodrik-Outmezguine, V.S., Okaniwa, M., Yao, Z., Novotny, C.J., McWhirter, C., Banaji, A., Won, H., Wong, W., Berger, M., de Stanchina, E., et al. (2016). Overcoming mTOR resistance mutations with a new-generation mTOR inhibitor. Nature *534*, 272–276.

Rowitch, D.H., and Kriegstein, A.R. (2010). Developmental genetics of vertebrate glial-cell specification. Nature *468*, 214–222.

Sadgrove, Ã.M., Wallraff, Ã.A., Hinterkeuser, Ã.S., Kirchhoff, F., and Hu, K. (2003). Seizures preferentially stimulate proliferation of radial glia-like astrocytes in the adult dentate gyrus : functional and immunocytochemical analysis. Eur. J. Neurosci. *18*, 2769–2778.

Sanai, N., Chang, S., and Berger, M.S. (2011). Low-grade gliomas in adults. J. Neurosurg. *115*, 948–965.

Scheffzek, K., Ahmadian, M.R., Wiesmüller, L., Kabsch, W., Stege, P., Schmitz, F., and Wittinghofer, A. (1998). Structural analysis of the GAP-related domain from neurofibromin and its implications. EMBO J. *17*, 4313–4327.

Schlessinger, J. (2000). Cell Signaling by Receptor Tyrosine Kinases A large group of genes in all eukaryotes encode for. Cell *103*, 211–225.

Schlomm, T., Iwers, L., Kirstein, P., Jessen, B., Köllermann, J., Minner, S., Passow-Drolet, A., Mirlacher, M., Milde-Langosch, K., Graefen, M., et al. (2008). Clinical significance of p53 alterations in surgically treated prostate cancers. Mod. Pathol. *21*, 1371–1378.

Schomas, D.A., Laack, N.N.I., Rao, R.D., Meyer, F.B., Shaw, E.G., Neill, B.P.O., Giannini, C., and Brown, P.D. (2009). Intracranial low-grade gliomas in adults: 30-year experience with long-term follow-up at Mayo Clinic. Neuro. Oncol. *11*, 437–445.

Schwartzbaum, J. a, Fisher, J.L., Aldape, K.D., and Wrensch, M. (2006). Epidemiology and molecular pathology of glioma. Nat. Clin. Pract. Neurol. *2*, 494–503.

Scully, S., Francescone, R., Faibish, M., Bentley, B., Taylor, S.L., Oh, D., Schapiro, R., Moral, L., Yan, W., and Shao, R. (2012). Transdifferentiation of glioblastoma stem-like cells into mural cells drives vasculogenic mimicry in glioblastomas. J. Neurosci. *32*, 12950–12960.

Seymour, T., Nowak, A., and Chipuk, J.E. (2015). Targeting aggressive cancer stem cells in glioblastoma. Front. Oncol. *5*, 1–9.

Shchors, K., Persson, A.I., Rostker, F., Tihan, T., Lyubynska, N., Li, N., Swigart, L.B., Berger, M.S., Hanahan, D., Weiss, W. a, et al. (2013). Using a preclinical mouse model of high-grade astrocytoma to optimize p53 restoration therapy. Proc. Natl. Acad. Sci. U.

S. A. *110*, E1480-9.

Sherr, C.J., and Mccormick, F. (2002). The RB and p53 pathways in cancer. Cancer Cell *2*, 103–112.

Sherr, C.J., and Roberts, J.M. (1999). CDK inhibitors : positive and negative regulators of G1-phase progression. Genes Dev. *13*, 1501–1512.

Sherriff, J., Tamangani, J., Senthil, L., Cruickshank, G., Spooner, D., Jones, B., Brookes, C., and Sanghera, P. (2013). Patterns of relapse in glioblastoma multiforme following concomitant chemoradiotherapy with temozolomide. Brain J. Radiol. *13*, 2–10.

Shi, J., Marinovich, a, and Barres, B. a (1998). Purification and characterization of adult oligodendrocyte precursor cells from the rat optic nerve. J. Neurosci. *18*, 4627–4636.

Shin, J., Padmanabhan, a., de Groh, E.D., Lee, J.-S., Haidar, S., Dahlberg, S., Guo, F., He, S., Wolman, M. a., Granato, M., et al. (2012). Zebrafish neurofibromatosis type 1 genes have redundant functions in tumorigenesis and embryonic development. Dis. Model. Mech. *5*, 881–894.

Simons, B.D., and Clevers, H. (2011). Review Strategies for Homeostatic Stem Cell Self-Renewal in Adult Tissues. Cell *145*, 851–862.

Simpson, P. (1979). Parameters of cell competition in the compartments of the wing disc of Drosophila. Dev. Biol. *69*, 182–193.

Simpson, P. (1981). Growth and cell competition in Drosophila. J. Embryol. Exp. *65*, 77–88.

Simpson, P., and Morata, G. (1981). Differential mitotic rates and patterns of growth in compartments in the Drosophila wing. Dev. Biol. *85*, 299–308.

Singh, S.K., Clarke, I.D., Terasaki, M., Bonn, V.E., Hawkins, C., Squire, J., and Dirks, P.B. (2003). Identification of a Cancer Stem Cell in Human Brain Tumors. Cancer Res. *63*, 5821–5828.

Singh, S.K., Clarke, I.D., Hide, T., and Dirks, P.B. (2004a). Cancer stem cells in nervous system tumors. Oncogene *23*, 7267–7273.

Singh, S.K., Hawkins, C., Clarke, I.D., Squire, J., Bayani, J., Hide, T., Henkelman, R.M., Cusimano, M.D., and Dirks, P.B. (2004b). Identification of human brain tumour initiating cells. Nature *432*, 396–401.

Slaughter, D.P., Southwick, H.W., and Smejkal, W. (1953). "field cancerization" in oral stratified squamous epithelium. Cancer *6*, 963–968.

Snippert, H.J., Flier, L.G. Van Der, Sato, T., Es, J.H. Van, Born, M. Van Den, Kroon-veenboer, C., Barker, N., Klein, A.M., Rheenen, J. Van, Simons, B.D., et al. (2010). Intestinal Crypt Homeostasis Results from Neutral Competition between Symmetrically Dividing Lgr5 Stem Cells. Cell *143*, 134–144.

Snippert, H.J., Schepers, A.G., Van Es, J.H., Simons, B.D., and Clevers, H. (2014). Biased competition between Lgr5 intestinal stem cells driven by oncogenic mutation induces clonal expansion. EMBO Rep. *15*, 62–69.

Soda, Y., Marumoto, T., Friedmann-Morvinski, D., Soda, M., Liu, F., Michiue, H., Pastorino, S., Yang, M., Hoffman, R.M., Kesari, S., et al. (2011). Transdifferentiation of glioblastoma cells into vascular endothelial cells. Proc. Natl. Acad. Sci. U. S. A. *108*, 4274–4280.

St Johnston, D., and Ahringer, J. (2010). Cell polarity in eggs and epithelia: Parallels and diversity. Cell *141*, 757–774.

Stolt, C.C., Schlierf, A., Lommes, P., Hillgärtner, S., Werner, T., Kosian, T., Sock, E., Kessaris, N., Richardson, W.D., Lefebvre, V., et al. (2006). SoxD Proteins Influence Multiple Stages of Oligodendrocyte Development and Modulate SoxE Protein Function. Dev. Cell *11*, 697–709.

Stupp, R., Mason, W., van den Bent, M., Weller, M., Fisher, B., Taphoorn, M.J.B.,

Belanger, K., Brandes, A. a, Marosi, C., Bogdahn, U., et al. (2005). Radiotherapy plus concomitant and adjuvant temozolomide for glioblastoma. N. Engl. J. Med. *9*, 196–197.

Sturm, D., Bender, S., Jones, D.T.W., and Lichter, P. (2014). Paediatric and adult glioblastoma : multiform (epi) genomic culprits emerge. Nat. Publ. Gr. *14*, 92–107.

Tamori, Y., and Deng, W.M. (2011). Cell competition and its implications for development and cancer. J. Genet. Genomics *38*, 483–495.

Torisu, Y., Watanabe, A., Nonaka, A., Midorikawa, Y., Makuuchi, M., Shimamura, T., Sugimura, H., Niida, A., Akiyama, T., Iwanari, H., et al. (2008). Human homolog of NOTUM, overexpressed in hepatocellular carcinoma, is regulated transcriptionally by β-catenin/TCF. Cancer Sci. *99*, 1139–1146.

Tyler, D.M., Li, W., Zhuo, N., Pellock, B., and Baker, N.E. (2007). Genes affecting cell competition in drosophila. Genetics *175*, 643–657.

Uhrbom, L., Dai, C., Celestino, J.C., Rosenblum, M.K., Fuller, G.N., and Holland, E.C. (2002). Ink4a-Arf Loss Cooperates with KRas Activation in Astrocytes and Neural Progenitors to Generate Glioblastomas of Various Morphologies Depending on Activated Akt 1. Cancer Res. *62*, 5551–5558.

Uhrbom, L., Nerio, E., and Holland, E.C. (2004). Dissecting tumor maintenance requirements using bioluminescence imaging of cell proliferation in a mouse glioma model. Nat. Med. *10*, 1257–1260.

Valente, L.J., Gray, D.H.D., Michalak, E.M., Pinon-hofbauer, J., Egle, A., and Scott, C.L. (2013a). Report p53 Efficiently Suppresses Tumor Development in the Complete Absence of Its Cell-Cycle Inhibitory. Cell ReportsReports *3*, 1339–1345.

Valente, L.J., Gray, D.H.D., Michalak, E.M., Pinon-Hofbauer, J., Egle, A., Scott, C.L., Janic, A., and Strasser, A. (2013b). P53 Efficiently Suppresses Tumor Development in the Complete Absence of Its Cell-Cycle Inhibitory and Proapoptotic Effectors p21, Puma, and Noxa. Cell Rep. *3*, 1339–1345.

Vidal, M., Larson, D.E., and Cagan, R.L. (2006). Csk-deficient boundary cells are eliminated from normal drosophila epithelia by exclusion, migration, and apoptosis. Dev. Cell *10*, 33–44.

Vincent, J.P., Kolahgar, G., Gagliardi, M., and Piddini, E. (2011). Steep Differences in Wingless Signaling Trigger Myc-Independent Competitive Cell Interactions. Dev. Cell *21*, 366–374.

Vousden, K.H., and Lu, X. (2002). Live or let die: the cell's response to p53. Nat. Rev. Cancer *2*, 594–604.

Wang, Z., and Sun, Y. (2010). Targeting p53 for Novel Anticancer Therapy. Transl. Oncol. *3*, 1–12.

Watson, A.L., Rahrmann, E.P., Moriarity, B.S., Choi, K., Conboy, C.B., Greeley, A.D., Halfond, A.L., Anderson, L.K., Wahl, B.R., Keng, V.W., et al. (2013). Canonical Wnt/ -catenin Signaling Drives Human Schwann Cell Transformation, Progression, and Tumor Maintenance. Cancer Discov. *3*, 674–689.

Weiss, M.B., Vitolo, M.I., Mohseni, M., Rosen, D.M., Denmeade, S.R., Park, B.H., and Weber, D.J. (2010). Deletion of p53 in human mammary epithelial cells causes chromosomal instability and altered therapeutic response. Oncogene *29*, 4715–4724.

Weller, M., Cloughesy, T., Perry, J.R., and Wick, W. (2012). Standards of care for treatment of recurrent. Neuro. Oncol. *10*, 1–24.

Wen, P., and Kesari, S. (2008). Malignant Gliomas in Adults. N. Engl. J. Med. *359*, 1850–1850.

Wiesmuller, L., and Wittinghofer, A. (1992). Expression of the GTPase Activating Domain of the Neurofibromatosis Type 1 (NF1) Gene in Escherichia coli and Role of the

Conserved Lysine Residue. Biochemistry *1*, 10207–10210.

Wolswijk, G., and Noble, M. (1989). Identification of an adult-specific glial progenitor cell. Development *400*, 387–400.

Yong, V.W.E.E., Moumdjian, R., Yong, F.P., Ruijs, T.C.G., Freedman, M.S., Cashman, N., and Antel, J.P. (1991). yInterferon promotes proliferation of adult human astrocytes in vitro and reactive gliosis in the adult mouse brain in vivo. Proc. Natl. Acad. Sci. *88*, 7016–7020.

Young, K.M., Psachoulia, K., Tripathi, R.B., Dunn, S.J., Cossell, L., Attwell, D., Tohyama, K., and Richardson, W.D. (2013). Oligodendrocyte dynamics in the healthy adult CNS: Evidence for myelin remodeling. Neuron *77*, 873–885.

Young, N.P., Crowley, D., and Jacks, T. (2011). Uncoupling cancer mutations reveals critical timing of p53 loss in sarcomagenesis. Cancer Res. *71*, 4040–4047.

Yu, X., Vazquez, A., Levine, A.J., and Carpizo, D.R. (2012). Allele-Specific p53 Mutant Reactivation. Cancer Cell *21*, 614–625.

Zhao Li, L., Lei, Q. and Guan, K. L., B. (2010). The Hippo-YAP pathway in organ size control and tumorgenesis: an updated version. Genes Dev. *24*, 862–874.

Zhu, Y., and Parada, L.F. (2002). The molecular and genetic basis of neurological tumours. Nat. Rev. Cancer *2*, 616–626.

Zhu, X., Bergles, D.E., and Nishiyama, A. (2007). NG2 cells generate both oligodendrocytes and gray matter astrocytes. Development *135*, 145–157.

Zhu, Y., Romero, M.I., Ghosh, P., Ye, Z., Charnay, P., Rushing, E.J., Marth, J.D., and Parada, L.F. (2001). Ablation of NF1 function in neurons induces abnormal development of cerebral cortex and reactive gliosis in the brain. Genes Dev. *15*, 859–876.

Zhuo, L., Theis, M., Alvarez-Maya, I., Brenner, M., Willecke, K., and Messing, A. (2001). hGFAP-cre transgenic mice for manipulation of glial and neuronal function in vivo. Genesis *31*, 85–94.

Ziosi, M., Baena-López, L.A., Grifoni, D., Froldi, F., Pession, A., Garoia, F., Trotta, V., Bellosta, P., Cavicchi, S., and Pession, A. (2010). dMyc functions downstream of yorkie to promote the supercompetitive behavior of hippo pathway mutant Cells. PLoS Genet. *6*.

Zong, H., Espinosa, J.S., Su, H.H., Muzumdar, M.D., and Luo, L. (2005). Mosaic analysis with double markers in mice. Cell *121*, 479–492.

Zong, H., Verhaak, R.G.W., and Canoll, P. (2012). The cellular origin for malignant glioma and prospects for clinical advancements. Expert Rev. 383–394.

Zong, H., Parada, L.F., and Baker, S.J. (2015). Cell of Origin for Malignant Gliomas and Its Implication in Therapeutic Development. Cold Spring Harb. Perspect. Biol. *1*, 1–12.